UNIVERSIDADE DA BEIRA INTERIOR
Ciências da Saúde

Development of different drug delivery systems for skin regeneration

Patrícia Isabel da Cruz Morgado

Master degree thesis in
Biomedical Sciences
(2nd cycle of studies)

Supervisor: Ilídio Joaquim Sobreira Correia, Ph.D.

Covilhã, June 2011

UNIVERSIDADE DA BEIRA INTERIOR
Ciências da Saúde

Desenvolvimento de diferentes sistemas de libertação controlada para a regeneração de feridas cutâneas

Patrícia Isabel da Cruz Morgado

Dissertação para obtenção do Grau de Mestre em
Ciências Biomédicas
(2º ciclo de estudos)

Orientador: Prof. Doutor Ilídio Joaquim Sobreira Correia

Covilhã, Junho de 2011

Acknowledgments

I would like to thank my supervisor, Professor Ilídio Correia, for all his dedication, trust and support that always showed me, and for making the possible and impossible to gather all the necessary conditions for the development of this study. To him I thank all the knowledge and confidence I gained during this time.

I must thank Professor António Miguel Morão for all his kindness in participating in this project and dedication he showed in its development.

I would also like to thank all my group colleagues for their advice, knowledge sharing and all the good and bad moments we spent together. Thanks for your friendship, kindness and patience.

To my friends for all the support and affection that have always given to me. To everyone with whom I always smile, studied and enjoyed myself.

Finally, I thank my family for the support that always showed in my decisions; to my parents for allowing me to finish another important stage in my life, to my grandmother and brother for the love and confidence that have always given to me and to my boyfriend for all the times that endured my despair and that calmed me in difficult times.

To all of you… a thank you…

Abstract

The human body has different fluids that are hostile environments for biologically active molecules. To overcome this arbitrary, several drug delivery systems have been developed. These systems not only protect all unstable biological active compounds from enzymatic degradation in the human body but also allow a sustained and targeted release of drugs. They contribute for decreasing drug dose required to achieve the desired therapeutic effect. Hydrogels, with their important characteristics, have been widely used in the development of these systems however, the quantity of drug loaded into them may be limited and the high water content of these polymeric matrices often results in relatively rapid drug release profiles. Nevertheless, due to their good physical and biological properties, hydrogels have been extensively used in the treatment of skin injuries. In order to take advantage of hydrogels for drug delivery and wound healing, different systems (nano and micrometric) have been developed and incorporated into hydrogels matrices. Nano and micro systems exhibit high encapsulation efficiencies of drugs and allow its release for a long period of time. Thus, the main goals of this master thesis work plan were to develop micrometric systems based on chitosan, alginate and a dextran hydrogel, and characterize their applicability in the treatment of skin injuries. Initially, the carriers were characterized according to their size, geometry, swelling behavior and biocompatibility. *In vitro* release studies allow us to analyze the release profile of a model protein (bovine serum albumin) when encapsulated into the microparticles. The same studies were done for microparticles loaded into a dextran hydrogel. Co-relating the swelling studies with the *in vitro* protein release studies a mathematical model based on the theory of hindered transport of large solutes in hydrogels was developed for theoretically describing the process of protein release. All the experimental results were interpreted with the aid of the developed model. Moreover it can contribute to decrease the number of experimental studies, reducing costs and saving time for the carrier development. After that, growth factors (vascular endothelial growth factor and endothelial growth factor) were encapsulated into chitosan microparticles that were then loaded into the dextran hydrogel. Subsequently *in vivo* studies were performed to characterize the applicability of the dextran hydrogel loaded with chitosan microparticles containing growth factors in wound healing. The *in vitro* and *in vivo* studies demonstrated that the developed carriers are biocompatible, accelerate the wound healing process and can be used to deliver other bioactive agents.

Keywords

Drug delivery systems, growth factors, *in vitro* and *in vivo* studies, mathematical modeling, wound healing.

Resumo

O corpo humano é composto por diferentes fluidos biológicos que são ambientes hostis para diversas moléculas bioactivas. Devido a este ambiente hostil, diversos sistemas de entrega controlada de fármacos têm sido desenvolvidos. Estes, não só protegem os compostos instáveis da degradação enzimática no corpo humano como, também, permitem a libertação desses compostos de uma forma controlada e, muitas vezes, direccionada, diminuindo, assim, a dosagem necessária para se obter o efeito terapêutico desejado. Até ao momento, os hidrogéis têm sido os materiais mais utilizados na produção deste tipo de sistemas. No entanto, a sua baixa eficiência de encapsulação e a elevada capacidade de absorverem água conduz a perfis de libertação do fármaco rápidos. Contudo, estes sistemas têm sido muito utilizados para o tratamento de feridas cutâneas devido às suas propriedades físicas e biológicas. Diferentes estudos têm sido efectuados, de forma a potenciar a utilização dos hidrogéis na libertação de fármacos e na regeneração de feridas. Novos sistemas (nano e micrométricos) têm sido produzidos e introduzidos no interior dos hidogéis. Estes apresentam eficiências de encapsulação de fármacos superiores e permitem que os mesmos sejam libertados durante um maior período de tempo. Assim, o plano de trabalhos deste mestrado teve como objectivos o desenvolvimento de sistemas micrométricos à base de quitosano e alginato e de um hidrogel de dextrano com o intuito de verificar a sua aplicabilidade no tratamento de feridas cutâneas. Deste modo, inicialmente os transportadores foram caracterizados quanto ao seu tamanho, geometria, capacidade de inchaço e biocompatibilidade. Estudos de libertação *in vitro* permitiram analisar o perfil de libertação de uma proteína modelo (albumina de soro bovino) quando encapsulada no interior das micropartículas. Os mesmos estudos foram efectuados para as micropartículas incorporadas no interior do hidrogel. Tendo por base os estudos de inchaço e os estudos de libertação *in vitro,* foi desenvolvido um modelo matemático baseado na teoria de transporte difuso de macromoléculas para descrever teoricamente o processo de libertação da molécula modelo usada no presente estudo. Todos os resultados experimentais foram interpretados com a ajuda do modelo desenvolvido, o qual pode reduzir o número de estudos experimentais necessários para desenvolver um determinado transportador, reduzindo os custos e o tempo necessário para o desenvolvimento destes novos sistemas para entrega direccionada e controlada de fármacos. Posteriormente, foram efectuados estudos *in vivo,* onde factores de crescimento (factor de crescimento vascular endotelial e factor de crescimento endotelial) foram encapsulados em micropartículas de quitosano. Através destes estudos verificou-se a aplicabilidade do hidrogel de dextrano e das micropartículas de quitosano com factores de crescimento encapsulados na regeneração de feridas cutâneas. Os estudos *in vitro* e *in vivo* demonstraram que os transportadores desenvolvidos são biocompatíveis, aceleram o processo de regeneração de feridas cutâneas e podem futuramente ser usados para libertar outros agentes bioactivos.

Palavras-chave

Cicatrização de feridas, estudos *in vitro* e *in vivo,* factores de crescimento, modelação matemática, sistemas de libertação controlada de fármacos.

Index

Chapter 1: Introduction

Chapter 2: Materials and Methods

Chapter 3: Modeling of Drug Release from Polymeric Systems

List of Figures

Chapter 1: Introduction

Chapter 2: Materials and Methods

Chapter 3: Modeling of Drug Release from Polymeric Systems

Chapter 4: Drug Delivery Systems for Wound Healing

List of Tables

List of Abbreviations

ρ_0	initial density of particles
ϕ_0	initial polymer volumetric fraction
ϕ	volume fraction of polymer
AAD	adipic acid dihydrazide
ATP	adenosine tryphosphate
BSA	bovine serum albumin
C_0	initial solute concentration inside the particles
$CaCl_2$	calcium chloride
CEA	cultured epidermal autograft
C_m	concentration near the particle's surface
C_{out}	concentration in the bulk of the outside solution
D	diffusion coefficient inside hydrogel
D_0	diffusion coefficient inside hydrogel in free solution
DexOx	oxidized dextran
DexOx+Ch	oxidized dextran loaded with chitosan microparticles
DexOx+EGF	oxidized dextran loaded with chitosan microparticles containing endothelial growth factor
DexOx+VEGF	oxidized dextran loaded with chitosan microparticles containing vascular endothelial growth factor
DexOx+VEGF/EGF	oxidized dextran loaded with chitosan microparticles containing vascular endothelial growth factor and endothelial growth factor
DMEM	Dulbecco's modified Eagle's médium
ECM	extracellular matrix
EDTA	ethylenediaminetetraacetic acid
EGF	epidermal growth factor
EtOH	ethanol
FBS	fetal bovine serum
FDA	Food and Drug Administration
FGF	fibroblast growth factor
GAG	glycosaminoglycan
HCl	chloride acid
IGF	insulin-like growth factor
ISO	International Standard Organization
K-	negative control
K+	positive control
K_m	mass transfer coefficient
LDH	lactate dehydrogenase

MTS	3-(4,5-dimethylthiazol-2-yl)-2,5-diphenyl-2H-tetrazolium bromide
MTT	3-(4,5-dimethylthiazol-2-yl)-2,5-diphenyltetrazolium bromide
PBS	phosphate buffered saline
PDGF	platelet-derived growth factor
PLA	poly(lactic acid)
PLGA	poly(lactide-co-glycolide)
PMS	phenazine methosulfate
R_{calc}	calculated percentage of protein release
R_{exp}	experimentally obtained value
r_f	radii of fibers
$R_{part,0}$	initial particle radius
r_s	hydrodynamic radius of the solute
S_0	size of the full thickness circular skin wound area
SC	stratum corneum
SEM	scanning electron microscopy
SDS	sodium dodecyl sulphate
S_N	size of the wound area on the indicated day
sw	swelling ratio
TBSA	total body surface area
TEM	transmission electron microscopy
TGF	transforming growth factor
TPP	tripolyphosphate
t_{samp}	sampling time
V_0	initial volume of the solution outside the particles
VEGF	vascular endothelial growth factor
VEGF+EGF	vascular endothelial growth factor and endothelial growth factor
$V_{part,0}$	initial total volume of particles
$v_{s,p}$	partial specific volumes of polymer
$v_{s,w}$	partial specific volumes of water
α	ratio of moles of protein transferred due to swelling to the total number of moles transferred
Φ	partition coefficient

Chapter 1
Introduction

1. Introduction

1.1. The Skin: structure and functions

The skin is the largest organ of the body in vertebrates and occupies an area of about $2m^2$, representing approximately one-tenth of the body mass (Balasubramani and RAVI, 2001; Metcalfe and Ferguson, 2007a). This complex organ has highly specialized functions. It protects the organism against toxins and microorganisms, allows regulation of body temperature, provides support to blood vessels and nerves, and prevents dehydration of all non-aquatic animals (Balasubramani and RAVI, 2001; Böttcher-Haberzeth et al., 2010; Clark et al., 2007; Rodrigues et al., 2008). Other critical functions of the skin are related with immune surveillance and sensory detection. Overall, skin is an indicator of general well being and health (Clark et al., 2007; Sachs and Voorhees, 2010). It can be considered an organ associated with physical attractiveness and beauty (Sachs and Voorhees, 2010).

Anatomically and functionally, skin has two distinctive layers: the epidermis and dermis (Figure 1), (Jones et al., 2002; Metcalfe and Ferguson, 2007a, b; Sheridan and Moreno, 2001). Some authors refer a third layer, the hypodermis or subcutaneous layer, that is mainly composed of fat and a layer of loose connective tissue (Metcalfe and Ferguson, 2007a, b).

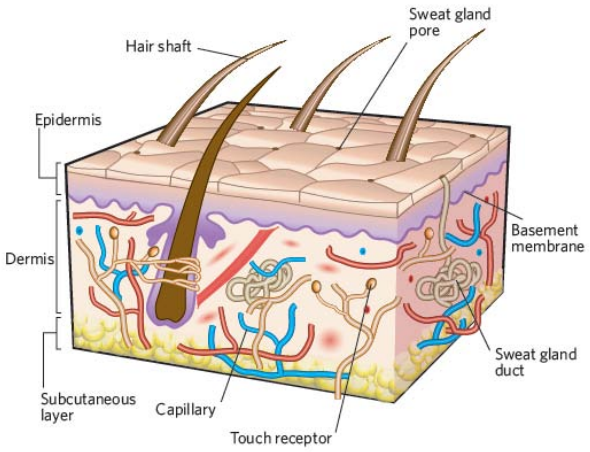

Figure 1 – The structure of human skin (adapted from (MacNeil, 2007)).

1.1.1. Epidermis

Epidermis, the outermost layer, is relatively thin, 0.1-0.2mm in depth, and totally cellular, but has sufficient thickness to provide vital barrier function (MacNeil, 2008; Metcalfe and Ferguson, 2007a, b; Wong and Chang, 2009). This layer is avascularized and is fed by diffusion from the capillaries of the papillary layer from dermis (Seeley et al., 2003). This layer is primarily composed of stratified squamous epithelium of keratinocytes, which derives from neuroectoderm and comprises over ninety percent of epidermal cells (Wong and Chang, 2009). The keratinocytes produce a protein called keratin, making them responsible for the

structural strength and permeability characteristics of the epidermis (Paul and Sharma, 2004; Seeley et al., 2003). The epidermis is also composed of melanocytes that contribute to skin color, Langerhans cells that are part of the immune system, and Merkel cells (specialized epidermal cells associated with nerve endings) responsible for detecting the touch and pressure surface (Seeley et al., 2003; Wong and Chang, 2009).

The cells in the deeper layers of the epidermis are responsible for the constant cell renewal, since they have a higher rate of replication. As there are new cells, older ones are pushed to the surface where they slough off. During this movement, cells change their shape and chemical composition, passing to secrete and accumulate keratin, a process known as keratinization. This process allows the identification of different phases of transition. Based on these stages, the different cells of the epidermis are divided into strata or layers, which are classified into: cornea, translucent, granular, spinous and basal (the top layer to the deepest) (Table 1) (Seeley et al., 2003).

1.1.2. Dermis

The dermis, or middle layer, is a connective tissue situated directly below the epidermis (Metcalfe and Ferguson, 2007a, b; Paul and Sharma, 2004; Wong and Chang, 2009). This layer is responsible for the elasticity and mechanical integrity of the skin, and contains blood vessels that are responsible for the nutrition of the epidermal layer (Jones et al., 2002). It contains receptors for touch, temperature and pain, as well as hair follicles and sweat ducts (MacNeil, 2008). This skin layer is composed of collagen (type I and III), the main type of fiber of your conjunctive tissue, with some elastin and glycosaminoglycans (GAGs). Fibroblasts are the major cell type present in the dermis. They are capable of producing remodeling enzymes such as proteases and collagenases, which play an important role in the wound healing process (Metcalfe and Ferguson, 2007a, b; Wong and Chang, 2009).

The two layers, epidermis and dermis, are connected by a basement membrane that is composed of various integrins, laminins, collagens, and other proteins that make important roles in regulating epithelial-mesenchymal cross-talk (Wong and Chang, 2009).

The dermis is divided into two layers: a deeper layer called reticular and a superficial layer nominated papillary. The reticular layer, the main component of the dermis, is composed of dense and irregular tissue, composed with a set of irregularly arranged fibers that are resistant to stretching in many directions, and is continuous with the hypodermis. Collagen and elastin fibers are, predominantly, oriented in a certain direction and cause lines of tension in the skin (Seeley et al., 2003). In turn, the papillary layer owes its name due to the extensions called papillae that point toward the epidermis. It also contains numerous blood vessels that supply nutrients to the overlying epidermis, removes waste products and help to regulate the body temperature (Seeley et al., 2003; Wong and Chang, 2009).

1.1.3. Hypodermis

The hypodermis, which has a deeper localization to the dermis, contains adipose tissue that is well vascularized and contributes to both the mechanical and the thermoregulatory properties of the skin. It separates the dermis from the underlying muscular fascia (Metcalfe and Ferguson, 2007a, b; Wong and Chang, 2009). This skin layer is composed of lax connective tissue with collagen and elastin fibers. The main types of cells formed in the hypodermis are fibroblasts, adipose cells and macrophages. This layer is often regarded as not being part of the skin, being sometimes called the subcutaneous tissue or superficial fascia (Seeley et al., 2003).

About half of the fat stored in the body is found in the hypodermis, although their number and location vary with age, sex and feeding (Seeley et al., 2003).

Table 1 – Comparison of the epidermis and dermis with the hypodermis (adapted from (Seeley et al., 2003)).

Portion	Structure	Function
Epidermis	Superficial part of the skin; stratified squamous epithelium; composed of four or five layers.	Barrier that prevents water loss and entry of chemicals and microorganisms; protects against abrasion and UV radiation; produces vitamin D; gives rise to the hair, nails and glands.
Corneum layer	The most superficial layer of the epidermis; 25 or more layers of pavement cells killed.	Provides structural strength; prevents water loss.
Translucent layer	Three to five layers of dead cells; it seems clear; present in thick skin, mostly absent from the thin skin.	Keratohyalin dispersion around the keratin fibers.
Granular layer	Two to five layers of cells flattened and losanged.	Production of granules of keratohyalin; lamellar bodies release fat cells; the cells die.
Spinous layer	Eight to ten layers of cells multifaceted.	Production of keratin fibers; form lamellar bodies.
Basal layer	Deeper layer of the epidermis; single layer of cubical or cylindrical cells; binds to the dermis.	Producing cells from the superficial layers; melanocytes produce and supply melanin.
Dermis	Deep part of the skin; connective tissue composed of two layers.	Responsible for structural strength and flexibility of skin.
Papillary dermis	The papillae protrude into the epidermis; lax connective tissue.	It brings the blood vessels close to the epidermis; the papillae give rise to fingerprints.
Reticular dermis	Carpet fibers of collagen and elastin; irregular dense connective tissue.	Top fibrous layer of the dermis; strong in many directions; form tension lines.
Hypodermis	Not part of the skin; lax connective tissue with abundant fat deposits.	Unites the dermis to underlying structures; nervous tissue provides the energy storage, insulation and cushioning; blood vessels and nerves innervating and irrigate the dermis.

1.2. Wounds: definition and classifications

As previously mentioned, skin is a complex tissue which provides an essential water, electrolyte, and bacteria-boundary to the outside world (MacNeil, 2008; Shaw and Martin, 2009a). Due to the various functions of the skin, any loss of skin integrity due to injury or illness, in addition to causing physical, mechanical and thermal damage, may also affect the physiological functions, resulting in disorders of the organism and ultimately in significant disability or even death (Clark et al., 2007; Rodrigues et al., 2008). Thus, skin disruption often leads to an increase in fluid loss, infection, scarring, compromised immunity and change in body image (Alemdaroglu et al., 2006). Many reasons can be pointed out for the loss of skin integrity, such as genetic disorders (bullous conditions), acute trauma, chronic wounds (e.g. venous, diabetic and pressure ulcers) or even surgical interventions (Dai et al., 2004; Shevchenko et al., 2010). However, thermal trauma, like burns, is one of the most common cause for major skin loss, where substantial areas of skin can be damaged and the possibility of skin regeneration is unlikely (Shevchenko et al., 2010). The mortality rate caused by burns has been decreasing since the last two decades with the advances in regenerative medicine. However it is still high if more than 70% of the total body surface area (TBSA) is injured or burned (Alemdaroglu et al., 2006).

According to the US Wound Healing Society, a wound can be described as a result of "disruption of normal anatomic structure and function" of the skin, resulting from physical or thermal damage or as a consequence of the presence of an underlying medical or physiological condition (Boateng et al., 2008). Wounds can be classified based on the nature of the repair process, on the number of skin layers and area of skin affected. Based on the type of the repair process, wounds can be classified as acute or chronic wounds (Boateng et al., 2008; Paul and Sharma, 2004).

Acute wounds are characterized by their ability to heal completely with minimal scarring within the expected time frame, normally 8-12 weeks (Boateng et al., 2008). The newly formed tissue has a similar structure and comparable functions to intact skin, however, its regeneration is uncommon (with notable exceptions such as early fetal healing) (Li et al., 2007). Mechanical injuries, due to external factors such as abrasions which are caused by frictional contact between the skin and hard surfaces, are the primary causes of acute wounds (Boateng et al., 2008; Li et al., 2007). Other examples of mechanical injuries include penetrating wounds caused by knives, gun shots and surgical wounds. Burns and chemical injuries (caused by radiation, electricity, corrosive chemicals and thermal sources) are another categories of acute wounds (Boateng et al., 2008). Chronic wounds represent a different kind of challenge for wound healing (Supp and Boyce, 2005). These are characterized by their slow healing, i.e., that have not healed beyond 12 weeks and often reoccur. Repeated tissue insults or underlying physiological conditions such as diabetes and other malignances, persistent infections, poor primary treatment and other patient related

factors, contributes to the disability of these wounds to heal faster (Boateng et al., 2008). These wounds involve a large surface area and have a high incidence in the general population, featuring an enormous medical and economic impact (Supp and Boyce, 2005). Pressure ulcers and leg ulcers (venous, ischaemic or of traumatic origin) are known as the most common chronic wounds (Boateng et al., 2008; Supp and Boyce, 2005).

Based on the number of layers and the area of affected skin, wounds can be divided into: epidermal, superficial and deep partial-thickness, and full-thickness ones (Paul and Sharma, 2004; Shevchenko et al., 2010). Epidermal injuries are normally caused by sunburns, light scalds or grazing, characterized by erythema and minor pain. In this type of lesions, only the epidermis is affected. As so, such injuries do not require specific surgical treatment and regenerate rapidly without any scarring (Shevchenko et al., 2010). Superficial partial-thickness wounds affect the epidermis and superficial parts of the dermis, with epidermal blistering and severe pain accompanying this type of injury, especially in the case of thermal trauma. The wound healing in this type of wounds is featured by epithelialization from the margins of the wound where basal keratinocytes change into a proliferating migratory cell type and cover the damaged area (Shevchenko et al., 2010). In the other hand, deep partial-thickness injuries involve greater dermal damaged that results in fewer skin appendages remaining and, therefore, they take longer to heal. Scarring and fibroplasia are more pronounced and intensive in this depth of injury when compared with superficial partial-thickness wounds (Shevchenko et al., 2010). Finally, in full-thickness injuries all epithelial-regenerative elements are completely destroyed. Wound healing is characterized by contraction, with epithelialization from only the edge of the wound, leading to cosmetic and functional defects. When the wound has more than 1 cm in diameter a skin grafting is usually required. These types of wounds cannot epithelialize on their own and may lead to extensive scarring, resulting in limitations in joint mobility and severe cosmetic deformities (Shevchenko et al., 2010).

1.3. Wound Healing

The wound healing process is extremely dynamic, interactive and difficult. It involves complex interactions of extracellular matrix (ECM) molecules, soluble mediators, various resident cells, and infiltrating leukocyte subtypes which, together, act to reestablish the integrity of damaged tissue and replace the lost one (Boateng et al., 2008; Branski et al., 2006; Eming et al., 2007). If this response is successful and the injury does not cause organism dead, these processes must be shut down in a precise sequence in the ensuing days for the recovery takes place (Gurtner et al., 2008).

It can be considered that a “healed wound” is one in which the connective tissues have been repaired, the wound is completely re-epithelialized and the skin has returned to its

normal anatomical structure and function without the need for continued drainage or dressing (Beldon, 2010; Enoch and Leaper, 2008).

In order to achieve the primary goal of wound healing (tissue integrity and haemostasis), there are five overlapping stages that need to be considered: haemostasis, inflammation, migration, proliferation and maturation (Boateng et al., 2008). These can be summarized in three main phases like haemostasis and inflammation, new tissue formation (proliferation) and tissue remodeling as shown in Figure 2 (Eming et al., 2007; Gurtner et al., 2008).

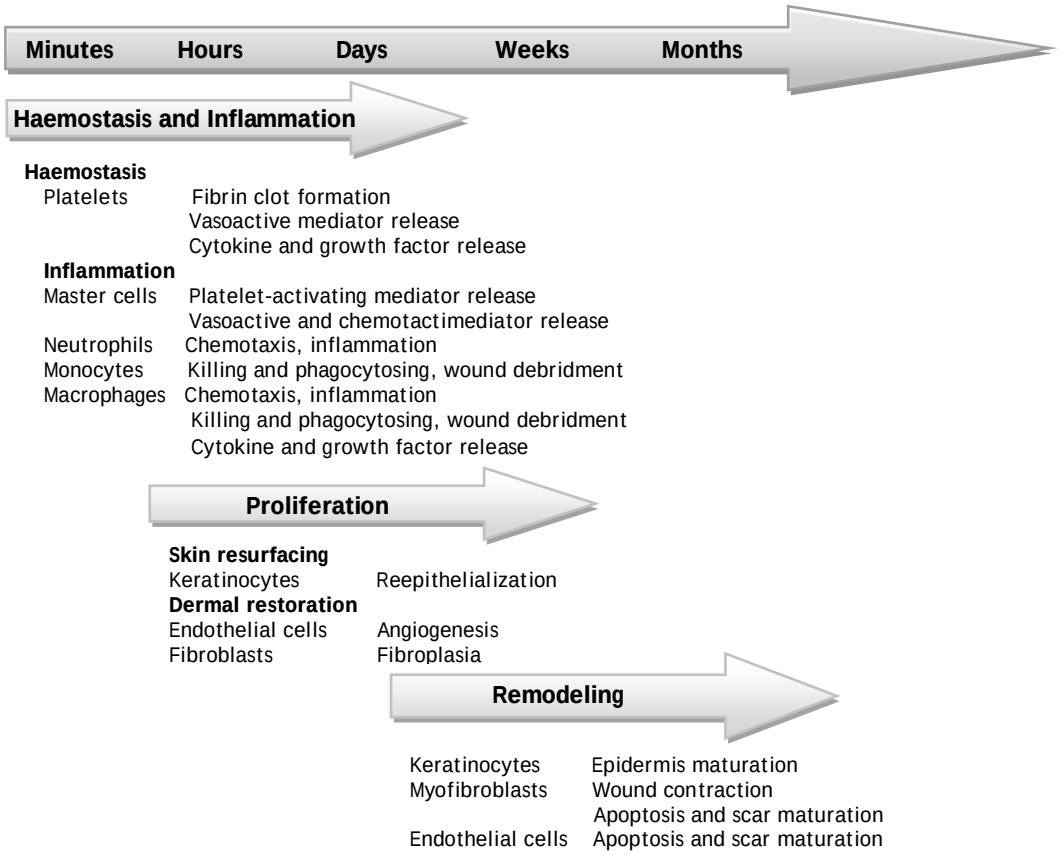

Figure 2 – Schematic representation of the main phases of wound healing, the major cell types and their effects (adapted from (Li et al., 2007)).

In contrast, embryonic wound healing is essentially a regenerative process, characterized by the absence of scarring and fibrosis (Böttcher-Haberzeth et al., 2010; Metcalfe and Ferguson, 2007b). Embryonic wounds exhibit a number of major differences from adult ones which scar, lack of fibrin clots and platelet degranulation, markedly reduce inflammatory response and distinctly elevate levels of molecules involved in skin morphogenesis and growth (Metcalfe and Ferguson, 2007b).

1.3.1 Haemostasis and Inflammation

Unless there is a severe arterial hemorrhage, haemostasis is achieved initially by the formation of a platelet plug, followed by a fibrin matrix, which becomes the scaffold for infiltrating cells (Auger et al., 2009; Gurtner et al., 2008; Ousey and McIntosh, 2009; Strodtbeck, 2001). The platelets degranulate and release their alpha granules, which secrete several growth factors, such as: platelet-derived growth factor (PDGF), insulin-like growth factor-1 (IGF-1), epidermal growth factor (EGF), transforming growth factor-ß (TGF-ß) and platelet factor-IV. They also contain dense bodies that store vasoactive amines, like serotonin, which increase the microvascular permeability (Enoch and Leaper, 2008). Owing to growth factors, the wound healing cascade is initiated by attracting and activating fibroblasts, endothelial cells and macrophages (Enoch and Leaper, 2008). Subsequently, four major amplification systems are activated (complement cascade, clotting mechanism, kinin cascade, plasmin generation), which contribute to haemostasis and the other staged of healing process. Finally, the clot (comprising fibrin, fibronectin, vitronectin, von Willbrand factor, thrombospondin) provides the provisional matrix for cell migration (Enoch and Leaper, 2008).

The inflammatory phase begins almost simultaneously with haemostasis, sometimes from within a few minutes of injury to 24h, and lasts for about 3 days. It plays a central role in wound healing, not only protecting the wound from invading microbes, but also by participating in the tissue repair processes (Boateng et al., 2008; Shaw and Martin, 2009b; Tsirogianni et al., 2006). In this phase, components of the coagulation cascade, inflammatory pathways and immune system are needed to prevent ongoing blood and fluid losses, to remove dead and dying tissues and to avoid infection (Figure 3) (Gurtner et al., 2008).

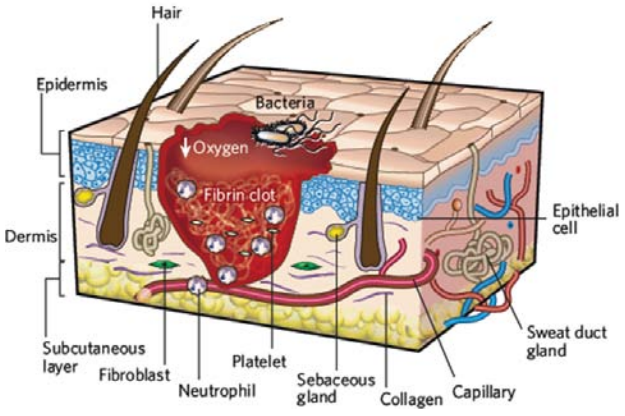

Figure 3 – First stage of wound repair: haemostasis and inflammation. The process of inflammation lasts until 48h after injury. The wound is characterized by a hypoxic (ischaemic) environment in which a fibrin clot has formed. Bacteria, neutrophils and platelets are abundant in the wound. Hair follicles and sweat duct glands, the normal skin appendages, are still present in the skin outside the wound (adapted from (Gurtner et al., 2008)).

Inflammation can be divided into two stages (early and late inflammatory phases) depending either on the time and duration of the response and the type of inflammatory cell involved (Enoch and Leaper, 2008; Li et al., 2007). In the early inflammatory phase (days 1-2), neutrophil granulocytes (polymorphonuclear leukocytes) are recruited to the wound in response to the activation of complement, the degranulation of platelets and the products of bacterial degradation, such as: fragments of ECM protein, TGF-ß, complement components (e.g. C3a, C5a) and formyl-methionyl peptide products from bacteria (Enoch and Leaper, 2008; Gurtner et al., 2008). The main function of polymorphonuclear leukocytes is to minimize bacterial contamination of the wound, thus preventing infection (Enoch and Leaper, 2008). After 2-3 days in the late inflammatory phase, monocytes appear in the wound area and differentiate into macrophages (Enoch and Leaper, 2008; Gurtner et al., 2008). Monocytes are attracted to the wound by a variety of chemoattractants like complement, clotting components, fragments of immunoglobulin G, breakdown products of collagen and elastin and cytokines (Enoch and Leaper, 2008). Macrophages are thought to be crucial for coordinating later events in response to injury and they function as phagocytic cells. They are the primary producers of growth factors responsible for the proliferation and production of the ECM by stimulating fibroblasts, endothelial and smooth muscle cells (Enoch and Leaper, 2008; Gurtner et al., 2008). These cells of the immune system also release proteolytic enzymes (e.g. collagenase) that help to debride the wound (Enoch and Leaper, 2008). Neutrophils are known to produce vascular endothelial growth factor (VEGF), while macrophages can also release PDGF, EGF, TGF-α, TGF-ß in addition to IGF (Auger et al., 2009).

At the end of this phase, collagen fibers are vertically oriented and do not connect the incision's edges; epithelial cell proliferation continues, yielding a thickened epidermal covering layer (Enoch and Leaper, 2008).

1.3.2. New tissue formation

The second stage of wound healing, which takes place 2-10 days after injury, is characterized by fibroblast migration, deposition of the ECM and formation of granulation tissue (Figure 4) (Branski et al., 2006; Enoch and Leaper, 2008; Gurtner et al., 2008).

This phase starts with the migration of keratinocytes over the injured dermis (Branski et al., 2006; Gurtner et al., 2008). Then, new blood vessels are formed (angiogenesis), and the sprouts of capillaries associated with fibroblast and macrophages restore the fibrin matrix with granulation tissue, thus forming a new substrate for keratinocyte migration at later stages of the repair process (Gurtner et al., 2008). These cells proliferate, mature and restore the barrier function of the epithelium (Gurtner et al., 2008). In the last part of this stage, fibroblasts are attracted to the wound by a number of factors, including PDGF and TGF-ß, and some differentiate into myofibroblasts, a type of contractile cells that, over time, bring the edges of the wound together (Enoch and Leaper, 2008; Gurtner et al., 2008).

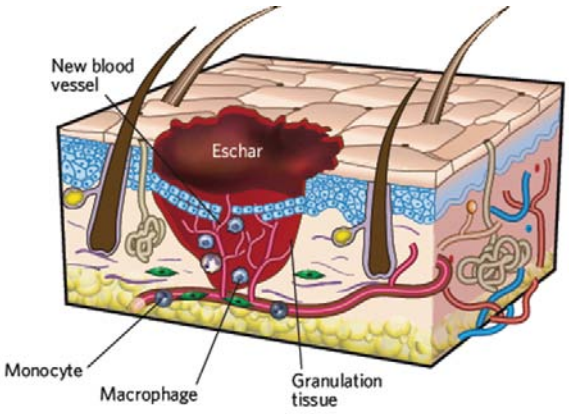

Figure 4 - Second stage of wound repair: new tissue formation. It is characterized by the formation of an eschar (scab). Most cells from the previous stage of repair have migrated from the wound, and new blood vessels grew. Epithelial cells under the eschar can be observed (adapted from (Gurtner et al., 2008)).

Fibroblasts and myofibroblasts interact, proliferate and produce the ECM proteins fibronectin, hyaluronan and, later, collagen and proteoglycans (Enoch and Leaper, 2008; Gurtner et al., 2008). Fibroblasts also secrete fibroblast growth factor (FGF) that can, along with the VEGF secreted by platelets and neutrophils, act as an angiogenic factor to stimulate endothelial cell proliferation and migration, thus promoting vascularization at the healing site (Auger et al., 2009). Epithelialization of the wound represents the final stage of the proliferative phase (Enoch and Leaper, 2008).

1.3.3. Remodeling

Remodeling is the last step of normal acute wound healing, also called maturation, during which all of the processes activated after injury cease. It begins 2-3 weeks after injury and lasts for a year or more (Auger et al., 2009; Gurtner et al., 2008). During this stage, the ECM components are modified by the balanced mechanisms of proteolysis and new matrix formed, and wound becomes gradually less vascularized (Auger et al., 2009). Most of endothelial cells, macrophages and myofibroblasts undergo apoptosis or exit from the wound, leaving a mass that contains few cells and consists mostly of collagen and other ECM components (Figure 5) (Gurtner et al., 2008). Although the initial granulation tissue is weak, during this stage, it will eventually gain strength over time due to the gradual replacement of immature type III collagen by mature type I collagen (Auger et al., 2009; Gurtner et al., 2008). This process is carried out by matrix metalloproteinases that are secreted by fibroblasts, macrophages and endothelial cells (Gurtner et al., 2008).

Further remodeling of the wound causes a decrease in the activity of metalloproteinases, an increase in activity of tissue inhibitors of enzymes, reduction in the density of macrophages and fibroblasts, stop in the outgrowth of capillaries, reduction in the blood flow and metabolic activity and decrease in size of the underlying contractile

connective tissue (Enoch and Leaper, 2008). Finally, the granulation tissue evolves into an avascular scar composed of inactive fibroblasts, fragments of elastic tissue, dense collagen and other components of the ECM. As the scar matures, fibronectin and hyaluronan are broken down and collagens bundles rise in diameter, increasing the tensile strength of the wound (Enoch and Leaper, 2008). However, the tissue never recover the properties of uninjured skin (Enoch and Leaper, 2008; Gurtner et al., 2008).

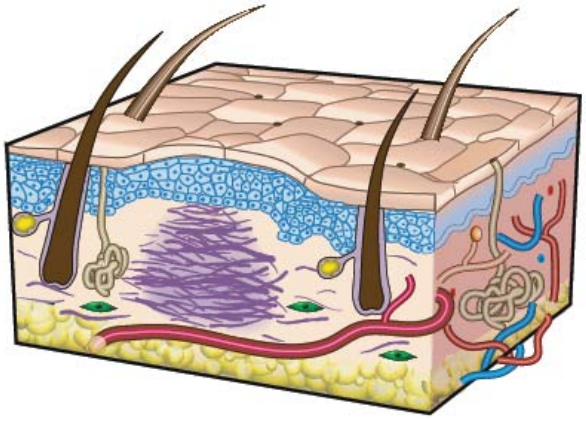

Figure 5 – Third stage of wound repair: remodeling. This stage lasts for a year or longer. It can be observed that disorganized collagen has been laid down by fibroblasts. The wound has contracted near its surface. The re-epithelialized wound is slightly higher that the surrounding surface; the healed region doesn't have normal skin appendages (adapted from (Gurtner et al., 2008)).

Sometimes, due to local and systemic factors, the normal process of healing is disrupted and this process can be divided into two types: non-healing or chronic wounds (as previously described in the text) and excessive wound healing (Enoch and Leaper, 2008). In cases of excessive wound healing, hypertrophic scars and keloids are formed resulting from overproduction of all components of the healing process, such as fibroblasts, collagen, elastin and proteoglycans (Enoch and Leaper, 2008). Hypertrophic scars are elevated and may fall down with time, while keloids continue to grow behind the margin of the original wound, like a benign tumor. Other type of scars can be defined as atrophic ones, that cause a valley or depression in the skin (Metcalfe and Ferguson, 2007b). All types of scarring can occur on all areas of the body, but some of them such as chest, knees and elbows are more susceptible to scarring (Metcalfe and Ferguson, 2007b). The main feature of the phenomenon scarring is called wound contraction. This is caused, at least in part, by the presence of myofibroblasts which develop characteristics of smooth muscles cells under the influence of TGF-ßs (Böttcher-Haberzeth et al., 2010).

1.4. Biomaterials and Tissue Engineering

Tissue engineering is emerging as an interdisciplinary field in biomedical engineering that integrates many concepts of science and engineering in order to design and develop biological substitutes that restore, maintain, or improve damaged tissues and organs functions (Clark et al., 2007; Desai, 2000; Harrison and Atala, 2007; Metcalfe and Ferguson, 2007b; Norman and Desai, 2006; Zhang and Webster, 2009). It has appeared as a solution to the a number of clinical problems that were not properly treated with the use of permanent replacement devices (Huebsch and Mooney, 2009). Major advances in transplantation of cells and organs, as well as in materials science and engineering have contributed for the continuous development of tissue engineering and regenerative medicine (Desai, 2000; Harrison and Atala, 2007; Norman and Desai, 2006).

Usually, there are three aspects considered in the production of any device for tissue engineering – the cells, the scaffold or biomaterial, and cell-material interaction: isolation of the cells from the patient by a small biopsy and their multiplication by cell culture techniques; amplification of the cell number and impregnation of these cells into a biodegradable scaffold or biomaterial; introduction of the construct cell-biomaterial into a functional tissue mass (Desai, 2000; Eisenbarth, 2007). It is know that the extracellular environment influences cell behavior in relation to morphology, cytoskeletal structure and function. Thus, when studying cell function and development of tissue substitute, it is important to reproduce as much as possible, the size, configuration and composition of the environment of cells, creating physiologically relevant models of cells and tissues (Desai, 2000; Ito et al., 2005).

Biomaterials, traditionally defined as materials used in medical devices, have been used since antiquity, but recently their degree of sophistication has increased significantly (Huebsch and Mooney, 2009). It gives the cells a temporary structure in which they further proliferate and differentiate in order to build the injured tissue, maintains the shape of the defect until the reconstruction process is finished and prevents the infiltration of the tissue in contact with the defect (Eisenbarth, 2007). The biomaterials used in tissue engineering applications are used in the form of carriers, hydrogels or scaffolds, and they can be derived from biological or synthetic origins (Eisenbarth, 2007; Lutolf and Hubbell, 2005). Usually, materials from natural sources (polypeptides, hydroxyapatites, hyaluronan, GAGs, fibronectin, collagen, chitosan, alginate and dextran) are advantageous because of their inherent properties of biological recognition, including presentation of receptor-binding ligands and susceptibility to cell-triggered proteolytic degradation and remodeling. Despite of these advantages, many issues have led the development of synthetic biomaterials as cellular substrates, including complexities associated with purification, immunogenicity and pathogen transmission. Examples of these materials include polyglycolide, polylactide, polytetrafluoroethylene and others (Lutolf and Hubbell, 2005; Metcalfe and Ferguson, 2007b).

A major disadvantage of synthetic materials is the lack of cell-recognition signals. However, new manufacturing processes are now being developed, which will allow the incorporation of cell-adhesion peptides into biomaterials, that are known to be involved in cellular interactions (Metcalfe and Ferguson, 2007b).

The biomaterials must have favorable properties in order to promote cell adhesion, proliferation and differentiation for the formation of the desired tissue (Eisenbarth, 2007; Huebsch and Mooney, 2009; Roach et al., 2007):

a. They should present similar mechanical properties to the injured tissue;
b. Must enable or support cell metabolism that build up a new tissue with suitable surface chemistry for cell attachment, proliferation and differentiation;
c. Have a three dimensional structure with interconnective pores for cell growth and nutrients flow. The substructure must be vascular supportive for almost all tissues and has to maximize the space for cellular adhesion, growth, ECM secretion, revascularization and adequate nutrient and oxygen supply;
d. It must be biodegradable along with the reconstruction of the newly build tissue and the products resultant of degradation must not affect the tissue regeneration and remodeling process;
e. It must be biocompatible. Biocompatibility is dependent on the site of implantation, the function and size of the implant and the duration of implantation with a key issue being the time-scale required for material-host tissue interactions to become established.

1.4.1. The role of biomaterials in skin regeneration

Large full-thickness skin defects, with more than 4 cm in diameter, resulting from burns, soft tissue trauma and disease leading to skin necrosis, will not heal well without a graft and represent a significant clinical problem that is far from being solved (Böttcher-Haberzeth et al., 2010; MacNeil, 2007). In the past, wounds were treated by allowing them to dry and hence, acquire a hard protective coating, the scab (Dos Santos et al., 2006). About 30 years ago, the wounds treatment was revolutionized with the discovery that a wound would heal faster when a moist dressing was applied rather than the traditional dry dressings such as gauze type materials produced from cotton or lint (Dos Santos et al., 2006). Other reasons to develop a material capable of promote skin regeneration are the following two: first, it is difficult to get autologous skin transplants when the defect exceeds 50-60% of the TBSA; second, most conventional skin grafting techniques in order to provide autologous defect coverage are based on transplanting split-thickness skin which is comprised throughout the epidermis but only for a portion of the dermis, and that frequently leads to scarring (Böttcher-Haberzeth et al., 2010; MacNeil, 2008). These problems could be reduced with the development of dermo-epidermal skin substitutes (Böttcher-Haberzeth et al., 2010).

There are many types of skin substitutes and they can be classified in a number of ways depending on their function in the wound (debridement, antibacterial, occlusive, absorbent, adherence), type of material used to produce the dressing (e.g. hydrocolloid, alginate, collagen), their origin (synthetic or natural), the physical form of the dressing (ointment, film, foam, gel) and according to the presence or absence of living cells (the use of autologous, allogeneic or xenogenic cells or tissues) (Auger et al., 2009; Boateng et al., 2008). They can also be classified into primary, secondary and island dressings (Boateng et al., 2008). Primary dressings are the ones that are in physical contact with the wound, while secondary dressings cover the primary ones. Island dressings possess a central absorbent region which is surrounded by an adhesive portion (Boateng et al., 2008).

The concern for the development of skin substitutes to improve wound healing is valid for extensive wounds that cannot heal spontaneously, since they are deep and do affect a high percentage of TBSA, and for smaller wounds which cannot heal due to inflammation or a deficiency in the other steps of wound healing process. Dressings can also be used in wounds that would heal by themselves, however very slowly, and the objective is a faster and/or better quality of healing (Auger et al., 2009).

Three factors are of paramount importance in the development of tissue-engineered materials: the safety of the patient, clinical efficacy and convenience of use (MacNeil, 2007; MacNeil, 2008). Tissue-engineered skin substitutes need to provide a barrier layer of renewable keratinocytes (the cells that form the upper barrier layer of skin), which is firmly bound to the underlying dermis. They must also attach well to the wound bed, maintain a moist environment at the wound/dressing interface, absorb the excess exudates without leakage to the surface of the dressing, be supported by new vasculature, provide thermal insulation, mechanical and bacterial protection, allow gaseous and fluid exchange, absorb wound odor, be non-adherent to the wound and easily removed without trauma, not be rejected by the immune system and be capable of self repair throughout a patient's life (Eldin et al., 2010; MacNeil, 2007; MacNeil, 2008). It should also have the ability to replace all the structures and functions of skin (Supp and Boyce, 2005).

The first milestones in skin research and skin tissue engineering focused on the enzymatic separation of the epidermis and dermis and the *in vitro* culture of keratinocytes (Böttcher-Haberzeth et al., 2010). Rheinwald and Green, in 1975, manipulated the growth of human primary epidermal cells on a layer of lethally irradiated 3T3 murine fibroblasts. After the first clinical application, cultured epidermal autografts (CEAs) were tested in almost all leading burn centers worldwide (Böttcher-Haberzeth et al., 2010; Green and Rheinwald, 1975; MacNeil, 2007). After that, Bell *et al* (1981) generated a dermo-epidermal substitute which was tested in an animal model and, subsequently, transformed into the product Apligraft® (Table 2) (Bell et al., 1981). This substitute contains both allogeneic fibroblasts and keratinocytes derived from neonatal foreskin (Böttcher-Haberzeth et al., 2010; Supp and Boyce, 2005). Another useful dermo-epidermal substitute is Integra®, a bilayered artificial

skin, composed of porous bovine collagen and chondroitin-6-sulfate glycosaminoglycan with a silicone membrane that functions as a temporary carrier (Böttcher-Haberzeth et al., 2010; MacNeil, 2007; Supp and Boyce, 2005). Futhermore, donor (cadaveric) skin is commonly used for managing serious burns and treating chronic wounds. Donor skin is currently an underused resource that could be especially valuable in the developed world (MacNeil, 2007). However, skin allografts isolated from cadavers, provide only temporary coverage because of host rejection (Clark et al., 2007). The most effective treatment will be based on the decellularization of each tissue and organ and it is dependent of many factors, including the tissue's cellularity, density, lipid content and thickness. It should be understood that every cell removal agent and method will alter ECM composition and cause some degree of ultrastructure disruption (Crapo et al., 2011). Triton X-100 and sodium dodecyl sulfate (SDS) are two typical detergents used to remove cells from tissues. SDS is typically more effective to remove cell residues from tissue compared to other detergents, but it is also more disruptive to ECM (Badylak et al., 2010; Crapo et al., 2011).

However, the most advanced skin substitute still do not incorporate many of the innate features of native skin such as glands, dermal microvascularization, pilosity and others specialized cells, responsible for the perception of heat, cold, pressure, vibration and pain. Other factor is the skin pigmentation that is not only a matter of aesthetics and quality of life, but also it provides protection against the UV radiation (Auger et al., 2009). For example, some researchers concluded that skin pigmentation can be controlled by keratinocytes and by the addition of melanocytes into skin substitutes (Auger et al., 2009). It is also possible to improve nerve regeneration in wound healing by controlling the amount of laminin present in the skin substitute (Auger et al., 2009). Other important factor in skin substitutes is that they can contribute for wound vascularization, preventing necrosis and loss of the epithelial covering. Some studies indicate that endothelial cells can spontaneously form into capillary-like structures and microvascular networks when cocultured with fibroblasts.

Another approach to improve vascularization is the use of angiogenic recombinant factors like VEGF and FGF. With the same idea, other factors such as PDGF or products like platelet-rich plasma (PDGF, EGF, VEGF, IGF-1 and TGF-β) can promote wound healing when added to the skin substitutes matrix improving the speed and the quality of healing (Auger et al., 2009). Finally, the emerging field of regenerative medicine aims to develop skin substitutes that can promote skin regeneration without scarring. It is believed that the inclusion of some factors and cells responsible for scar less healing in an embryo (e.g. TGF-β3) into collagen composite scaffolds, will optimize the healing process by providing an aesthetic and functional skin (Auger et al., 2009; Balasubramani and RAVI, 2001).

Table 2 - Tissue-engineered products, with or without living cells (Auger et al., 2009; Böttcher-Haberzeth et al., 2010; MacNeil, 2008; Pham et al., 2007; Supp and Boyce, 2005).

Commercial Product	Description	Application
Epidermal substitutes		
Epicel®	Cultured epidermal autograft (autologous keratinocytes grown in the presence of murine fibroblasts)	Full- and partial-thickness burns and chronic ulcers treatment
Epidex®	Cultured epidermal autograft (autologous outer root sheet hair follicle cells)	Full- and partial-thickness burns and chronic ulcers treatment
Laserskin® (Vivoderm®)	Subconfluent autologous keratinocytes seeded on esterified laser-perforated hyaluronic acid matrix	Full- and partial-thickness burns and chronic ulcers treatment
BioSeed-S®	Autologous oral mucosal cells on a fibrin matrix	Partial-thickness burns and chronic ulcers treatment
Myskin®	Cultured epidermal autograft (autologous keratinocytes grown in the presence of irradiated murine fibroblasts)	Partial-thickness burns and chronic ulcers treatment
CellSpray®	Preconfluent autologous keratinocytes delivered into a suspension for spray	Partial-thickness burns and chronic ulcers treatment
Dermal substitutes		
Dermagraft®	Bioabsorbable polyglactin mesh scaffold seeded with human allogeneic nenonatal fibroblasts	Full-thickness diabetic foot ulcers treatment
Alloderm®	Acellular donated allograft human dermis	Full- and partial-thickness wounds treatment
EZ-Derm®	Aldehyde-crosslinked porcine dermal collagen	Full- and partial-thickness wounds treatment
Repliform®	Acellular human dermal allograft	Urological plastic surgery applications
Cymetra®	Micronized particulate acellular cadaveric dermal matrix	Wound filler in plastic surgery
Biobrane®	Porcine collagen chemically bound to silicone/nylon membrane	Temporary covering of partial-thickness burns and wounds
Hyalograft 3D®	Esterified hyaluronic acid matrix seeded with autologous fibroblasts	Full- and partial-thickness wounds treatment
Matriderm®	Bovine dermal collagen type I, III, V and elastin	Full- or partial-thickness wounds treatment
ICX-SKN®	Allogeneic fibroblasts set in a natural human collagen matrix	Phase II trial pending
Bilayer substitutes		
Integra®	Thin polysiloxane (silicone) layer; cross-linked bovine tendon collagen type I and shark glycosaminoglycan (chondroitin-6-sulfate)	Full- or partial-thickness wounds treatment
OrCel®	Human allogeneic neonatal keratinocytes on gel-coated non-porous side of sponge; bovine collagen sponge containing human allogeneic neonatal fibroblasts	Treat skin graft donor sites and mitten-hand surgery for epidermolysis bullosa
Apligraf®	Human allogeneic neonatal keratinocytes; bovine collagen type I containing human allogeneic neonatal fibroblasts	Venous and diabetic foot ulcers treatment
TissueTech® autograft system	Combination of Hyalograft 3D® and Laserskin®	Full- and partial-thickness burns and chronic ulcers treatment

1.5. The Role of Growth Factors in Wound Healing

As previously stated, regeneration is characterized by a constant change in the environment to which cells are exposed to (Metcalfe and Ferguson, 2007b). Thus, the regeneration of any type of tissue requires an interaction between different phenotypes of cells, local and systemic functioning mediators such as growth factors and hormones, and the ECM within which these events occur (Chen et al., 2006). Growth factors are proteins that induce a change in the cellular function by inducing proliferation or differentiation. They play a role in the modulation of tissue growth and development (Karakeçili et al., 2008) and bind to specific high-affinity receptors on the cell-surface to stimulate cell growth (Alemdaroglu et al., 2006). Exogenous application of growth factors has been extensively used for the treatment of chronic wounds, where growth factors are present in lower concentrations (Branski et al., 2006). Despite such clear rationale suggesting the probability of enhancing wound healing trajectories with topical growth factor application, clinical success has been limited when a single growth factor is applied. This is due to the fact that the application of a single growth factor only has a transient effect in the enhancement of wound healing (Branski et al., 2006).

Among the various growth factors involved in skin regeneration, EGF and VEGF play an important role in this process. VEGF is a multifunctional molecule with several important biological activities that depend on both the stage of development and physiological function of the organ in which it is expressed (Breen, 2007). VEGF has many beneficial functions involved in regulating physiological angiogenesis associated with exercise and metabolism, ovarian follicular development and function, and wound healing (Breen, 2007). It acts as an endothelial cell mitogen, chemotactic agent, induce vascular permeability, maintenance and protection of both vascular endothelial and non-endothelial cells in mature mammals (Bao et al., 2009; Breen, 2007). Compared with other angiogenic growth factors (e.g. bFGF and TGF-ß) VEGF is unique for its effects on multiple components of the wound-healing cascade; it promotes the closure of chronic wounds exhibiting hypoxia and compromised vascularity (Bao et al., 2009; Barrientos et al., 2008; Metcalfe and Ferguson, 2007a, b).

As previously described, VEGF is produced by many cell types that participate in wound healing mechanism, such as endothelial cells, fibroblasts, smooth muscle cells, platelets, neutrophils, and macrophages (Bao et al., 2009). The addition of VEGF alone or in combination with other growth factors may be important for the treatment of nonhealing wounds and other ischemic processes. It may also have a future role as adjunctive therapy to accelerate healing and prevent combinations in surgical revascularization, anastomoses and plastic surgeries (Bao et al., 2009).

EGF is a small polypeptide of 53 amino acid residues that is secreted by platelets, macrophages and fibroblasts. It acts in a paracrine fashion on keratinocytes (Alemdaroglu et al., 2006; Barrientos et al., 2008; Karakeçili et al., 2008). It has been implicated in wound healing and homeostasis in a number of tissues including colon, skin, mammary gland and

liver (Metcalfe and Ferguson, 2007b). It is also known to be present at high levels in saliva and may accelerate healing of skin lesions in animals when they lick their wounds (Metcalfe and Ferguson, 2007b). *In vivo* studies have shown that EGF is effective for the acceleration of epithelization in human and animal wounds. It stimulates the proliferation of keratinocytes in culture, and its topical administration accelerates dermal regeneration of partial thickness burns or split-thickness incisions *in vivo* (Alemdaroglu et al., 2006). It has been reported that repeated treatment with EGF increases the epithelial cell proliferation in a dose dependent manner, and accelerates the wound healing process, whereas a single EGF treatment has no noticeable effect on the wound-healing rate (Kwon et al., 2006). Therefore, EGF may still be useful to individuals with chronic wounds if delivered by a system, polymers, or electrospun nanofibers since such techniques maintain a continuous growth factor concentration, sustaining its presence in the wound and preventing its rapid degradation (Barrientos et al., 2008).

1.6. Hydrogels and Drug Delivery Systems

Several biological active molecules such as peptides, proteins (e.g. growth factors), oligonucleotides and genes, are easily degraded in the body fluids (Bhavsar et al., 2009); (Guse et al., 2006; Prabaharan and Mano, 2008). Usually, these compounds must be administrated several times in order to have the desired therapeutic effect. Drug delivery systems have been developed in order to allow a sustained and targeted release, decreasing the number of therapeutic doses administrated and also contributing to increase the efficacy of the therapy (Guse et al., 2006; Hiemstra et al., 2007; Kenawy et al., 2009; Kim et al., 2009; Reddy and Swarnalatha, 2010; Siepmann and Siepmann, 2008). The goal of an ideal drug delivery system is to deliver a drug to a precise site, in specific time and with a right release pattern. The traditional medical forms (tablets, injection solutions, etc.) provide drug delivery with peaks, often above the required dose (Figure 6). The constant drug level in blood or sustained drug release to avoid multiple doses and bypassing the hepatic “first-pass” metabolism are the main challenges for every delivery system (Stamatialis et al., 2008). The therapeutic time window can be applied for the tissue engineering based on drug delivery. To obtain specialized function in the body, normal tissues also require temporally specified stimulation during their development (Enoch and Leaper, 2008; Kim et al., 2009).

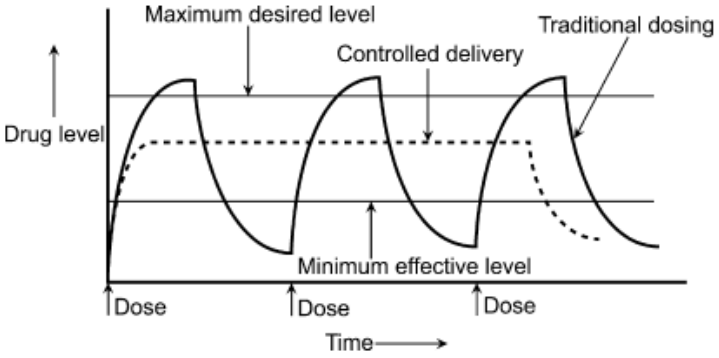

Figure 6 – Scheme of the therapeutic time window. The various cases; maximum, minimum, traditional dose and controlled delivery are indicated (adapted from (Stamatialis et al., 2008)).

As an extension of the pulsatile release system, a temporally programmed drug release system is an excellent solution to supply multiple drugs (Kim et al., 2009). Drug delivery systems can be categorized into two major groups: time-controlled systems and stimuli-induced release systems. In this last case the drug is released in response to internal/external stimuli such as changes in pH, temperature or glucose levels in blood, for example (Caldorera-Moore and Peppas, 2009; Hamidi et al., 2008). The drug can also be released at the site of action, through the functionalization of the system structure with specific ligands that are recognized by membrane receptors like integrins (Petrie and García, 2009).

The interest in hydrogels, three-dimensional polymeric networks capable of absorbed high amounts of water (Hamidi et al., 2008), has been growing after the establishment of the first synthetic hydrogels by Wichterle and Lim in 1954 (Lin and Metters, 2006; Wichterle and Lim, 1960). Since then, the growth of hydrogel technologies have increased in many fields (Lin and Metters, 2006) of tissue engineering and regenerative medicine such as diagnostics, cellular immobilization, separation of biomolecules or cells, and barrier materials to regulate biological adhesions (Hoare and Kohane, 2008).

The hydrogels affinity to absorb high amounts of water is attributed to the presence of hydrophilic groups such as –OH, -CONH-, -$CONH_2$-, and –SO_3H in polymers forming hydrogel structures. Because of these groups, the polymer is thus hydrated to different degrees (sometimes more than 90%wt) depending on the nature of the aqueous environment and polymer composition (Hamidi et al., 2008). However, the hydrogel can be formed from polymers with hydrophobic characteristics (e.g., poly(lactic acid) (PLA) or poly(lactide-co-glycolide) (PLGA)) which have limited water absorbing properties (< 5-10%) (Hamidi et al., 2008). Hydrogels can also be classified based on a variety of characteristics, such as the nature of side groups (neutral or ionic), mechanical and structural features (affine and phantom), method of preparation (homo- or co-polymer), physical structure (amorphous, semicrystalline, hydrogen bounded, supermolecular, and hydrocolloidal), and responsiveness

to physiologic environment stimuli (pH, ionic strength, temperature, electromagnetic radiation, and so on) (Hamidi et al., 2008). They can be prepared from natural or synthetic polymers. Although hydrogels made from natural polymers may show mechanically sub-optimal characteristics and may contain pathogens or evoke immune/inflammatory responses, they do offer several advantageous properties like biocompatibility, biodegradability, and biologically recognizable moieties that support cellular activities (Hamidi et al., 2008; Lin and Metters, 2006). On the other hand, synthetic polymers do not possess these inherent bioactive properties, but usually have well-defined structures that can be modified to yield tailorable degradability and functionality (Lin and Metters, 2006; Lo and Jiang, 2010).

The capacity of hydrogels to absorb high amounts of water and the physiochemical similarity of hydrogels to the native ECM, both compositionally (particularly in the case of carbohydrate-based hydrogels) and mechanically make them biocompatible. Furthermore, biodegradability or dissolution may be designed into hydrogels via enzymatic, hydrolytic, or environmental (e.g. pH, temperature, or electric field) pathways (Hoare and Kohane, 2008). They are also relatively deformable which make them suitable to adjust to the shape of the surface in which they are applied. Finally, the muco- or bioadhesive properties of hydrogels can be advantageous in their immobilization at the site of application or in their use on surfaces that are not horizontal (Hoare and Kohane, 2008). These suitable properties that resemble natural tissues, make hydrogels particularly attractive for micro and nanofabrication applications in tissue-engineering to produce delivery drugs systems and scaffolds (Figure 7) (Peppas et al., 2006).

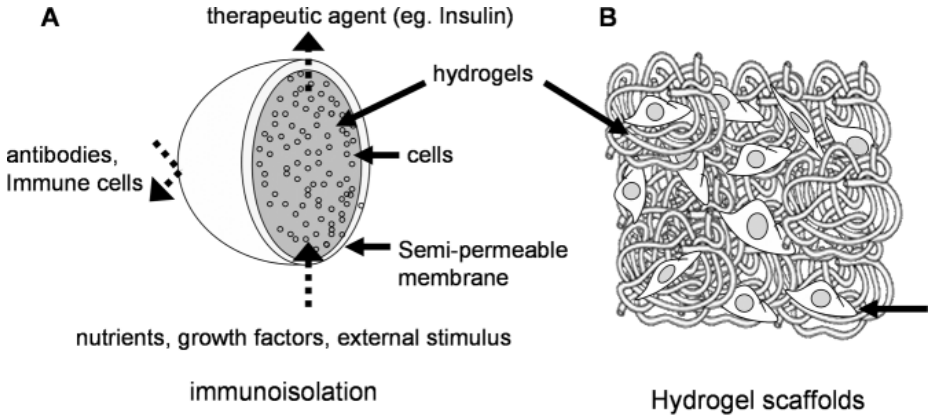

Figure 7 – Role of hydrogels in tissue engineering. Schematic diagram of the use of hydrogels in microencapsulation (A) and as a tissue-engineering scaffold (B) (adapted from (Peppas et al., 2006)).

Hydrogels also possess most of the desirable characteristics of an "ideal dressing" and they have been commonly used for wound healing since they can absorb the excess of wound exudates, protect the wound from secondary infection, leave no residue, be malleable and effectively promote the healing process by providing a moisturized wound healing environment (Anumolu et al., 2010; Boateng et al., 2008; Hamidi et al., 2008; Yang et al., 2010; Yoo and Kim, 2008). These materials are nonreactive with biological tissue, permeable

to metabolites, non-adherent and cool the surface of the wound, which may lead to a marked reduction in pain and therefore have high patient acceptability (Boateng et al., 2008). Because they are soothing and absorptive, hydrogels are especially valuable for partial-thickness wounds, such as superficial thermal burns, friction blisters, chemical peels, dermabrasion, facial resurfacing, and ulcers (Yoo and Kim, 2008).

Although, hydrogels have good physical properties that make them suitable to be used as drug delivery systems, the quantity of drug loaded into them may be limited, particularly in the case of hydrophobic drugs, and the high water content and large pores size of most hydrogels, often results in relatively rapid drug release profiles (Brandl et al., 2010; Hoare and Kohane, 2008). Fast release not only limits the efficacy of the applied drug delivery systems, but also carries the risk of causing harmful side-effects due to the exposure to high drug concentrations (Brandl et al., 2010). Each of these issues significantly restricts the practical use of hydrogel-based delivery therapies in the clinic (Hoare and Kohane, 2008).

To overcome these restrictions, different strategies have been explored to reduce the release rate of drug from hydrogels, such as the enhancement of the interactions between the drug and the hydrogel matrix and/or increase the diffusive barrier to drug release from the hydrogel (Hoare and Kohane, 2008). Microspheres, liposomes, multilayer hydrogels and other types of particle-based drug delivery vehicles have shown to be useful for long-term release. To do so, a lot of effort has been done to overcome the inherent pharmacological limitations of hydrogels by co-formulating particulate systems into the hydrogel matrix, as demonstrate in Figure 8 (Hoare and Kohane, 2008).

The use of these formulations brings some advantages such as: the increase of the biocompatibility in a particulate vehicle by "hiding" the microparticles within the hydrogel, prevent microparticle migration away from their target site *in vivo*, and the hydrogel phase may also change the kinetic protein release profile observed in microparticles by providing an additional diffusion barrier to drug release, moderating or eliminating the burst release typically observed with microparticles and extending the release of drugs (Hoare and Kohane, 2008).

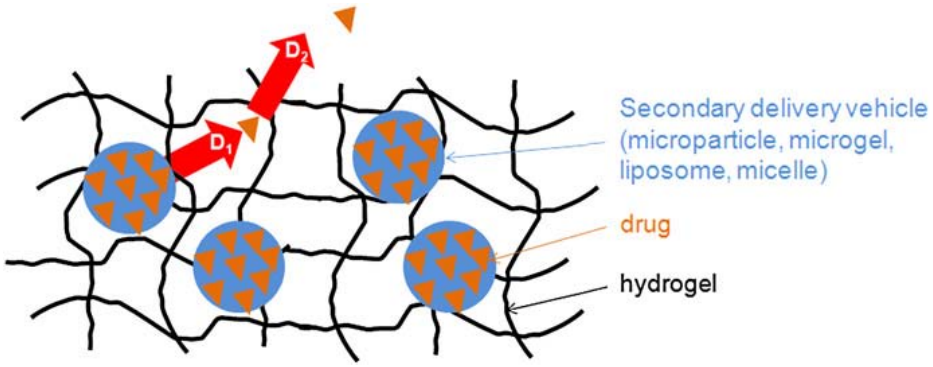

Figure 8 – Illustration of a composite hydrogel containing drug encapsulated in a secondary controlled release vehicle (e.g. microparticles, nanoparticles, microgels, lipossomas, micelles). D_1 and D_2 represent the diffusion coefficients of drug out the hydrogel (D_1 = release from secondary release vehicle; D_2 = diffusion through hydrogel) (adapted from (Hoare and Kohane, 2008)).

Micro- and nanotechnologies can offer new opportunities towards the development of better, intelligent medical devices that have the possibility to profoundly impact medical therapeutic techniques. Advances in the micro- and nano-fabrication methods have provided new means for the production of micro- and nano-devices for drug and gene delivery, tissue engineering, biosensors, and diagnostic systems (like protein and DNA microarrays) (Caldorera-Moore and Peppas, 2009).

The cells that built the human body are on the order of 100-1000μm, and their components have dimensions in the order of nanometers. Cell-cell interactions and cell-biomaterial interactions occur at the microscale range. Thus, creating devices that will interact with cells at the micro level will potentially avoid extreme damage of entire tissues or even organs, and reduce inflammatory response while better targeting and treating the problem (Caldorera-Moore and Peppas, 2009). In these systems, the drug is dissolved, entrapped, encapsulated or attached to a particle matrix and depending on the method used for preparation, nano- or microparticles (nano- or microspheres) or capsules can be obtained. Nano- or microcapsules are vesicular systems in which the drug is confined to a cavity surrounded by a boundary structure, e.g., polymeric, while nano- or microspheres are matrix spherical systems in which the drug is physically and uniformly dispersed (Figure 9) (Hamidi et al., 2008).

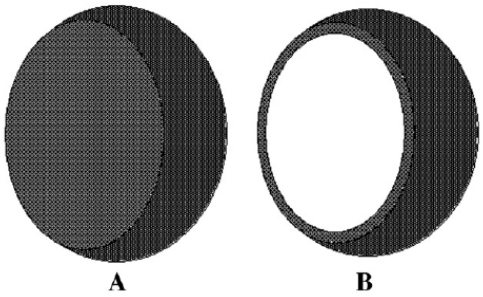

Figure 9 – Schematic representation of a nano- or micropshere (A) and a nano- or microcapsule (B). In nano- or microspheres the whole particle consists of a continuous polymer network. Nano- or microcapsules present a core-shell structure with a liquid core surrounded by a polymer shell (adapted from (Hamidi et al., 2008)).

Microsphere-based matrices have been widely used in skin repair. Recently, researchers have proved that chitosan scaffolds with FGF loaded in gelatin microparticles were effective in accelerating wound closure of pressure ulcers (Huang and Fu, 2010). Similarly, alginate beads-VEGF delivery system was used for both the improvement of wound healing and vascular tissue engineering (Huang and Fu, 2010). The use of a vehicle to deliver growth factors is very advantageous over direct administration of the growth factors, since these proteins rapidly diffuse from the target site and are enzymatically digested or deactivated. Thus, incorporating growth factors into appropriate vehicles allows a controlled release of these molecules at the target area over an extended period of time. Furthermore, the growth factor is protected against proteolysis for prolonged retention of activity *in vivo* (Huang and Fu, 2010).

Stratum corneum (SC), part of epidermis, represents the main physical barrier of the skin (10μm thick), so that for a substance permeating across the skin, diffusion through the SC is the rate limiting step (Prow et al., 2011; Stamatialis et al., 2008). Drugs can also potentially pass through the skin via hair follicles and sweat ducts (Figure 10). The rate of penetration through the SC controls the drug delivery, since drug transport through the deeper layers as well as through the vessel walls is much faster (Stamatialis et al., 2008).

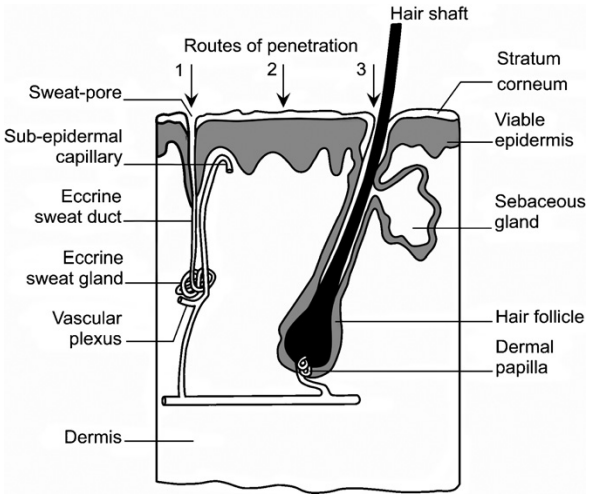

Figure 10 – Cross section of the human skin with the representation of the principal routes of drug penetration in the body (Stamatialis et al., 2008).

1.7. Mathematical Modeling of Drug Delivery

The application of mathematical modeling in drug delivery has become a field with enormous importance for academic and industrial activities. Computer simulations, in comparison with other scientific disciplines (e.g. aviation and aerospace), are likely to became an integral part of future research and development in pharmaceutical technology (Siepmann and Siepmann, 2008). Taking into account some important aspects like the type of administration, drug dose incorporated and drug release profile, mathematical predictions will allow for good estimates of the required constitution, geometry, dimensions and preparation procedure of the respective dosage forms. Thus, mathematical modeling in drug delivery allows the researchers to save time and to reduce costs since the number of experimental studies needed to develop a new and/or optimize an existing system can significantly be reduced (Siepmann and Siepmann, 2008). The use of a mathematical model in drug delivery systems began in 1961 with Professor Takeru Higuchi (Higuchi, 1960). Since then, several models have been proposed, including empirical/semi-empirical as well as mechanistic realistic ones. Empirical/semi-empirical models are purely descriptive and not based on real physical, chemical and/or biological phenomena, while mechanistic mathematical theories are based on real phenomena, such as diffusion, swelling, dissolution, erosion, precipitation and/or degradation. With these models the relative importance of

several processes that are involved (e.g. drug diffusion and polymer swelling) can be estimated (Siepmann and Siepmann, 2008).

The mathematical models that have been developed to predict the release of an biological active agent from a hydrogel device as a function of time are based on the rate-limiting step for controlled release and are categorized into three main sectors: diffusion-controlled, swelling-controlled and chemically-controlled (Lin and Metters, 2006). The first one is the most widely applicable mechanism for describing drug release from hydrogels. It uses Fick's law of diffusion with either constant or variable diffusion coefficients. When the diffusion of a drug is faster than the hydrogel swelling, swelling-controlled drug release occurs. To model this mechanism usually it is necessary to involve moving boundary conditions, where molecules are released at the interface of swollen and dry phases of the hydrogels. Finally, chemically-controlled release is used to describe molecule release determined by reactions that occur within a delivery matrix, such as cleavage of polymer chains via hydrolytic or enzymatic degradation, reversible or irreversible reactions that occur between the polymer network and the releasable drug (Lin and Metters, 2006).

Chapter 2
Materials and Methods

2. Materials and Methods

2.1. Materials

2.1.1. Drug delivery systems produced with alginate and chitosan

Alginate and chitosan are two natural polysaccharides extensively used in the production of drug delivery systems. Alginic acid and it's salts [Ca, Mg, Na & K] are derived from brown algae and belong to a family of polysaccharides composed of α-L-guluronic acid (G) and ß-D-mannuronic acid (M) residues, arranged in homopolymeric blocks of each type (MM, GG) and heteropolymeric blocks (MG) (Sachan et al., 2009; Takka and Gürel, 2010). In Figure 11 it is possible to observe the chemical structure of alginic acid sodium salt used during the development of this thesis workplan. This polymer can be reversibly gelled in aqueous solutions when mixed with divalent cations like Ca^{2+}, Mg^{2+}, Ba^{2+} (Draget et al., 1997; Uludag et al., 2000). It has been used for the production of drug delivery systems to deliver drugs, stem cells and other human cells and for tissue engineering applications because of its biocompatibility, non-immunogenicity and relatively low cost (Davidovich-Pinhas et al., 2009; Gadad et al., 2009; Heile et al., 2009; Orive et al., 2003). It has also been widely used in wound dressings, as an injectable delivery vehicle of cells and proteins, including various growth factors (Huang and Fu, 2010).

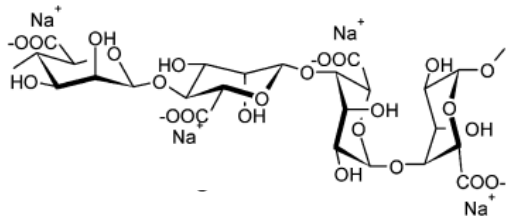

Figure 11 – Chemical structure of sodium alginate (adapted from (Mazumder et al., 2009))

Chitosan is a deacetylated derivative of chitin, a natural polysaccharide found primarily in the exoskeletons of arthropods and some fungi (Gaspar et al., 2011; Ribeiro et al., 2009). It is a linear polysaccharide comprising copolymers of glucosamine and N-acetyl glucosamine linked by ß (1-4) glycosidic bonds (Figure 12) (Ribeiro et al., 2009). It has been used for many biomedical applications, including wound dressing, production of drug delivery systems, and tissue engineering applications, due to its biocompatibility, low toxicity, structural similarity to natural GAGs, and degradation by enzymes such as chitosanase and lysozyme (Huang and Fu, 2010). Chitosan microparticles can be produced by ionic cross-linking between the positive charges of the amino groups of chitosan and negative charges of tripolyphosphate ions (TPP) (Luangtana-anan et al., 2010). In addition, chitosan was found to enhance blood coagulation and accelerates the wound healing; thus, it can act as an ideal wound dressing because of its positive-charge, film-forming capacity, mild gelation characteristics and strong tissue-adhesive property (Huang and Fu, 2010).

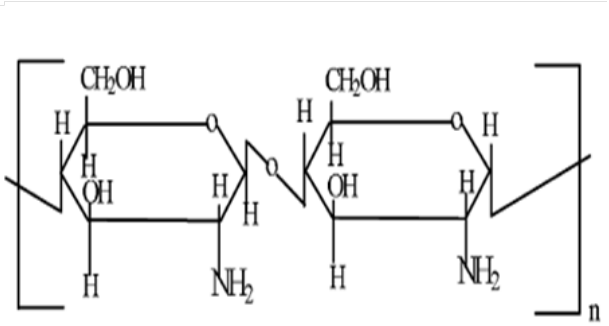

Figure 12 – Chemical structure of chitosan (adapted from (Kumar and Majeti, 2000)).

2.1.2. Dextran as a wound dressing

Dextran, a natural glucose-containing polysaccharide, is a very versatile starting polymer for hydrogel synthesis (Maia et al., 2009). It is a polysaccharide composed of straight chain consists of α-1,6 glycosidic linkages between glucose molecules, while branches begin from α-1,4 linkages and there are three hydroxyl groups per anhydroglucose unit, which makes it very soluble in water. These hydroxyl groups (Figure 13) can be easily modified and ready to form hydrogel by either direct attachment or through a crosslinker (Chen et al., 2006; Lo and Jiang, 2010). It is biocompatible and can be degraded through the action of dextranases in various organs in the human body, including liver, spleen, kidney and colon (Maia et al., 2009).

The oxidation of dextran by sodium periodate is an easy and well-known way to functionalize dextran with aldehyde moieties. These aldehyde moieties in conjugation with N-nucleophiles, have been tested on the synthesis of pro-drugs, as a spacer in enzyme immobilization or for growth factor controlled release (Huang and Fu, 2010; Maia et al., 2005; Maia et al., 2009). Dextran hydrogels have also been used for stabilizing and delivering FGFs for tissue healing (Huang and Berkland, 2009).

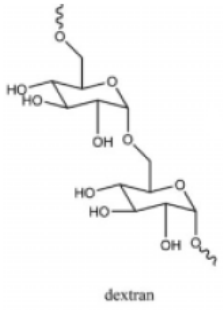

Figure 13 – Dextran molecular structure (adapted from (Lo and Jiang, 2010)).

2.2. Methods

2.2.1. *In vitro* assays

The increasing use of biomaterials in clinical medicine to augment or replace failing organ function has heightened the need to apply different assays to study the safety and efficacy of new medical devices (Kirkpatrick et al., 2005; Kumari et al., 2010)..

The materials to be implanted in the human body must be sterile to avoid subsequent infection that can lead to a significant illness or possibly death (Omokanwaye et al., 2010). Several sterilization methods have been used such as autoclaving, UV irradiation, ethanol immersion and gamma sterilization (Zhao et al., 2010). These methods have been reported to impact the surface properties of biomaterials consequently affecting cell behavior. Some studies reported that UV and ethanol sterilization give rise to a higher surface free energy inducing higher initial cell adhesion and proliferation compared to autoclaving (Zhao et al., 2010). On the other hand, gamma irradiation, due to high levels of energy, is one of the most adequate methods to sterilize materials that would be incorporated into human body (Hasiwa et al., 2008; Zuleta et al., 2010). However, gamma sterilization approach is difficult, expensive and can induce unfavorable changes on materials (Hasiwa et al., 2008). Thus, an effective sterilization method should lead to a balance between the required sterility level and minimum detrimental effect on the properties of the biomaterial, while being cost-effective, simple and readily available (Omokanwaye et al., 2010).

The biocompatibility of the different materials developed can be estimated through animal experimentation and *in vitro* techniques (Kirkpatrick et al., 2005). The cytotoxicity of a material should, firstly, be evaluated through *in vitro* studies. Cell cultures offers an excellent method to screen potential biomaterials, reducing the number of animal needed, time and costs (Kirkpatrick et al., 2005; Kumari et al., 2010). However, it must never be forgotten that cell culture represents a reduction in the complexity of the entire organism generally to a single cell type grown as a unique sheet of cells (monolayer) (Kirkpatrick et al., 2005). Cell viability may be evaluated using a variety of methods, depending on the cell or tissue type, and choosing the best assay can became a difficult task (Capasso et al., 2003; Promega, 2008). One of the things that should be taken into account when choosing a method is what information we want to evaluate at the end of a treatment period. The different assays are available to measure a variety of different markers that indicate the number of dead cells (cytotoxicity assay), the number of live cells (viability assay), the total number of cells or the mechanism of cell dead (e.g. apoptosis) (Promega, 2008). Several methods are used to determine the cytotoxic effects of a test compound and they are based either on colorimetric methods or on microscopy analysis (Capasso et al., 2003; Ganapathy-Kanniappan et al., 2010). These last methods require the use of dyes (e.g. tripan blue), which are selectively incorporated by living cells, while colorimetric ones are based on color development of the growth medium after reaction of cell metabolites with chemical agents of

the assay solution (Capasso et al., 2003). The most commonly used colorimetric methods are adenosine triphosphate (ATP) depletion, lactate dehydrogenase (LDH) release, 3-(4,5-dimethylthiazol-2-yl)-2,5-diphenyltetrazolium bromide (MTT) and 3-(4,5-dimethylthiazol-2-yl)-2,5-diphenyl-2H-tetrazolium bromide (MTS) assays (Ganapathy-Kanniappan et al., 2010).

In this research work, two of these colorimetric assays were used, MTS and LDH release assays. The information gathered through the use of both methods is the opposite: the MTS assay indicates the percentage of viable cells, while the LDH assay indicates the percentage of dead cells (Capasso et al., 2003; Marques et al., 2002). The tetrazolium-based MTS assay is a commonly used tool in cytotoxicity evaluation due to its simplicity, speed, reproducibility, and compatibility with multi-well formats (Ganapathy-Kanniappan et al., 2010). The MTS is reduced by a mitochondrial enzyme (succinate dehydrogenase) present in viable cells into a colored formazan product (Figure 14), with maximal absorbance at 490nm. The quantity of formazan product is directly proportional to the number of living cells in the sample (Capasso et al., 2003; Ganapathy-Kanniappan et al., 2010).

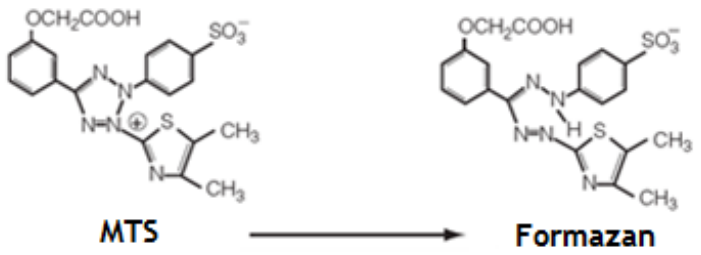

Figure 14 – Reduction of MTS to formazan (adapted from (Promega, 2008))

LDH is an oxidative enzyme which converts lactate into pyruvate (Figure 15) during glycolisis (Watanabe et al., 1995). This cytosolic enzyme has been used for many years to measure the loss of cellular membrane integrity. Thus, indirect measurement of LDH activity, which is present in the cytoplasm of intact cells, can occur only if the cells are lysed. LDH activity is directly proportional to the number of damaged cells (Marques et al., 2002).

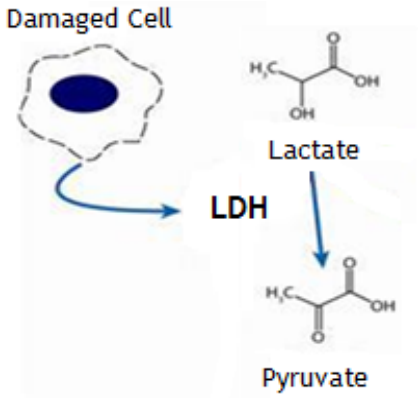

Figure 15 – Schematic representation of LDH activity (adapted from (Promega, 2008)).

2.2.2. *In vivo* assays

As previously stated, *in vitro* assays allow to evaluate the behavior of cells in contact with biomaterials developed. However, *in vitro* testing cannot replace the data obtained through the study of a system *in vivo* (Ratner, 2004). Local responses triggered by biomaterials can be evaluated through various qualitative and quantitative methods depending on the type of study such as: histological, histochemical and immunohistochemical tests, microscopic analysis like transmission electron (TEM) and scanning electron (SEM) microscopies for tests based on observation, mechanical tests, and methods for irritation and hypersensitivity (Kiyozumi et al., 2007; Ratner, 2004).

Histological analysis and visualization (e.g. TEM and SEM) techniques are used to determine the morphological changes of tissues, cells and biomaterials (Kiyozumi et al., 2007). Through histological analysis it is possible to make a qualitative assessment of the cell type, number of components of the ECM and the thickness of the fibrous layer around the biomaterial (Ratner, 2004). In a different way, through immunohistochemistry it is also possible to recognize specifically the cells and components of ECM around the biomaterial using specific antibodies for each component which will be identified (Ratner, 2004). Finally, the irritation tests are based on standard 10993-10, 2002 by International Standard Organization (ISO) and show the reaction of the animal's body when in contact with chemicals released from biomaterials. Can be viewed at any skin, intestinal mucosa and eye irritation or hypersensitivity (ISO, 2003; Kirkpatrick et al., 2005).

In vitro and *in vivo* assays are performed in order to evaluate if the biomaterials satisfy the international regulamentations defined by Food and Drug Administration (FDA) and ISO guidelines, in order to be applied in humans (Park and Lakes, 2007).

Chapter 3

Modeling of Drug Release from Polymeric Systems

3. Modeling of Drug Release from Polymeric Systems for Biomedical Applications

3.1. Abstract

In recent years different hydrogel-based drug delivery systems have been developed to satisfy the ever-increasing needs in the medical fields. Nano and micro fabrication methods have been used to prepare carriers that protect biological active compounds from enzymatic degradation in the human body and allow a sustained and targeted drug release.

The present study describes the production and characterization of different drug carriers: alginate and chitosan microparticles and a dextran hydrogel loaded with the two types of microparticles. A mathematical model based on the theory of hindered transport of large solutes in hydrogels and the contribution of polymer swelling to mass transfer was developed for theoretically describing the process of protein release.

Swelling and *in vitro* release studies of a model protein (bovine serum albumin) were performed for the different carriers studied. All the experimental results were interpreted with the aid of the developed model. The cytotoxic profile of the carriers was also evaluated using human fibroblast cells as model. The results obtained revealed that cells adhered and proliferated in the presence of the drug delivery carriers, which is fundamental for its application in the biomedical field.

Keywords: biocompatibility, controlled release, drug delivery systems, mathematical modeling, mass transfer mechanism, swelling studies.

3.2. Introduction

The human body has different fluids that are hostile environments for biologically active molecules (Bhavsar et al., 2009). Different systems have been developed in order to protect all unstable biological active compounds, such as peptides, proteins, oligonucleotides, and genes, from degradation in the body fluids (Guse et al., 2006; Prabaharan and Mano, 2008). Proteins usually have a short half-life inside organisms and, therefore, need to be administrated several times in order to have the desired therapeutic effect (Guse et al., 2006; Hiemstra et al., 2007; Siepmann et al., 2008). To overcome these limitations, the production of drug delivery systems that allow a sustained and targeted release is fundamental to decrease the number of therapeutic doses administrated and also contribute to increase the efficacy of the therapy (Guse et al., 2006; Hiemstra et al., 2007; Kenawy et al., 2009; Kim et al., 2009; Reddy and Swarnalatha, 2010; Siepmann et al., 2008). Controlled drug delivery technology is one of the multiple areas that integrates the human health care sciences (Prabaharan and Mano, 2008).

Hydrogels, are three-dimensional polymeric networks capable of absorbing high amounts of water (Hamidi et al., 2008). These systems have been widely applied for the controlled drug delivery of macromolecules, including therapeutic proteins and nucleic acids (Brandl et al., 2010; Lin and Metters, 2006). However, despite of their attractive physical properties (such as porosity, deformability and muco- or bioadhesive characteristics), the quantity of drug loaded into hydrogels may be limited and the high water content of most hydrogels often results in relatively rapid drug release profiles (Brandl et al., 2010; Hoare and Kohane, 2008). Fast release not only limits the efficacy of the applied drug delivery systems, but also carries the risk of provoking harmful side-effects due to the exposure to high drug concentrations (Brandl et al., 2010).

Natural or synthetic polymers, lipids, surfactants and dendrimers have also been employed to produce different nano and micro drug carriers (Acharya et al., 2010). Among them, polysaccharides have attracted great interest as a result of their outstanding physical and biological properties (Patel et al., 2010). These polymeric carriers can increase the bioavailability and the percentage of drug delivery to specific target cell by the functionalization of the polymer with specific ligands that are recognized by membrane receptors like integrins (Petrie and García, 2009). Thus, the drug is released only at the site of action, in response to internal/external stimuli such as changes in pH, temperature or glucose levels in blood, for example (Avgoustakis, 2009; Reddy and Swarnalatha, 2010). Several methods, using polymer templates, have been developed to prepare homogenous particles such as optically encoded microparticles or mesoporous silicon particles (Acharya et al., 2010).

In this study we produced chitosan and alginate microparticles that were incorporated into a dextran hydrogel (Maia et al., 2005; Maia et al., 2009). Chitosan and alginate are attractting the attention of different researchers worldwide since they present characteristics like biocompatibility, biodegradability, pH sensitivity, and mucoadhesive property, that are fundamental for their application as drug carriers (Guse et al., 2006; Siepmann et al., 2008; Takka and Gürel, 2010; Yu et al., 2009; Yu et al., 2010; Zolnik and Burgess, 2008). Dextran, a natural glucose-containing polysaccharide, is a very versatile starting polymer for hydrogel synthesis (Maia et al., 2009).

Mathematical modeling for simulate the drug release from carriers requires a fundamental understanding of the processes involved and can be used to decrease the number of experimental studies required for carrier development, thereby reducing costs and saving time (Siepmann et al., 2008; Siepmann and Siepmann, 2008).

The main goals of this research work were to develop a mass transfer model of a generic protein from the inside of a hydrogel to the outside, when the hydrogel undergoes swelling and apply the developed model to interpret experimental protein release profiles from alginate and chitosan microparticles. The theory of hindered transport of large spherical solutes in hydrogels (Phillips, 2000) is used here to estimate the protein diffusion coefficient inside the particles, under dynamic conditions. The model also considers the occurrence of

protein partition between the inside and the outside of the particles, then, the protein is transferred from the surface of the particles to the bulk of the outside solution. Depending on the type of polymer that constitutes the hydrogel, previous theories consider that swelling may affect the rate of drug delivery by decreasing it due to the increase of the length of the diffusion pathways, or by increasing it, in those cases where the effect of enhanced mobility is dominant (Siepmann et al., 2008). Here, we propose that, besides these two effects, swelling may also contribute to decrease the rate of protein transfer due to the uptake of outside solution into the particle that swells or, in the case of shrinking (*i.e.*, negative swelling) to increase the rate of protein transfer as a result of solution release from the inside of the particles. The model was then extended to the case of protein transfer mediated by a second hydrogel, such as that of modified dextran, during the process of protein release. The mathematical model developed here is of general applicability to similar drug delivery systems produced using other materials and other solutes than proteins, provided that these solutes are nearly spherical.

3.3. Materials

Chitosan (medium molecular weight), alginic acid sodium salt, adipic acid dihydrazide (AAD), sodium periodate, diethylene glycol, bovine serum albumin (BSA), calcium chloride ($CaCl_2$), TPP, phosphate-buffered saline (PBS), dialysis membranes (MWCO $\approx$ 12.000 Da), amphotericin B, Dulbecco's modified Eagle's medium (DMEM-F12), L-glutamine, MTS, penicillin G, streptomycin, trypsin and ethylenediaminetetraacetic acid (EDTA) were purchased from Sigma-Aldrich (Portugal). Dextran (Dextran T500; Mw: 500000 Da) was purchased from Pharmacia LKB, Sweden. Pierce® BCA protein assay reagent A and B were purchased from Thermo Scientific (Portugal). Tris Base was purchased from Fisher Scientific (Portugal). Human Fibroblast Cells (Normal Human Dermal Fibroblasts adult, criopreserved cells) were purchased from PromoCell (Spain). Fetal bovine serum (FBS) was purchased from Biochrom AG (Germany).

3.4. Methods

3.4.1. Alginate and chitosan microparticles preparation

The alginate microparticles were prepared by internal gelation technique, accordingly to a procedure previously described in the literature (Li et al., 2009; Yu et al., 2008). Initially, sodium alginate was dissolved in milli-Q water. Then BSA (2mg/mL) was added to this solution. The moisture was stirred during 5 minutes to ensure a complete mixing of the protein in the solution. The gelation medium was prepared by dissolving $CaCl_2$ in distilled water. Finally, 20mL of sodium alginate solution was loaded into a syringe and, using a syringe pump (KdScientific, KDS-100, Sigma) at a rate of 100 mL/h, the solution was extruded through a needle, with an internal diameter of 0.45mm, into a 100mL of the gelation

medium, under magnetic stirring. The microparticles formed were then washed with distilled water. Subsequently, chitosan microparticles were prepared by the same technique with negatively charged TPP ions. Chitosan solution was prepared by dissolving chitosan in an acetic acid solution (Grech et al., 2010). BSA-loaded microparticles were obtained by the addition of BSA to the chitosan solution at a concentration of 5mg/mL. Then, the microparticles were formed by drop-wise 20mL of chitosan solution into a 100mL of TPP solution, using the syringe pump at the same rate previously described. The microparticles were stirred for 5 minutes and washed with distilled water prior to further use (Luangtana-anan et al., 2010).

3.4.2. Dextran hydrogel synthesis

An aqueous solution of dextran was oxidized with sodium periodate solution at room temperature, accordingly to a procedure previously described in the literature (Maia et al., 2009). The reaction was stopped after 4 h, adding diethylene glycol. The resulting solution was dialyzed for 3 days against water, using a dialysis membrane and then lyophilized during 72 h (ScanVac CoolSafe Freeze Drying, LaboGene™, Denmark). Finally, the hydrogel was prepared by dissolving the oxidized dextran (DexOx) in PBS and mixed with AAD solutions (Maia et al., 2005; Maia et al., 2009). Microparticles loaded with BSA were added to DexOx before its reticulation with AAD.

3.4.3. Determination of the encapsulation efficiency

During microparticles preparation, samples of $CaCl_2$ and TPP solution were collected and the protein content was determined via BCA method on a UV-VIS Spectrophotometer (UV-1700 PharmaSpec, Shimadzu) at 570nm. The encapsulation efficiency was determined through the following equation (1) (Yu et al., 2009; Yu et al., 2008):

$$Encapsulation\ Efficiency\ (\%) = \frac{Protein\ fed - Protein\ loss}{Protein\ fed} \times 100\% \qquad \text{Eq. (1)}$$

3.4.4. *In vitro* protein release study

Protein loaded microparticles (100 microparticles/test tube) were immersed in 2mL of Tris buffer (pH 5 and 7.4). The test tubes with microparticles were immersed in a shaking water bath at 37ºC. At specific times, the supernatant was completely removed and replaced by 2mL of fresh buffer solution (13 measurements were done in the first 10 hours and then 1 measurement was done every 12h, until 82 hours). The concentration of protein release was determined using BCA method, as described earlier in the text (Hongmei et al., 2009; Liu et al., 2008; Yu et al., 2008). The same procedure was used to determine the amount of protein released (2) from the microparticles incorporated into the hydrogel.

$$R(\%) = \frac{M_t}{M_\infty} \times 100\% \quad \text{Eq. (2)}$$

where M_t is the amount of protein released from the microparticles at time t and M_∞ is the amount of protein pre-loaded in microparticles.

3.4.5. Swelling studies

The swelling properties of microparticles were characterized in Tris buffer at pH 5 and pH 7.4. Microparticles (300mg) were placed in a test tube containing 2mL of swelling solution (Tris buffer) and allowed to swell at 37ºC. At predetermined intervals, the swollen microparticles were removed and weighed. The wet weight of the swollen microparticles was determined by blotting them with filter paper to remove surface moisture, immediately followed by weighing on an electronic balance, and reimmersed into the swelling media. The same operation continues until the weights of the swollen microparticles were constant (Anal and Stevens, 2005; El-Sherbiny et al., 2010; Li et al., 2009). The swelling degree was determined as follows, see equation 3:

$$SW(\%) = \frac{Wt - Wo}{Wo} \times 100\% \quad \text{Eq. (3)}$$

where W_t is the final weight of microparticles and W_0 is the initial weight microparticles.

3.4.6. Scanning electron microscopy analysis

The morphology of microparticles was characterized by SEM. Alginate and chitosan microparticles were air-dried overnight and then mounted on an aluminium board using a double-side adhesive tape and covered with gold using an Emitech K550 (London, England) sputter coater. The samples were then analyzed using a Hitachi S-2700 (Tokyo, Japan) scanning electron microscope operated at an accelerating voltage of 20 kV and at various amplifications (Gaspar et al., 2011; Ribeiro et al., 2009; Takka and Gürel, 2010; Yu et al., 2008).

3.4.7. Proliferation of human fibroblast cells in the presence of the different drug carriers

Human fibroblast cells were seeded in T-flasks of 25 cm^3 with 6mL of DMEM-F12 supplemented with heat-inactivated FBS (10% v/v) and 1% antibiotic/antimycotic solution. After the cells reached confluence, they were subcultivated by a 3-5 minutes incubation in 0.18% trypsin (1:250) and 5mM EDTA. Then cells were centrifuged, resuspended in culture

medium and seeded in T-flasks of 75 cm^3. Hereafter, cells were kept in culture at 37°C in a 5% CO_2 humidified atmosphere inside an incubator (Maia et al., 2009; Ribeiro et al., 2009).

To evaluate cell behavior in the presence of the microparticles and the hydrogel herein produced, human fibroblast cells were seeded with microparticles and dextran in 96-well plates at a density of $5x10^4$ cells/well, for 24 hours. Before cell seeding, plates and the materials were sterilized by UV irradiation for 30 minutes (Ribeiro et al., 2009). Cell growth was monitored using an Olympus CX41 inverted light microscope (Tokyo, Japan) equipped with an Olympus SP-500 UZ digital camera.

3.4.8. Characterization of the cytotoxic profile of the carriers

To evaluate the cytotoxicity of the carriers, human fibroblast cells, at a density of $5x10^4$ cells/well, were seeded in a 96-well plate with microparticles and dextran hydrogel with and without microparticles, and cultured with DMEM-F12 at 37°C, under a 5% CO_2 humidified atmosphere. The plates with materials were UV irradiated for 30 minutes, before cell seeding. After an incubation of 24 hours, the mitochondrial redox activity of the viable cells was assessed through the reduction of the MTS into a water-soluble brown formazan product. The medium of each well was then removed and replaced with a mixture of 100µL of fresh culture medium and 20µL of MTS/phenazine methosulfate (PMS) reagent solution. The cells were incubated for 4 hours at 37°C, under a 5% CO_2 humidified atmosphere. The absorbance was measured at 492 nm using a microplate reader (Sanofi, Diagnostics Pauster).

Wells containing cells in the culture medium without materials were used as negative control. Ethanol (EtOH) 96% was added to wells containing cells as a positive control (Palmeira-de-Oliveira et al., 2010; Ribeiro et al., 2009).

3.4.9. Statistical analysis

Statistical analysis of cell viability results was performed using one-way analysis of variance (ANOVA) with the Dunnet's post hoc test. A value of $p<0.05$ was considered statistically significant (Ribeiro et al., 2009). Results of cells in the presence of different carriers were compared with negative and positive controls.

3.5. Model Development and Theoretical Simulations

The process of BSA release from microparticles is modeled here by considering that the solute (protein) diffuses from the inside of the particles, which are spherical, to the solution, where its diffusion coefficient is considerably higher than inside the particles. In the proposed model hindered diffusion of the solute is assumed to occur inside the particles due to hydrodynamic and steric effects that depend on the hydrogel structure and solute size. In order to estimate solute diffusion coefficients inside the hydrogels it is used here the approach proposed by Phillips *et. al.* (2000), in which it is assumed that the hydrogel is a

liquid-filled medium with randomly oriented cylindrical polymer fibers. The radii of the fibers, r_f, are of the same order of magnitude as the polymer molecular chains. Using this approach, the diffusion coefficient inside the hydrogel, D, can be estimated from the corresponding values in free solution, D_0, corrected according to the following relationship (Phillips, 2000):

$$\frac{D}{D_0} = e^{-0.84 f^{1.09}} e^{-a\phi^b} \qquad \text{Eq. (4)}$$

where ϕ is the volume fraction of the polymer that constitutes the particles and f a parameter which is defined as:

$$f = \phi\left(1+\frac{r_s}{r_f}\right)^2 \qquad \text{Eq. (5)}$$

where r_s is the hydrodynamic radius of the solute. Parameters a and b only depend on the ratio $\lambda = r_f / r_s$ and are given by:

$$a = 3.727 - 2.460\,\lambda + 0.822\,\lambda^2 \qquad \text{Eq. (6)}$$

$$b = 0.358 - 0.366\,\lambda - 0.0939\,\lambda^2 \qquad \text{Eq. (7)}$$

As it can be seen from these equations, for estimating D it is therefore only required the knowledge of r_f and ϕ, apart from D_0.

Equilibrium of solute distribution between the particle and the outside solution at the interface particle/solution should play a key role in the process of protein release if significant interactions occur between the solute and the particle's polymer. The ratio between the solute concentrations inside and outside the particles is defined here as a partition coefficient, Φ, a quantity that can be experimentally determined.

Polymer swelling during protein release should be also considered in the model. In the case of particles that continuously increase their volume, there will be a continuous uptake of the surrounding solution into the particle and in the case of a particle that shrinks, the solution inside the particles is released from the particle to the outside (see Figure 16). The possible occurrence of any one of these processes may contribute significantly to protein transfer. Apart from these effects, polymer swelling also affects the protein diffusion coefficient, according to equation (4) by changing the value of ϕ and it has the effect of decreasing the concentration gradients inside the particle due to the increase of the particle radius.

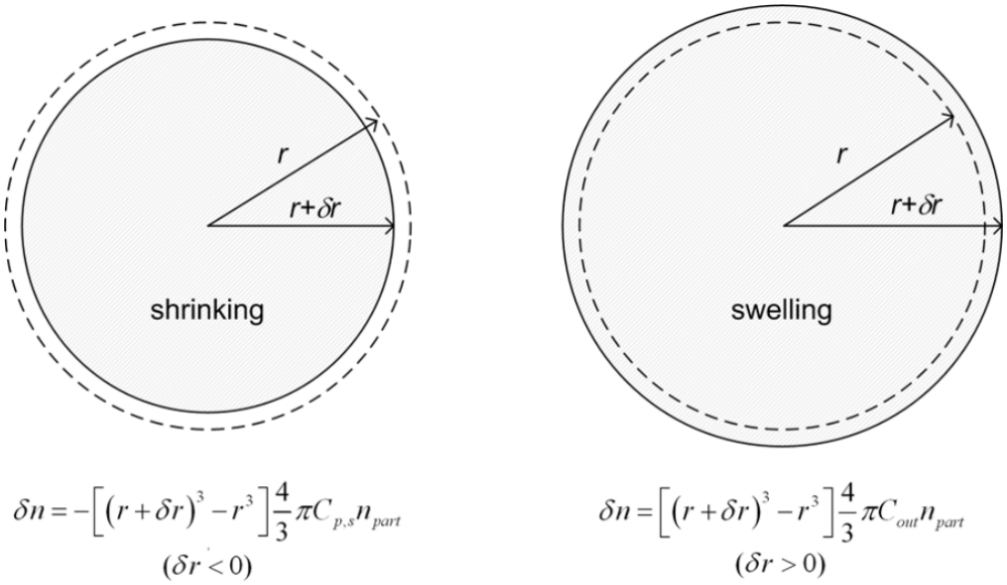

Figure 16 - Mechanism of protein transfer from the particles to the outside (in the case of shrinking) and from the outside solution into the particles (in the case of swelling). δn indicates the number of moles of protein transferred to or from the solution, in each case, for the time increment used in the simulations, δt. $C_{p,s}$ is the protein concentration at the particle's surface and C_{out} the concentration in the outside solution. δr is the change in the particle radius between simulations times t and $t+\delta t$.

Finally, it is also necessary to consider the mass transfer process in the surrounding solution, which is conventionally modeled by defining a mass transfer coefficient, which relates the concentration gradient from the particle's surfaces to the bulk of the solution with the solute molar flux:

$$J = k_m(C_m - C_{out}) \qquad \text{Eq. (8)}$$

where k_m is the mass transfer coefficient, C_m is the concentration near the particle's surface and C_{out} the concentration in the bulk of the outside solution, which was continuously stirred in the performed experiments.

Calculations were carried out using a *Matlab* routine designed for the purpose. It was assumed that the polymer volumetric fraction, ϕ, has an initial value, ϕ_0, and continuously changes in time, according to swelling data experimentally obtained. Fiber radii, r_f, for both alginate and chitosan were obtained from the literature (Morris et al., 2009; Phillips, 2000). From these two parameters D was estimated along the time using equation (4). Other parameters required for the calculations are the initial particle radius, $r_{part,0}$, the initial total volume of particles, $V_{part,0}$, the initial volume of the solution outside the particles, V_0 and the sampling times. According to the experimental method used in this work, the solution outside the particles was removed and replaced by a fresh buffer solution of volume V_0, at each sampling time. This procedure, of course strongly affects the mass transfer process, since this periodic replacement acts as a powerful driving force. An arbitrary value was considered for the initial solute concentration inside the particles, C_0, which is not required to be known if

one is only interested in estimating the percentage of protein release. The concentration in the solution outside the particles was considered to be 0 immediately after each replacement.

3.6. Results and Discussion

3.6.1. Morphology and optical properties of the carriers

Macroscopic images of the microparticles are shown in Figure 17. The microparticles produced presented spherical shape and the mean diameters of the alginate and chitosan microparticles were about 2mm and 1.5mm, respectively. Compared with the alginate microparticles prepared by Yu and co-workers (2008), the microparticles herein produced were similar in shape and morphology, however, they had a lower diameter which may result from the use of a syringe-pump in the production process (Yu et al., 2008). This system not only reduced the size of microparticles, but also allowed obtaining carriers with similar geometry. Chitosan microparticles had a similar diameter to those obtained by Grech *et al* (2010) (Grech et al., 2010).

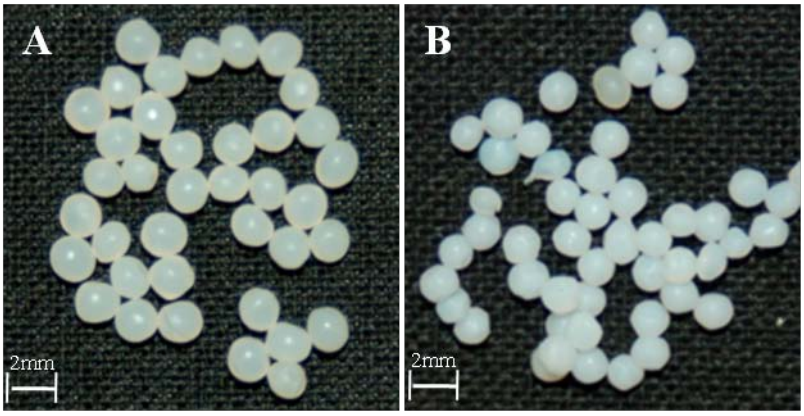

Figure 17 - Images of alginate (A) and chitosan (B) microparticles.

The diameter of both microparticles can be reduced by air-drying. Figures 18A and B shows SEM images of the microparticles herein produced. An average diameter of 905µm for alginate microparticles and 759µm for chitosan microparticles can be determined from the SEM images. Alginate and chitosan carriers produced were approximately spherical (Figures 18A and B) with a slightly wrinkled surface (Figures 18C and D). As previously reported in other studies, their surface properties result from water loss during the air-drying process (Lee et al., 2004). Usually, accordingly to what is described in the literature, the chitosan microparticles have a smoother surface compared to that of alginate microparticles, which usually show a more irregular and rough surface (Ko et al., 2002; Yu et al., 2008).

The encapsulation efficiency of BSA in alginate and chitosan microparticles was estimated to be approximately 81.3% and 60.7%, respectively. Such results can be explained by the method used to prepare chitosan microparticles, and also by the obtained result

discussed in section 3.6.3 that shows that the volumetric fraction of the polymer is smaller in the case of alginate, therefore, the diffusion into the interior of the carrier is faster.

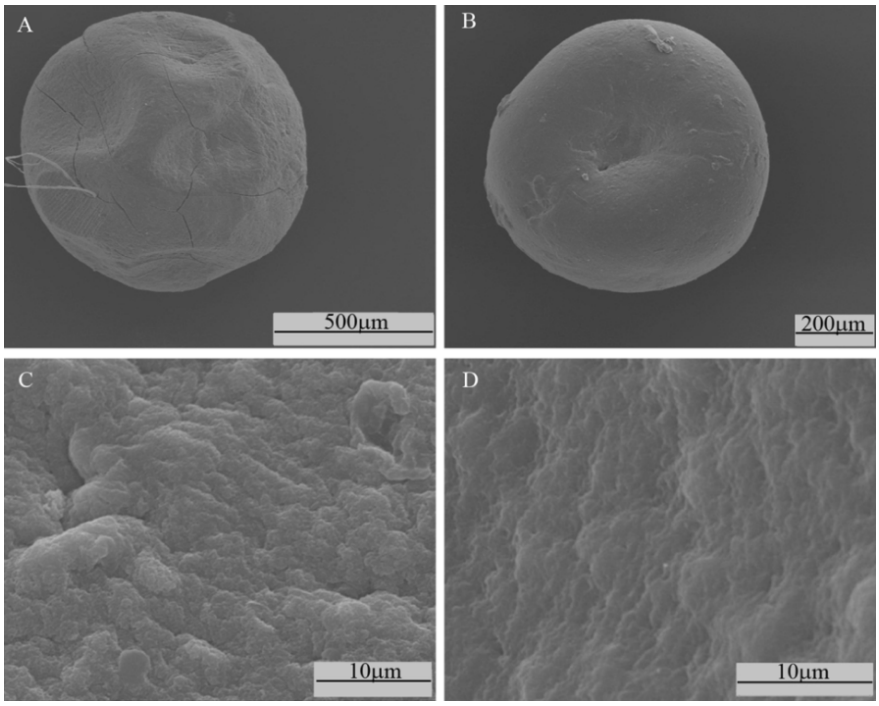

Figure 18 - SEM images of alginate microparticles 80x (A), chitosan microparticles 100x (B), surface of alginate microparticles 2000x (C) and surface of chitosan microparticles 2000x (D).

To overcome this limitation and to obtain microparticles with similar amounts of BSA, the amount of protein added to chitosan microparticles was higher than that used for alginate microparticles produced. However, the quantity of BSA encapsulated in both carriers was relatively high and was similar to the data previously reported in the literature (Liu et al., 2008; Yu et al., 2008).

A hydrogel of dextran was also produced to encapsulate the microparticles previously developed. This hydrogel was produced by dextran oxidation carried out in solution with sodium periodate. The degree of oxidation, as already described by Maia *et al*. (2009), can be correlated with the capacity of hydrogel to dissolve and swell, thus having implications for the durability of the hydrogel. The oxidation conditions were selected in order to obtain the best stability, according to the previous work of Maia *et al* (2009). After freeze-drying of the DexOx solutions, these acquire a spongy morphology similar to cotton, as shown in Figure 19A. After the addition of PBS, the DexOx was dissolved and with the addition of AAD, the dissolved dextran acquires consistency, forming a hydrogel within 20-30 min. As described above, the microparticles were incorporated into the dextran hydrogel as depicted in Figure 19B.

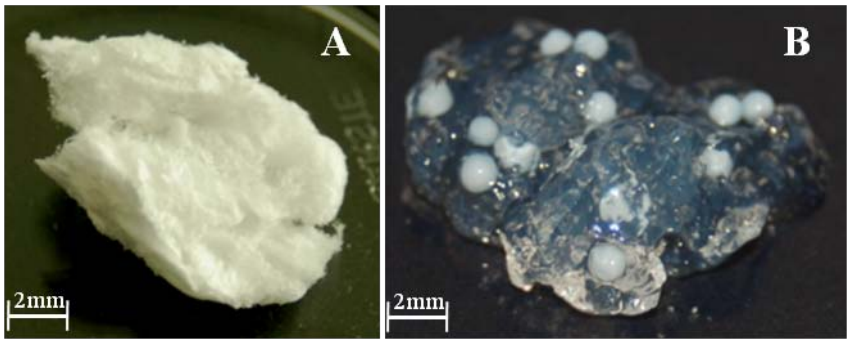

Figure 19 - Images of freeze-drying oxidized dextran (A) and dextran hydrogel with microparticles incorporated (B).

3.6.2. Evaluation of the cytotoxic profile of the different carriers

The cytocompatibility of alginate and chitosan microparticles and dextran hydrogel with and without microparticles incorporated was characterized through *in vitro* studies. As already mentioned, human fibroblasts cells were seeded at the same initial density in the 96-well plates, with or without materials to assess its cytotoxicity. Cell adhesion and proliferation was noticed in wells where cells were in contact with the microparticles and with the hydrogel with and without microparticles (Figures 20A - E) and in the negative control (Figure 20F). In the positive control, no cell adhesion or proliferation was observed. Dead cells with their typical spherical shape are shown in Figure 20G. The observation of cell growth in the presence of carriers demonstrated that alginate and chitosan microparticles and DexOx hydrogel are biocompatible.

To further evaluate the biocompatibility of the materials, MTS assay was also performed. The MTS assay results (Figure 21) showed that cell viability was higher for the negative control, in which cells were seeded just with DMEM-F12, followed by those that were seeded in the presence of the carriers. As should be expected the positive control showed almost no viable cells. The MTS assay showed a significant difference between positive control ($p < 0.05$) and the negative control and cells exposed to carriers after 24 hours of incubation. These results demonstrated that the polymers do not affect cell viability and can be used as drug delivery systems.

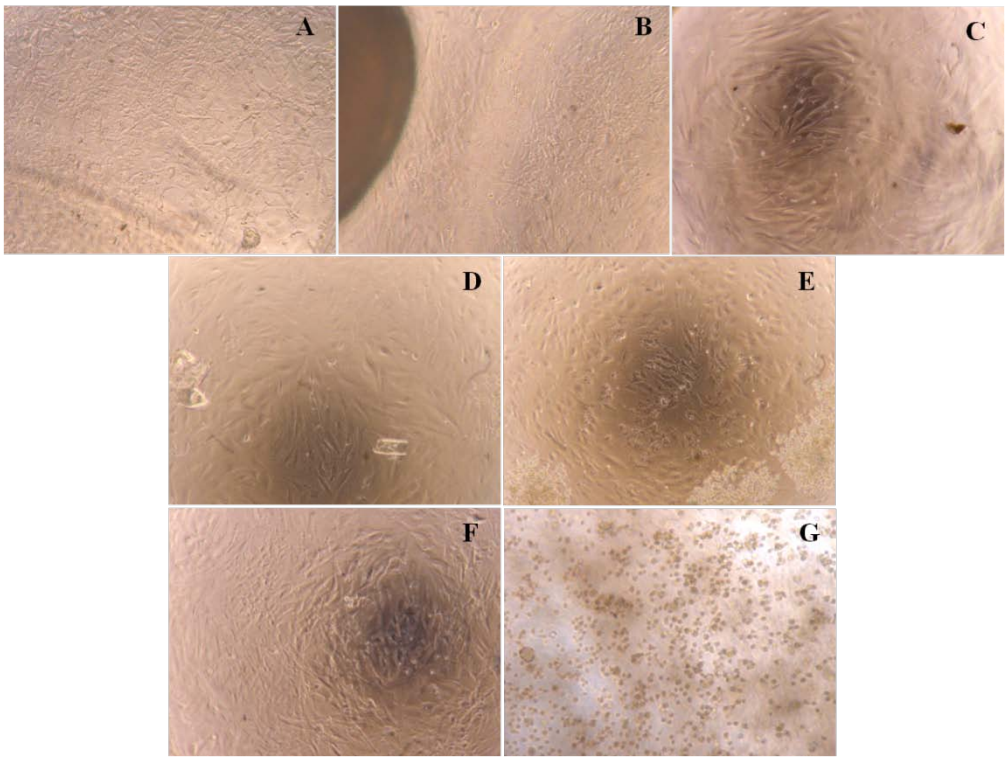

Figure 20 - Microscopic photographs of human fibroblast cells after being seeded in contact with the carriers: alginate microparticles (A), chitosan microparticles (B), oxidized dextran (C), oxidized dextran with alginate microparticles (D), oxidized dextran with chitosan microparticles (E), negative control (F) and positive control (G) Original magnification x100.

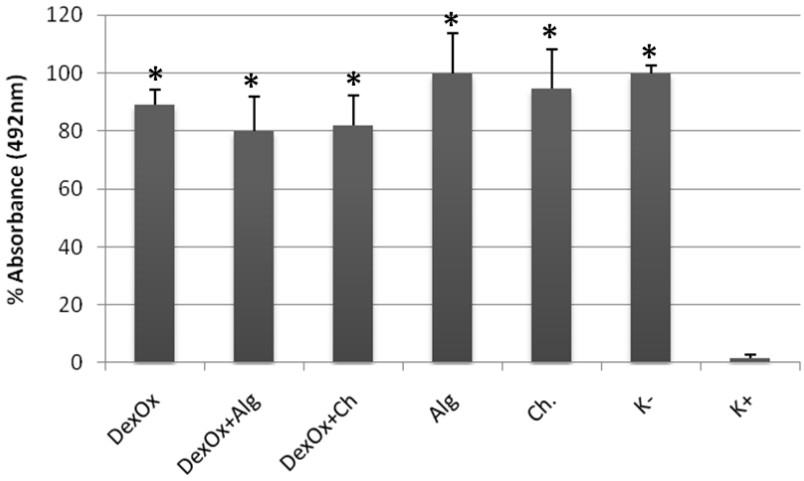

Figure 21 - Cellular activities measured by the MTS assay after 24h in contact with the carriers. Oxidized dextran (DexOx); alginate microparticles incorporated into oxidized dextran (DexOx+Alg); chitosan microparticles incorporated into oxidized dextran (DexOx+Ch); alginate microparticles (Alg); chitosan microparticles (Ch); negative control (K-); positive control (K+). Each result is the mean ± standard error of the mean of at least three independent experiments. Statistical analysis was performed using one-way ANOVA with Dunnet's post hoc test (*$p < 0.05$).

3.6.3. Modeling of BSA release from alginate and chitosan microparticles

Swelling data for both microparticles herein produced is shown in Figure 22. As it can be seen, for those produced with alginate the swelling ratio is positive and increases along the time, being approximately independent on the pH. Considering that alginate has some tendency to dissolve at high pH values, due to the carboxylate groups that impart some tendency to the polymer to dissolve (Yu et al., 2008), it can be concluded that this process is slow in the time scale used in the experiments, therefore, one can assume for modeling purposes that particle dissolution is negligible.

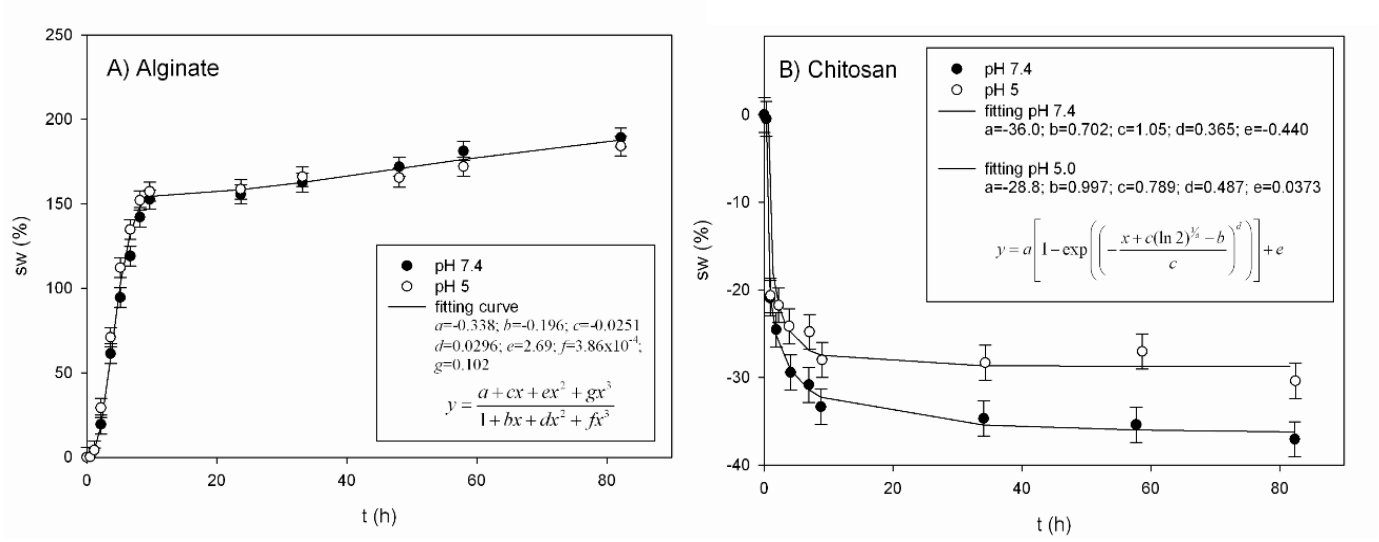

Figure 22 - Swelling ratio as a function of the time at 37ºC for: alginate microparticles (A) and chitosan microparticles (B).

In the case of chitosan, a completely different behavior was found, since the swelling ratio is negative and it decreases along time, indicating that the mass of the particles decreases. This decrease depends on the pH, being more pronounced at pH 7.4 than pH 5. However, considering that chitosan has a higher tendency to dissolve at low pH values rather than high, this strongly suggests that, like in the case of alginate, polymer dissolution should not be the mechanism responsible for the observed decrease in the swelling ratio. Yet, another possibility should be considered, which is the occurrence of polymer shrinking. This process also depends on the pH. At low pH, the amino groups of chitosan are protonated and this leads to repulsion between the polymer chains, thereby allowing more water to remain inside the gel network. As the pH increases, the amino groups become deprotonated and the repulsion between the polymer chains decrease, allowing a faster shrinking. Greater values of swelling ratio at low rather than higher pH values have been previously reported in literature for chitosan particles prepared by other methods than the one used here (Butler et al., 2006; Rohindra et al., 2004; Wang et al., 2008).

From the data shown in Figure 22, the volumetric fraction of the polymer, ϕ, can be estimated from the indicated swelling ratio values using the following relationship:

$$\phi = \phi_0 \left(v_{s,w} \rho_0 \left(\frac{sw}{100} \right) + 1 \right)^{-1} \quad \text{Eq. (9)}$$

where ϕ_0 is the initial polymer volumetric fraction, sw is the swelling ratio and ρ_0 is the initial density of the particles. The latter can be estimated as:

$$\rho_0 = \frac{\phi_0}{v_{s,p}} + \frac{1-\phi_0}{v_{s,w}} \quad \text{Eq. (10)}$$

being $v_{s,p}$ and $v_{s,w}$ the partial specific volumes of the polymer and water, respectively. For alginate $v_{s,p}$ corresponds to 0.6 cm^3/g (Amsden, 2001), for chitosan 0.57 cm^3/g (Morris et al., 2009) and for water it can be assumed 1 cm^3/g. The results of protein release from alginate and chitosan microparticles are shown in Figure 23.

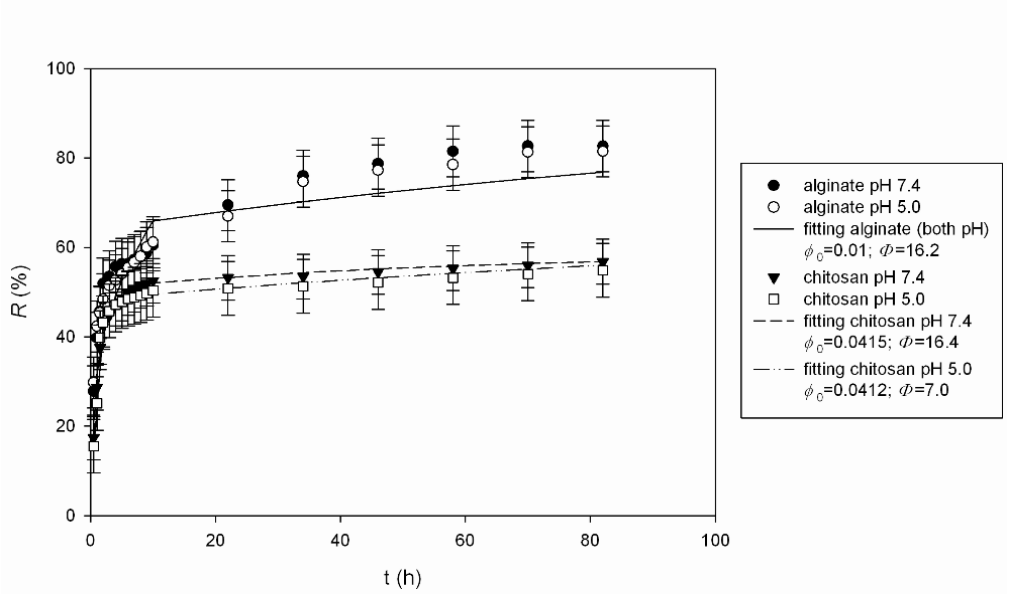

Figure 23 - Protein release (*R*) from alginate and chitosan microparticles. Experimental data obtained at different pH values and theoretical curves obtained by fitting of the indicated parameters.

As it can be seen, the solution's pH has a small effect on the protein's release rate, being slightly higher at pH 7.4; this indicates that alginate, although it has some tendency to dissolve at higher pH, as previously indicated, the dissolution process is slow enough to prevent a faster protein release from the hydrogel matrix at the higher pH. For alginate r_f has been estimated to be 3.6 Å, by x-ray analysis (Phillips, 2000), and values of ϕ between 0.006 to 0.05 have been reported (Amsden, 1998). As it can be seen in Figure 23 a very good

agreement between the experimental data and the model was found using ϕ_0=0.01, k_m=5x10^{-6} m/s and ϕ=16.24; these values were determined by minimizing the following error function:

$$\varepsilon(\phi_0, k_m, \Phi) = \sum \left| R_{\text{calc}}(\phi_0, k_m, \Phi, t_{samp}) - R_{\text{exp}}(t_{samp}) \right| \qquad \text{Eq. (11)}$$

where, R_{calc} is the calculated percentage of protein release at each sampling time t_{samp}, and R_{exp} the corresponding experimentally obtained value.

The partition coefficient, Φ, was determined by fitting for ϕ_0=0.01. The obtained value of Φ indicates that the protein interacts with the polymer and that interaction was attractive. The relative contributions to mass transfer of the two mechanisms included in the proposed model (mass transfer from the particles to the solution by hindered diffusion and mass transfer back to the particles due to positive swelling) can be estimated along the time of the experiments, by evaluating the ratio of the moles of protein transferred due to swelling to the total number of moles transferred; this ratio will be denoted as α. The estimated values of α, obtained by simulation using the previously determined parameters ϕ_0, k_m and Φ are shown in Figure 24A. As it can be seen, α cyclically oscillates in the whole range of the possible values, *i.e.*, between 0 and 1; each time the outside solution is refreshed α drops to very low values but, as the solute accumulates in the outside solution, the driving force for diffusion decreases and protein uptake by the particles due to swelling becomes progressively more important, reaching a point where mass transfer due to swelling becomes the dominant mechanism ($\alpha \approx 1$). As it can be seen in Figure 24B, this causes a severe decrease in the rate of solute accumulation in the outside solution.

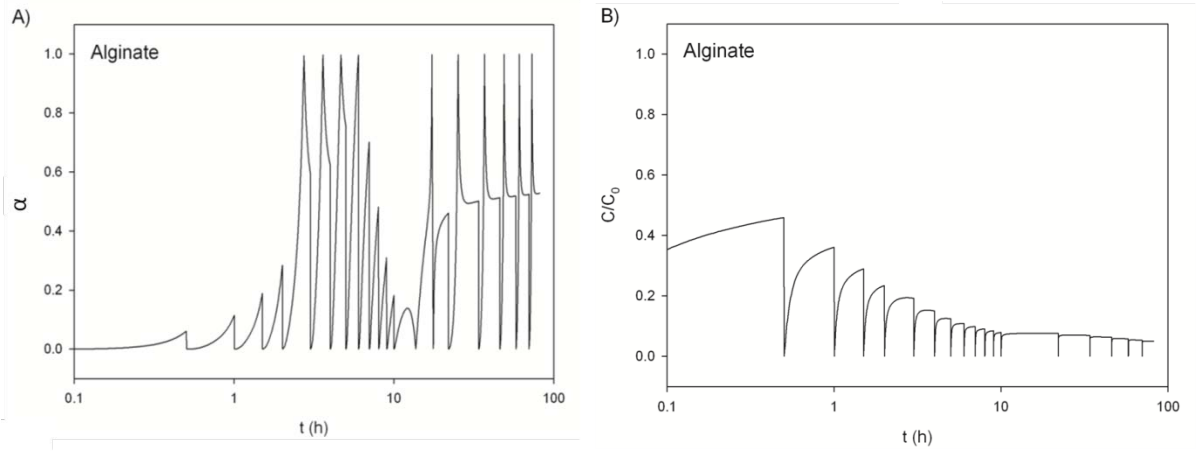

Figure 24 - Simulation of BSA release from alginate microparticles, with ϕ_0=0.01, k_m=5x10^{-6} m/s and Φ = 16.2. Swelling contribution to mass transfer, estimated through the parameter α. Relative protein concentration in the outside solution, C/C_0.

In the case of chitosan microparticles, r_f can be estimated to be 3.5 Å (Morris et al., 2009). Using the data obtained at pH=7.4 (see also Figure 23), the values of ϕ_0=0.0415 and Φ=16.4 were obtained by fitting, using k_m=5x10^{-6} m/s; at pH=5 it was obtained ϕ_0=0.0412 and Φ=7.0 using the same value of k_m. As it can be concluded from the fittings, the two values of ϕ_0 obtained at different values of pH are consistent with each other and considerably higher than the value found for alginate. The obtained values of Φ are both higher than 1, indicating an attractive interaction between the polymer and the protein, as in the case of alginate. The lower value of Φ obtained at pH=5.0 was probably due to the fact that chitosan has positive charge at that pH, and BSA is approximately neutral since its isolectric point is 4.8. In the case of chitosan, contrary to that of alginate, polymer dissolution may occur at a low pH, more specifically below pH 6.5, the value of its pKa; however, as it can be seen in Figure 23, the protein release curves obtained at pH 5 and pH 7.4 are very similar, again indicating that dissolution should be very slow and it is not a relevant process affecting the rate of protein transfer.

Comparing the obtained values of protein release between chitosan and alginate, it can be concluded that those are considerably smaller for chitosan, independently on the pH, although swelling in the case of chitosan is negative, and this affects the rate of protein transfer. Therefore, the lower rate of protein release for chitosan should be essentially explained by the lower diffusion coefficients inside the particles, as a result of the higher values of ϕ. In fact, from the obtained values of ϕ_0, the initial diffusion coefficients in chitosan should be near 10^2 times lower than in alginate microparticles. Moreover, throughout the time of the experiments the values of ϕ in the case of chitosan should increase due to shrinking reaching 0.066 at pH=7.4 and 0.059 at pH=5.0, in contrary to the case of alginate microparticles, for which ϕ should increase due to swelling, reaching 0.0034. This results in a difference in the diffusion coefficients between alginate and chitosan of about 3 orders of magnitude by the end of the experiments, *i.e.*, after 82 h. The relative contribution of swelling to mass transfer in the case of chitosan is shown in Figure 25. As it can be seen, the swelling process has a significant contribution to mass transfer in the beginning, but its contribution rapidly decreases. This is consistent with the observation that in the case of chitosan, the swelling ratio becomes approximately constant after nearly 10 h (see Figure 22).

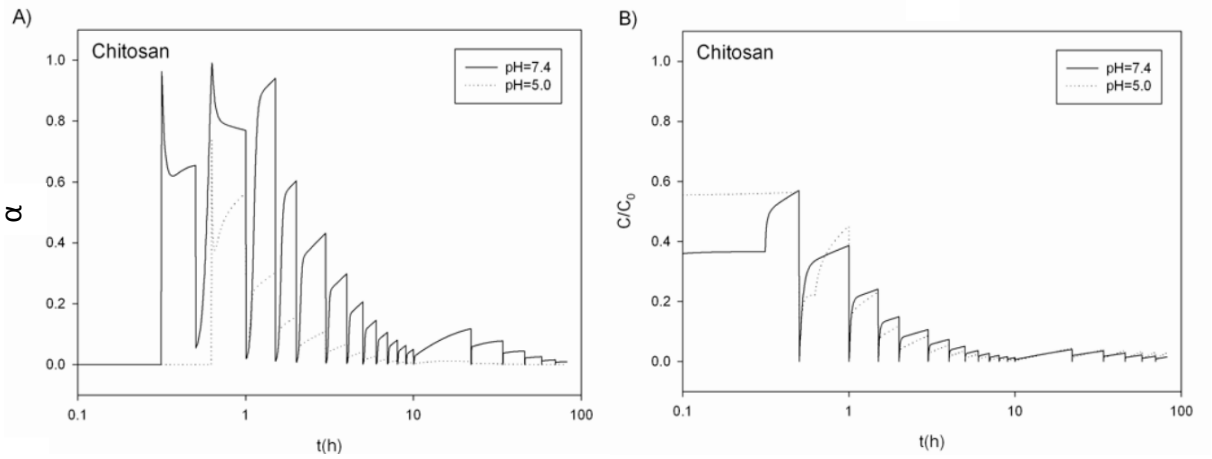

Figure 25 - Simulation of BSA release from chitosan microparticles. Swelling contribution to mass transfer, estimated through the parameter α. Relative protein concentration in the outside solution, C/C_0. Parameters used: ϕ_0=0.0415 and Φ= 16.4 at pH 7.4, ϕ_0=0.0412 and Φ= 7.0 at pH=5.0.

The results of BSA release from a suspension of microparticles in a dextran hydrogel are shown in Figure 26. Data was obtained for alginate and chitosan. In each case, 8 particles were placed inside 2 mL of hydrogel and 2 mL of the Tris buffer (outside solution) was used. The same experimental sampling procedure was used. To increase the release time of the protein, the microparticles were incorporated within the hydrogel.

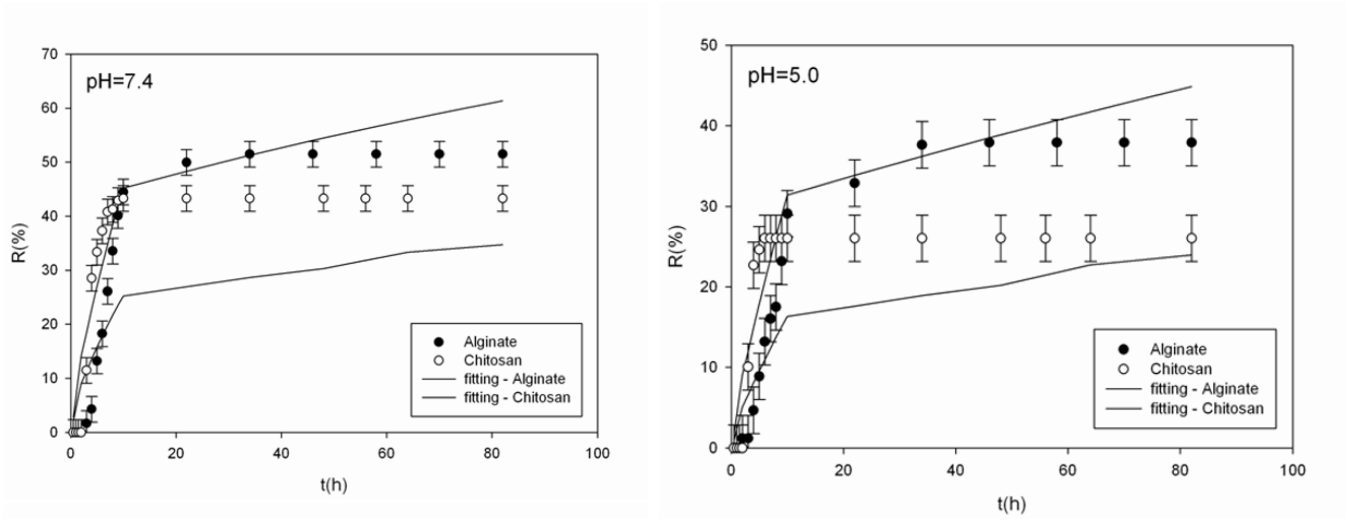

Figure 26 - BSA release (*R*) from alginate and chitosan microparticles incorporated into dextran hydrogel at pH 5 and 7. Experimental data obtained at different pH values and theoretical curves obtained by fitting of the indicated parameters.

As it can be seen this is in fact achieved, however, the amount of protein released is decreased by incorporating the microparticles into the hydrogel, since a pseudo-stationary state is observed. In order to model this system, a simplified approach is proposed in which it is considered that the particles are randomly placed inside the hydrogel, which is modeled

ideally as a sphere. The protein diffuses inside the particles according to the hindered transport model previously applied. The particles may swell or shrink according to the previous study, and the same mass transfer mechanism is assumed to occur. It is also assumed that the dextran hydrogel does not swells or shrinks during the process of protein transfer and, therefore, water does not accumulate inside the gel, being transferred to (or from) the particles from (or to) the outside solution, in the case of swelling or shrinking of the microparticles. A partition equilibrium is considered between the particles and the hydrogel, where it is assumed that the protein concentration is always homogeneous, except near the interfaces hydrogel/microparticles and hydrogel/outside solution (see Figure 27). For modeling protein mass transfer using this simplified approach one must consider the mass transfer coefficient at the interfaces, $k_{m,1}$ and $k_{m,2}$, the partition coefficient between the particles and the hydrogel, $\Phi_{i,H}$ and that one between the hydrogel and the outside solution, Φ_{HOS}. For the sake of simplicity, and in order to decrease the number of adjustable parameters, it was considered that the product $\Phi_{i,H}\Phi_{HOS}$ for a certain particle type corresponds to the previously determined value of Φ_i, at a certain pH, where *i* designates the type of particle (*i*=1 denotes alginate, *i*=2 chitosan). This implies that $\Phi_{HOSpH=7.4}=16.2/\Phi_{1,HpH=7.4}=16.4/\Phi_{2,HpH=7.4}$ and $\Phi_{HOSpH=5.0}=16.2/\Phi_{1,HpH=5.0}=7.0/\Phi_{2,HpH=5.0}$. Therefore, in order to obtain the full set of parameters needed for modeling, it is required to find just one of the $\Phi_{i,H}$ at each pH value. This was done by fitting, using all the data obtained in the tests performed with the dextran hydrogel, by adjusting the value of $\Phi_{1,H}$, and considering $k_{m,1}=k_{m,2}=5\text{x}10^{-6}$ m/s. The optimal values obtained were $\Phi_{1,H}$=1.02 at pH=7.4 and $\Phi_{1,H}$=0.62 at pH=5.0. This implies that $\Phi_{2,H}$(pH=7.4)=1.03, Φ_{HOS}(pH=7.4)=15.9, $\Phi_{2,H}$(pH=5.0)=0.267, Φ_{HOS}(pH=5.0)=26.2. Although the fittings are less satisfactory for the system with the dextran hydrogel than without the hydrogel, the results are indicative that BSA strongly interacts with the hydrogel, especially at pH=5.0, and this should explain, essentially, the lower values of protein release that are obtained when using the dextran hydrogel as an intermediate medium for mass transfer. Also, it is possible that some physical or chemical changes of the dextran hydrogel may occur during the process of protein release leading to an increase in the amount of protein retained inside the drug carrier system, thereby contributing to the observed pseudo-stationary state. In fact, if the drug carrier system remained unchanged throughout the time, the cyclic renewal of the outside solution would ensure a continuous increase in the amount of protein released as a function of time and that was not observed.

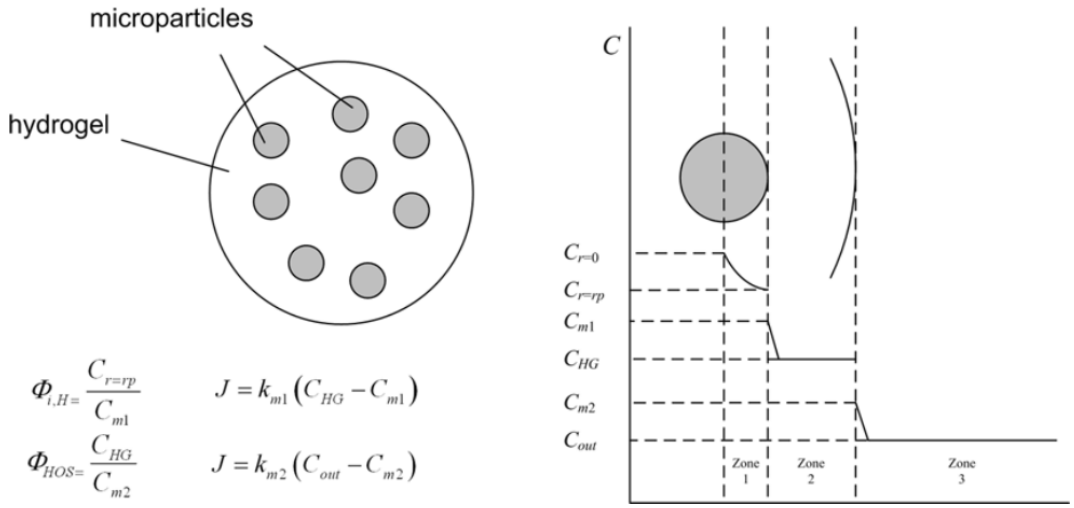

Figure 27- Proposed model to describe the mass transfer process of the protein from the microparticles placed inside a hydrogel (*HG*) to the outside solution. Partition coefficients and mass transfer coefficient definitions. Zone 1: particles interior; Zone 2: bulk of the hydrogel; Zone 3: outside solution.

3.7. Conclusions

In the present work, drug delivery systems based on alginate and chitosan microparticles, and dextran hydrogel were produced. The microparticles were characterized in terms of size, geometry, encapsulation efficiency for a model protein (BSA) and swelling behavior. Cytotoxicity assays demonstrated that all the carriers are biocompatible and they can be used as drug delivery systems.

Co-relating *in vitro* BSA release studies with swelling data from both microparticles, a mathematical model was proposed here for describing the mass transfer process of the protein to an outside buffer solution, with and without mediation of the dextran hydrogel. Comparing the relative importance of the two mass transfer mechanisms considered in the model (hindered diffusion and swelling) it is concluded that the occurrence of particle swelling during protein release significantly affects the mass transfer rate. In the case of chitosan swelling is negative, *i.e.*, shrinking is observed, which has a positive contribution to the global mass transfer process; however, only initially that contribution is significant and diffusion becomes the dominating process as the particle swelling ratio stabilizes.

The experimental results also showed that a higher percentage of the protein is released in the case of alginate microparticles, for the same period of time, independently on the pH. This result can be explained using the developed model by the higher polymer volume fraction of chitosan microparticles, ϕ, since this parameter strongly affects the diffusion coefficients inside the particles. Also, it can be concluded that the interactions between the protein and both polymers studied are always attractive, at the pH values studied, considering that the obtained values of Φ were always found to be higher than 1.

The use of a dextran hydrogel to mediate protein transfer from the microparticles to the outside solution was successfully tested, since the protein is effectively transferred to the outside solution at a lower rate, as expected. However, the percentage of protein release was affected, which was possibly due to the strong attractive interaction identified between the dextran hydrogel and BSA.

Chapter 4

Drug Delivery Systems for Wound Healing

4. Development of New Carriers to Deliver Bioactive Molecules for Wound Healing

4.1. Abstract

Skin injuries (skin wounds, burns and scars) are traumatic events, which are seldom accompanied by complete structural and functional restoration of the original tissue. Different strategies have been developed in order to turn the wound healing process faster and less painful. In the present study *in vitro* and *in vivo* assays were carried out to evaluate the applicability of a dextran hydrogel loaded with chitosan microparticles containing two growth factors (vascular endothelial growth factor and endothelial growth factor) in the wound healing process. The carriers' morphology was characterized by scanning electron microscopy. The cytotoxicity of carriers with growth factors and their degradation by products was evaluated *in vitro* through MTS and LDH assays, using human fibroblast cells. The evaluation of the applicability of the carriers containing growth factors in the treatment of dermal burns in Wistar rats was performed by induction of full-thickness transcutaneous dermal wounds. Wound healing was monitored through macroscopic and histological analysis. The *in vitro* and *in vivo* studies disclosed that these systems are biocompatible, may aid the re-establishment of skin architecture and they can be used for the release of other bioactive agents.

Keywords: wound healing, drug delivery systems, biocompatibility, growth factors, *in vivo* and *in vitro* studies.

4.2. Introduction

Wound healing is a complex biological process, which includes a wide range of cellular, molecular and physiological pathways (Kim et al., 2008). Moreover, this process is slow and rarely accompanied by a complete structural and functional restoration of skin functions, which has repercussions in life quality and productivity of millions of people around the world (Balasubramani et al., 2001). Skin generally needs to be covered with a dressing immediately after damaged. The application of skin substitutes is need for blood clotting, protection of the wound from loss of fluid and proteins, electrolyte disturbances, and to improve aesthetic appearance of the wound site (Jayakumar et al., 2011; Kumbar et al., 2008). Skin substitutes have been demonstrating enough emphasis during these years (Boateng et al., 2008a; Ribeiro et al., 2009; Sezer et al., 2007). Traditional dressings like cotton wool, natural or synthetic bandages and gauzes were replaced by modern dressings that have been improved to retain and create a moist environment around the wound, facilitating the wound healing. The modern dressings are mainly classified according to the

materials from which they are produced including hydrocolloids, alginates and hydrogels, and generally occur in the form of gels, thin films and foam sheets (Boateng et al., 2008a). Ideally, a desirable wound dressing must adhere to the wound site, be porous enough to allow diffusion of wastes, nutrients and excess water, prevent dehydration and also be biocompatible, biodegradable and with good mechanical properties (Kim et al., 2008; Kokabi et al., 2007; Seal et al., 2001).

Hydrogels have different properties that are fundamental for their application as wound dressing. They can absorb the excess of wound exudates, protect the wound from secondary infection, be produced with different shapes, and effectively promote the healing process by providing a hydrated wound healing environment (Anumolu et al., 2010; Hamidi et al., 2008; Yang et al., 2010). These materials are nonreactive with biological tissue, permeable to metabolites, non-adherent and cool the surface of the wound, which may lead to a marked reduction in pain and therefore have high patient acceptability (Boateng et al., 2008b). In situ, forming hydrogels are capable of fulfilling the damage area and thus is advantageous over the preformed ones. These systems have also been applied for the controlled drug delivery of therapeutic agents (antimicrobials or growth factors) into the damaged area (Brandl et al., 2010; Delair, 2010; Lin and Metters, 2006).

Besides their good properties to be used as drug delivery systems, hydrogels present some disadvantages: their encapsulation efficiencies are low and their release profiles are fast which in addition to limiting the effectiveness of the applied system may cause secondary effects on the patient being subjected to high concentrations of drugs (Brandl et al., 2010; Hoare and Kohane, 2008). To increase their broadband of applications, new micro and nano drug carriers have been incorporated into the polymeric matrices to overcome the hydrogels limitations described in chapters 1 and 3 (Acharya et al., 2010).

In recent studies, chitosan has been used to deliver bioactive molecules such as EGF and VEGF in order to observe their influences in skin regeneration (Bao et al., 2009; Ribeiro et al., 2009). EGF, bFGF, granulocyte-macrophage colony-stimulating factor, human growth hormone, IGF, PDGF, TGF-β, and VEGF have been reported to contribute to wound healing process (Klenkler and Sheardown, 2004; Roskoski, 2007). As reported in the literature, repeated treatment with EGF increases the epithelial cell proliferation, synthesis of the ECM and accelerates the wound healing process (Alemdaroglu et al., 2006; Breen, 2007; Kwon et al., 2006). VEGF plays an important role in the vascular system, including the ability to induce new vessel growth and increase vascular permeability, being a good candidate for wound healing, as previously reported in chapter 1.

In this study, VEGF and EGF were encapsulated into chitosan microparticles. Then the microparticles were incorporated into the dextran hydrogel, potentially suitable for controlled delivery of growth factors. Dextran hydrogels have been used for stabilizing and delivering FGFs for tissue healing (Huang and Berkland, 2009). The combination of these two systems were advantageous since the wound was covered, protected and hydrated by the dextran hydrogel and, at same time, the hydrogel acted as a support for the microparticles

introduced inside it, extending the growth factors release for a longer period of time. The biocompatibility of the carriers was studied through *in vitro* and *in vivo* assays. Moreover, the potential applications of these systems in the acceleration of wound healing were also evaluated.

4.3. Materials

Chitosan (medium molecular weight), AAD, sodium periodate, diethylene glycol, TPP, PBS, dialysis membranes (MWCO ≈ 12.000 Da), amphotericin B, DMEM-F12, L-glutamine, MTS, LDH assay, penicillin G, streptomycin, trypsin, EDTA, EGF and VEGF were purchased from Sigma-Aldrich (Portugal). Dextran (Dextran T500; Mw: 500000 Da) was purchased from Pharmacia LKB, Sweden. Human Fibroblast Cells (Normal Human Dermal Fibroblasts adult, criopreserved cells) were purchased from PromoCell (Spain). FBS was purchased from Biochrom AG (Germany).

4.4. Methods

4.4.1. Chitosan microparticles production

Chitosan microparticles were prepared by internal gelation technique with negatively charged TPP ions. Chitosan solution was prepared by dissolving chitosan in an acetic acid solution (Grech et al., 2010). Then, the microparticles were formed using an electrospinning apparatus. Chitosan solution was placed in a 10mL plastic syringe with a needle of 0.45mm being used as the nozzle. The needle was connected to a high-voltage generator (CZE 1000R, Spellman, UK) at a voltage of 9 KV and an aluminum foil (under the TPP solution below agitation) served as the counter electrode (Wang et al., 2010). The chitosan solution was drop-wise into TPP solution. The feed rate of the solution was controlled through a syringe pump (KdScientific, KDS-100, Sigma) at a rate of 10mL/h (Wang et al., 2010). The microparticles were stirred for 5 minutes prior to further use. VEGF, EGF and VEGF/EGF-loaded microparticles were obtained by dissolution the growth factors into chitosan solution at a concentration of 10µg/mL (Stojadinovic et al., 2007).

4.4.2. Dextran hydrogel synthesis

The dextran hydrogel was prepared using the procedure previously described in chapter 3. Chitosan microparticles were incorporated into the hydrogel before its reticulation with AAD.

4.4.3. Proliferation of human fibroblast cells in the presence of the carriers

Human fibroblast cells were seeded in T-flasks of 25 cm^3 with 6mL of DMEM-F12 supplemented with heat-inactivated FBS (10% v/v) and 1% antibiotic/antimycotic solution. After the cells attained confluence, they were subcultivated by a 3-5 minutes incubation in 0.18% trypsin (1:250) and 5mM EDTA. Then cells were centrifuged, resuspended in culture medium and seeded in T-flasks of 75 cm^3. Hereafter, cells were kept in culture at 37°C in a 5% CO_2 humidified atmosphere inside an incubator (Maia et al., 2009; Ribeiro et al., 2009). To evaluate cell behavior in the presence of the carriers, they were placed in 96-well plates and sterilized by UV radiation for 30 minutes before cell seeding. Then, DMEM-F12 was added to each well and was left in contact with vehicles for 24 hours. Meanwhile, human fibroblast cells were cultured in 96-well plates at a density of $5x10^4$ cells per well. After 24 hours, the cell culture medium was removed and replaced by the one that was previously placed in contact with carriers for 24h. This procedure was repeated during 2 days. Cell growth was monitored using an Olympus CX41 inverted light microscope (Tokyo, Japan) equipped with an Olympus SP-500 UZ digital camera.

4.4.4. Characterization of the cytotoxic profile of the carriers

To evaluate the cytotoxicity of the carriers, human fibroblast cells were seeded in a 96-well plate, at a density of $5x10^4$ cells/well. At the same time, in another plate, the culture medium was added to the sterilized polymers, and left there for 24h and 48h. After this time of incubation, the cell culture medium was removed and replaced with 100µL of medium that was in contact with the drug delivery systems. Then cells were incubated at 37ºC in a 5% CO_2 humidified atmosphere for more 24h and 48h for each case. Subsequently, cell viability was assessed through the reduction of the MTS into a water-soluble brown formazan product (n=5), by an adaptation of the method previously described in the literature (Maia et al., 2009). The medium of each well was then removed and replaced with a mixture of 100µL of fresh culture medium and 20µL of MTS/PMS reagent solution. The cells were incubated for 4 hours at 37°C, under a 5% CO_2 humidified atmosphere. The absorbance was measured at 492 nm using a microplate reader (Sanofi, Diagnostics Pauster). Wells containing cells in the culture medium without materials were used as negative control. EtOH 96% was added to wells containing cells as a positive control (Palmeira-de-Oliveira et al., 2010; Ribeiro et al., 2009). Futhermore, cell integrity was assessed through the release of LDH. For this assay, after the incubation of the cells with carriers the medium of each well (50µL) (sample supernatants) was transferred to a fresh 96-well plate and the LDH assay mixture (100µL) was added to each sample of medium. After 20-30 minutes the enzymatic activity was stopped by the addition of chloride acid (HCl). The absorbance was measured at 492nm (Jin et al., 2009). Wells containing cells in the culture medium without carriers were used as negative control.

To positive control, cells were died by the addition of LDH assay lysis solution (Albrecht et al., 2009; Potter and Stern, 2011).

4.4.5. Scanning electron microscopy analysis

The morphology of microparticles and the hydrogel with/without adhered human fibroblast cells were characterized by SEM. Cells ($6x10^4$ cells per well) were seeded with sterilized chitosan microparticles and DexOx (with and without microparticles) in 48-well plates, over a coverslip, for 48 hours. Samples were fixed in 2.5% glutaraldehyde overnight. Then, they were frozen in a glass container using liquid nitrogen and freeze-dried for 3h. Chitosan microparticles without cells were air-dried overnight. Finally, the carriers were mounted on an aluminium board using a double-side adhesive tape and covered with gold using an Emitech K550 (London, England) sputter coater. The samples were then analyzed using a Hitachi S-2700 (Tokyo, Japan) scanning electron microscope operated at an accelerating voltage of 20 kV and at various amplifications (Gaspar et al., 2011; Ribeiro et al., 2009; Takka and Gürel, 2010; Yu et al., 2008).

4.4.6. *In vivo* studies

A total of 30 female Wistar rats (8-10 weeks) were used, weighting between 150-200g. The animal protocols followed in the present study were approved by the Ethics Committee of Centro Hospitalar Cova da Beira and were performed according to the guidelines set forth in the National Institutes of Health Guide for the care and use of laboratory animals. Animals were individually anesthetized with an IP injection of Ketamine (40mg/kg) and Xylazine (5mg/kg) for surgery and for the induction of the skin lesion. The operative area of skin was shaved and disinfected using EtOH and the dorsal skin of the animals was exposed to water at 95 ± 1ºC for 10 seconds. After 2 hours, damaged tissue was removed with surgical scissors and forceps. Wounds of 2 cm of diameter were created with no visible bleeding (Ribeiro et al., 2009). The animals were divided into six groups: in group 1, wounds were filled with DexOx loaded with chitosan microparticles containing VEGF (DexOx+VEGF); group 2, wounds were filled with DexOx loaded with chitosan microparticles containing EGF (DexOx+EGF); group 3, wounds were filled with DexOx loaded with chitosan microparticles containing VEGF and EGF (DexOx+VEGF/EGF); group 4, wounds were filled with DexOx loaded with chitosan microparticles (DexOx+Ch); group 5, wounds were filled with VEGF and EGF dissolved in PBS every two days (VEGF/EGF); group 6 was used as control and wounds were covered with PBS. After surgery, animals were kept in separate cages and were fed with commercial rat food and water *ad libitum*. All animals showed good general health condition throughout the study, as assessed by their weight gain. The animals were sacrificed after 7, 14 and 21 days (Ribeiro et al., 2009).

4.4.7. Histology study

Tissue specimens were obtained from the wound area by sharp dissection at days 7, 14 and 21. The material from skin lesions and organs (brain, heart, lung, liver, spleen and kidney) was obtained by necropsy, was formalin fixed and paraffin embedded for routine histological processing. A 3µm section obtained from each paraffin block was stained with hematoxylin and eosin (H&E). Then, samples were evaluated by two blind observers using a light microscope with specific image analysis software from Olympus. Skin fragments with no carriers or growth factors were used as normal control. The assessment of the brain, heart, lung, liver, spleen and kidney was performed looking for any morphological alteration (Ribeiro et al., 2009).

4.4.8. Evaluation of the wound size

Images of the wound area were taken by a digital camera (Nikon D50) and analyzed with image analysis software Image J (Scion Corp., Frederick, MD). Measurement of the wound closure area was defined by the limits of grossly evident epithelyzation, with all surface areas in a two-dimensional plane calibrated against the adjacent metric ruler. The percentage of wound size was calculated using the following formula:

$$\frac{S_N}{S_0} \times 100\ (\%) \qquad \text{Eq. (12)}$$

where S_0 is the size of the full thickness circular skin wound area (2 cm diameter) on day 0, and S_N is the size of the wound area on the indicated day (Ribeiro et al., 2009).

4.4.9. Statistical analysis

For each measurement of the surface of the burn wounds, a minimum of three animals were used. The results obtained were expressed as mean ± standard error of the mean. Differences between groups were tested by one-way ANOVA with Dunnet's post hoc test. Computations were performed using a MYSTAT 12 statistical package (Systat Software, a subsidiary of Cranes Software International Ltd.).

4.5. Results and Discussion

The *in vitro* protein release studies at pH 5 and the production of a dextran hydrogel described in chapter 3 had a purpose of incorporating the chitosan microparticles with growth factors encapsulated into the dextran hydrogel, to be used with therapeutic purposes (to accelerate the wound healing process). As described in literature, the skin surface has long been recognized to be acidic, with a pH of 4.2 – 5.6 measured in humans (Prow et al., 2011). This pH is influenced by sex and anatomical site, sweat, sebum and hydration and has a

number of functions, including antimicrobial defense, the maintenance of the permeability barrier and restriction of inflammation, between others (Prow et al., 2011). As described previously, hydrogels are good candidates to be used as wound dressings due to their good physical and chemical properties. Growth factors are proteins involved in all phases of the wound healing process. Chitosan microparticles were chosen, instead of the alginate ones, based on the *in vitro* protein release studies. The percentage of BSA released from chitosan microparticles was lower than alginate ones, thus the protein is released in a longer period of time, decreasing the number of applications in the wound. So, incorporating the growth factors into chitosan microparticles and these into the dextran hydrogel allow to increase the time release of growth factors and accelerate the healing process.

4.5.1. Morphology of the carriers

Carriers' morphology was analysed through SEM (Figure 28). In the present study, chitosan microparticles were prepared by an adaption of the ionotropic gelation method (Hamidi et al., 2008), that involved an electrospraying technique. This gelation process is due to the formation of inter or intra crosslinkages between and within chitosan chains, mediated by the polyanions of TPP (Hamidi et al., 2008). Through the use of electrospraying process the diameter and the surface of chitosan microparticles were decreased. Microparticles presented a spherical shape (Figure 28A) and with an average diameter of approximately 255 ± 0.9 µm, three times lower than the diameter of chitosan microparticles produced by the method described in chapter 3. As depicted in Figure 28B the chitosan carriers produced had a slightly smoother surface, accordingly to what was previously described in the literature (Ko et al., 2002; Yu et al., 2008).

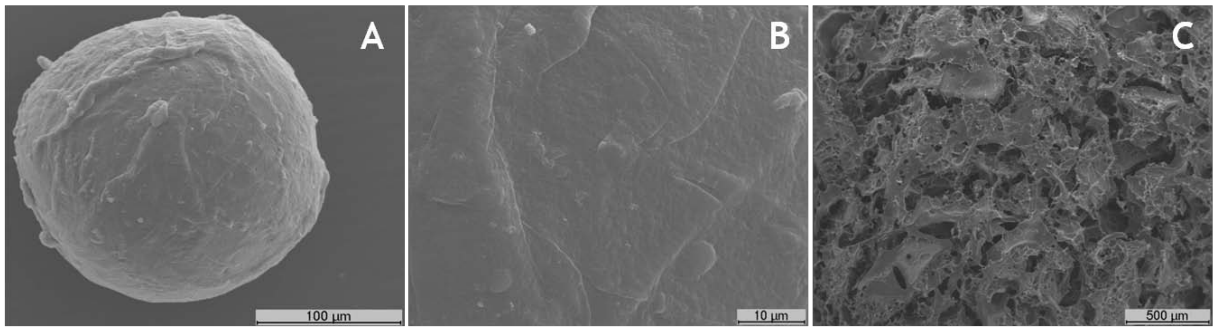

Figure 28 – SEM images of chitosan microparticles 400x (A), surface of chitosan microparticles 2000x (B) and surface of oxidized dextran 50x (C).

Electrospraying is a slightly modified form of the electrospinning process that is widely used for making micro/nanofibers (Arya et al., 2009). The principle of electropraying is essentially the same as that of electrospinning where the most important variable between them is the polymer concentration used in the process, which is relatively smaller in the case of electrospraying (Arya et al., 2009; Maeng et al., 2010; Wang et al., 2010). As described in

other studies, the average diameter of the micro/nano carriers depends on various parameters in the electrospinning process such as: needle diameter, electrospraying distance, polymer concentration and voltage applied (Arya et al., 2009; Maeng et al., 2010). The parameters used in this study are described in Table 3.

Table 3 – Parameters used for the synthesis of chitosan microparticles.

Parameters used	
Neddle gauge	25G
Electrospraying distance	10 cm
Chitosan concentration	1.5% (w/v)
Acetic acid concentration	1% (w/v)
Voltage	9 KV

SEM analysis of DexOx hydrogel (Figure 28C) revealed a highly interconnected interior structure. Both small and macromolecules could freely diffuse into DexOx. Keeping in mind the wound dressing application, the interconnected section of DexOx promotes drainage, prevents the build-up of exudates, and may be an optimum wound bed for autografting (Ribeiro et al., 2009). These results were in agreement with experimental data obtained by other researchers (Weng et al., 2008). The interconnectivity can provide more space and increased surface area-to-volume ratio of hydrogel scaffolds for cell growth, tissue invasion, local angiogenesis, and facilitate nutrient transport (Huang et al., 2011).

4.5.2. Evaluation of the cytotoxic profile of the carriers

The cytocompatibility of dextran hydrogel loaded with chitosan microparticles with/without growth factors incorporated was first characterized through *in vitro* studies. As already mentioned, human fibroblasts cells were seeded at the same initial density in the 96-well plates, with or without materials to assess its cytotoxicity during 48h. Cell adhesion and proliferation was observed in wells where cells were in contact with carriers (Figures 29) and in the negative control (K-), during the 48h. In the positive control (K+), dead cells with their typical spherical shape were visualized. The observation of cell growth in the presence of carriers demonstrated that all of them are biocompatible.

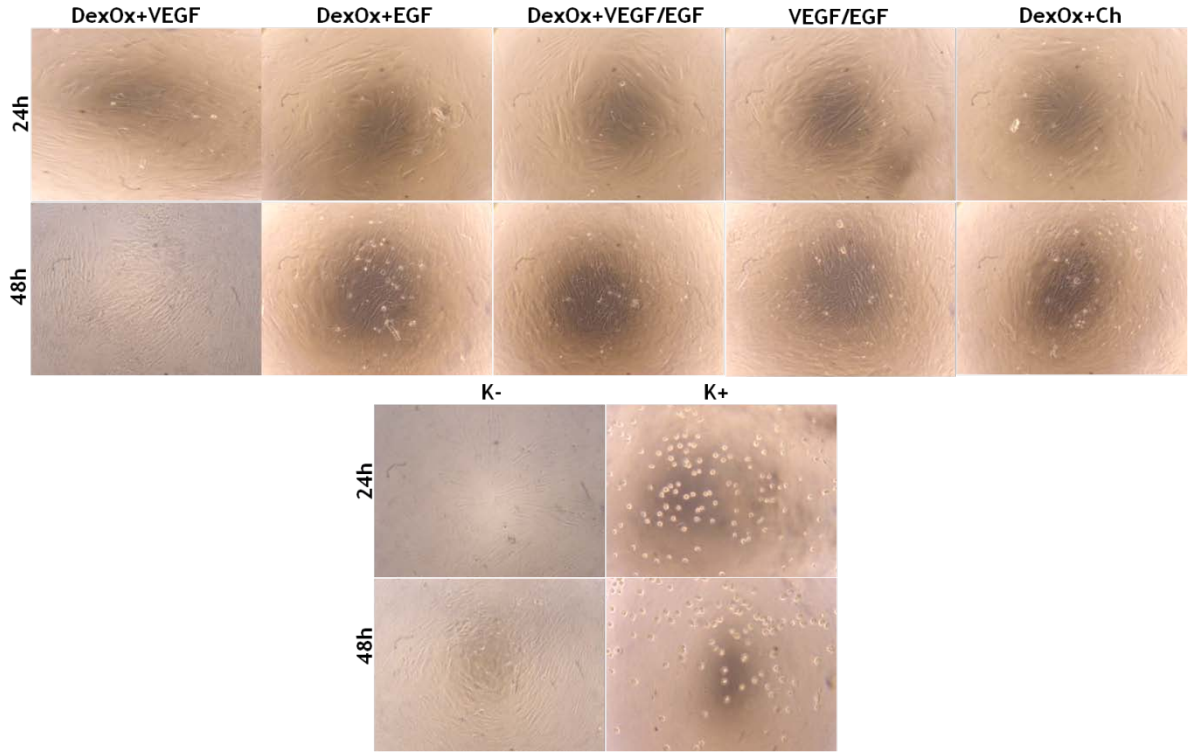

Figure 29 – Microscopic photographs of human fibroblasts cells after being seeded in the presence of the carriers during 24h and 48h. DexOx+VEGF: oxidized dextran loaded with chitosan microparticles containing VEGF; DexOx+EGF: oxidized dextran loaded with chitosan microparticles containing EGF; DexOx+VEGF/EGF: oxidized dextran loaded with chitosan microparticles containing VEGF and EGF; VEGF/EGF: VEGF and EGF dissolved in cultured medium, DexOx+Ch: oxidized dextran loaded with chitosan microparticles; K-, negative control; K+, positive control. Original magnification x100.

The proliferation of human fibroblasts cells in the presence of materials after 48h was also visualized through SEM (Figures 30).

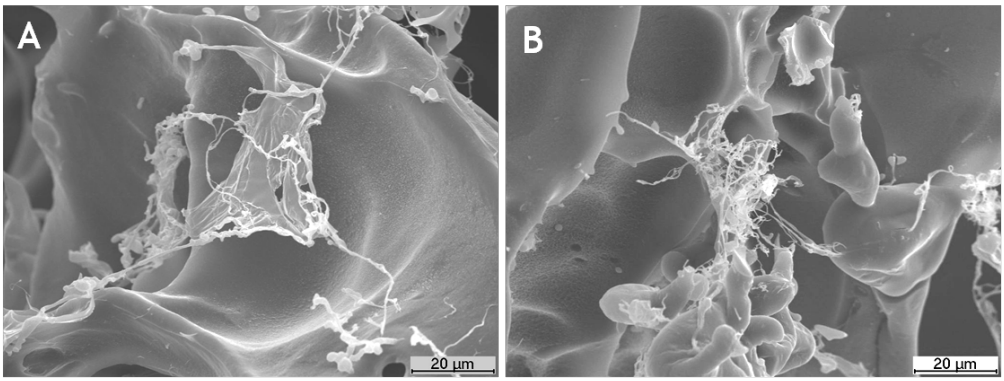

Figure 30 – SEM images of human fibroblast cells in contact with oxidized dextran hydrogel. Original magnification x1000 (A) and oxidized dextran hydrogel with chitosan microparticles incorporated. Original magnification x1000 (B).

To further evaluate the biocompatibility of the carriers, MTS and LDH assays were also performed. The MTS assay results (Figure 31) showed that cells in contact with the samples had higher viability than the positive control, but slightly lower than the negative

control (except for DexOx+VEGF/EGF sample at 24h), during the two times of incubation. It also showed a significant difference between positive control ($p < 0.05$) and the negative control and cells exposed to carriers, but no difference between samples after 24 and 48 hours of incubation. These results demonstrated that the vehicles do not affect cell viability and can be used as drug delivery systems for wound healing.

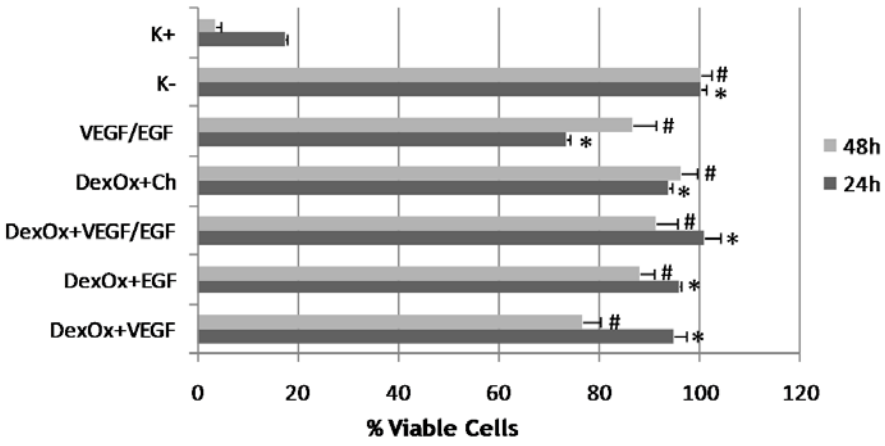

Figure 31 – Cellular activities measured by the MTS assay after 24h and 48h. Positive control (K+); negative control (K-); VEGF and EGF (VEGF/EGF); oxidized dextran loaded with chitosan microparticles (DexOx+Ch); oxidized dextran loaded with chitosan microparticles containing VEGF and EGF (DexOx+VEGF/EGF); oxidized dextran loaded with chitosan microparticles containing EGF (DexOx+EGF); oxidized dextran loaded with chitosan microparticles containing VEGF (DexOx+VEGF). Each result is the mean ± standard error of the mean of at least three independent experiments. Statistical analysis was performed using one-way ANOVA with Dunnet's post hoc test (*$p<0.05$; $^{\#}p<0.05$).

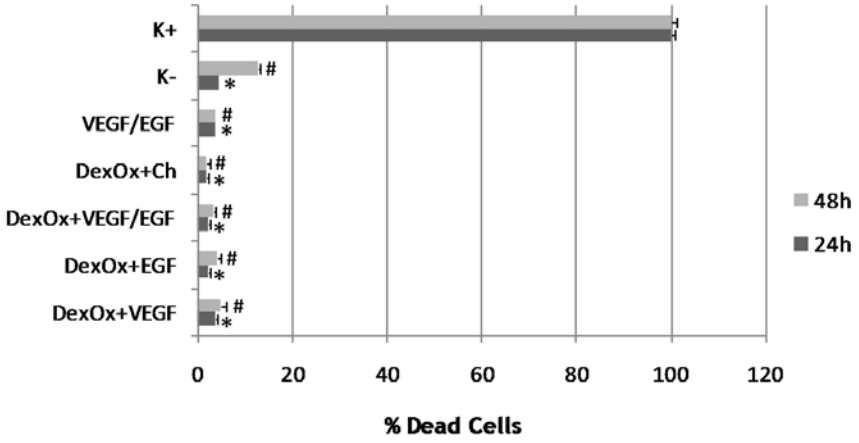

Figure 32 – Cellular integrity measured by the LDH assay after 24h and 48h. Positive control (K+); negative control (K-); VEGF and EGF (VEGF/EGF); oxidized dextran loaded with chitosan microparticles (DexOx+Ch); oxidized dextran loaded with chitosan microparticles containing VEGF and EGF (DexOx+VEGF/EGF); oxidized dextran loaded with chitosan microparticles containing EGF (DexOx+EGF); oxidized dextran loaded with chitosan microparticles containing VEGF (DexOx+VEGF). Each result is the mean ± standard error of the mean of at least three independent experiments. Statistical analysis was performed using one-way ANOVA with Dunnet's post hoc test (*$p<0.05$; $^{\#}p<0.05$).

LDH activity, the second method used to evaluate cell viability, is an indicator of membrane integrity as described in chapter 2 (Potter and Stern, 2011). From Figure 32 it is possible to say that no significantly enhanced LDH release was detected after 24h and 48h of cells being seeded in the presence of the carriers. The LDH assay also showed a significant difference between positive control ($p<0.05$) and the negative control and cells exposed to vehicles, but no difference between samples after the times of incubation. These results reinforced the idea that the carriers are biocompatible and do not affect cell integrity and viability.

4.5.3. *In vivo* evaluation of the wound healing process

In order to characterize the applicability of the different carriers in wound healing, Wistar rats were used and divided into six groups, as previously described in the text. Group 4 (DexOx+Ch), group 5 (VEGF/EGF) and group 6 (normal control) were set as control. Group 5 was used to verify if the capacity to accelerate skin regeneration was only due to growth factors or owing to the system consisting of dextran hydrogel loaded with chitosan microparticles containing growth factors. Moreover, the application of dextran hydrogel loaded with chitosan microparticles without growth factors (group 4), would examine if the effect on wound contraction was concerning to the use of growth factors or simply due to the materials used. Finally, group 6, where the wounds were only treated with PBS, was used to verify if the wound contraction would be due to the use of the materials and growth factors or if they did not have the capacity to promote skin regeneration.

Figure 33 shows a set of typical wound beds after the surgical procedure and application of the carriers. The healing patterns were observed after 2, 5, 7, 9, 12, 14, 16, 19 and 21 days. From the macroscopic analysis, the wound beds of group treated with DexOx+VEGF/EGF were considerably smaller than those of the control groups (groups 4-6).

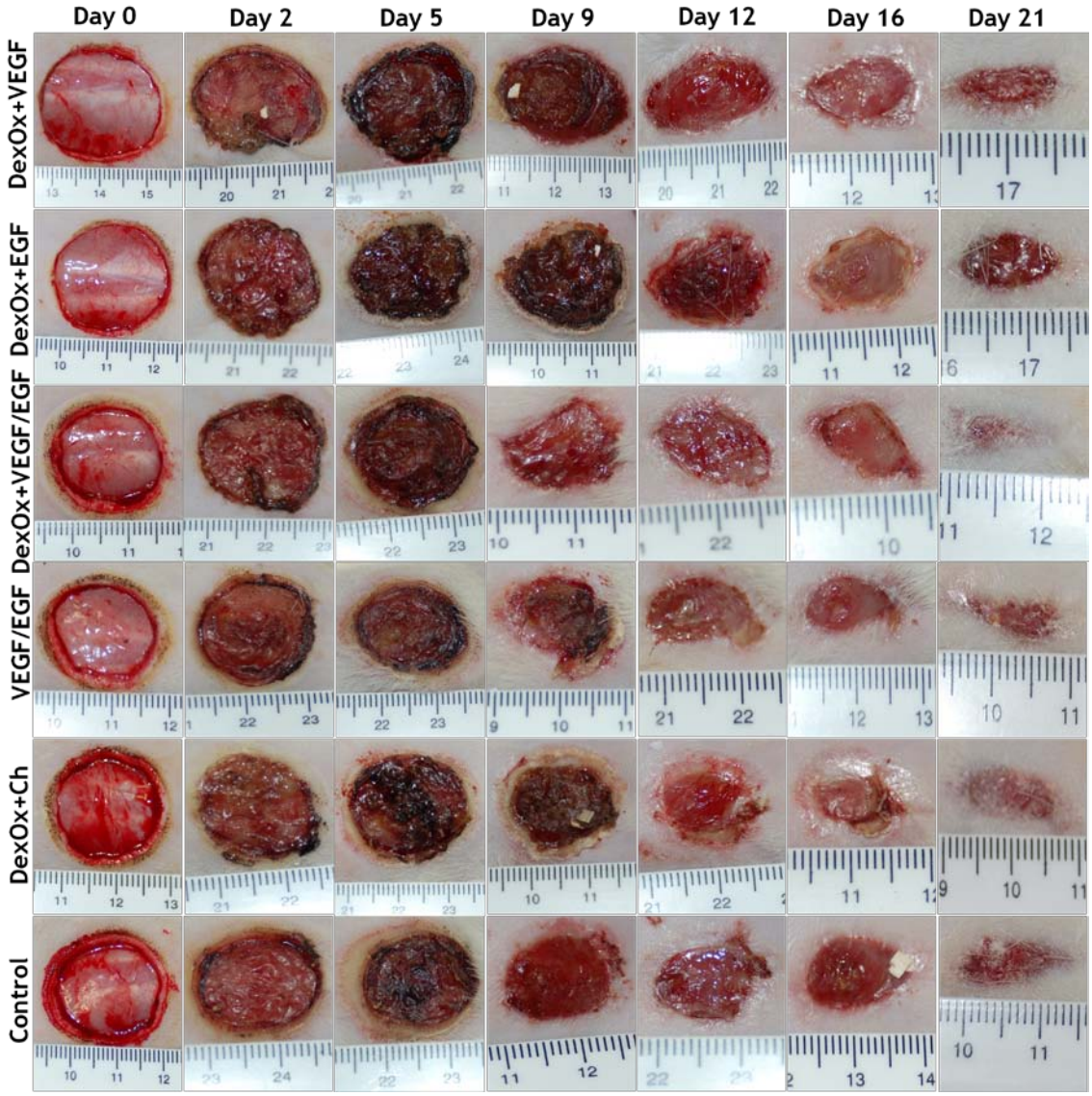

Figure 33 – Typical macroscopic wound-healing panorama over 21 days. A deep third-degree burn wound with 2cm diameter was induced at the dorsal skin of each female Wistar rat. All went through various healing phases such as inflammation, eschar, tissue formation and tissue remodeling on the 2nd, 6th, 9th, 12th, 16th and 21st day after injury.

From Figure 34 it is possible to notice that the wound area of the control animals increased during the first days. Such increase of wound area was not observed in the animals treated with DexOx+VEGF, DexOx+EGF and DexOx+VEGF/EGF. In the group treated with DexOx+EGF, it was noticed that the wound area was significantly higher between the 7th and 14th days compared with the control group treated with PBS (group 6). The wound area of DexOx+VEGF group was always lower than the DexOx+EGF and control groups. Finally, it is possible to conclude that the best conditions to improve the wound healing process are those where DexOx+VEGF/EGF was used.

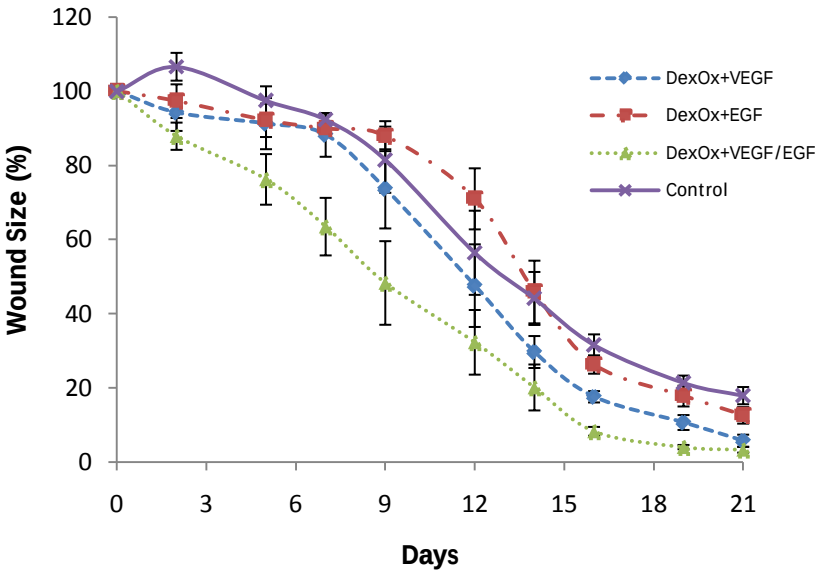

Figure 34 - Effect of DexOx+VEGF, DexOx+EGF and DexOx+VEGF/EGF on burn wound compared to the control group. The surface area of the burn wounds was calculated as described in methods and reported at each time point as the percentage of the surface area at baseline. Each point represents the mean ± standard error of the mean of at least three independent experiments.

From the observation of Figure 35 it is possible to verify that the ability of DexOx+VEGF/EGF to accelerate the wound healing process is due to the combination of the two carriers (dextran hydrogel and chitosan microparticles) with the two growth factors (VEGF and EGF). The wound area of the animals treated only with DexOx+Ch and VEGF/EGF was always higher than the animals' group treated with DexOx+VEGF/EGF.

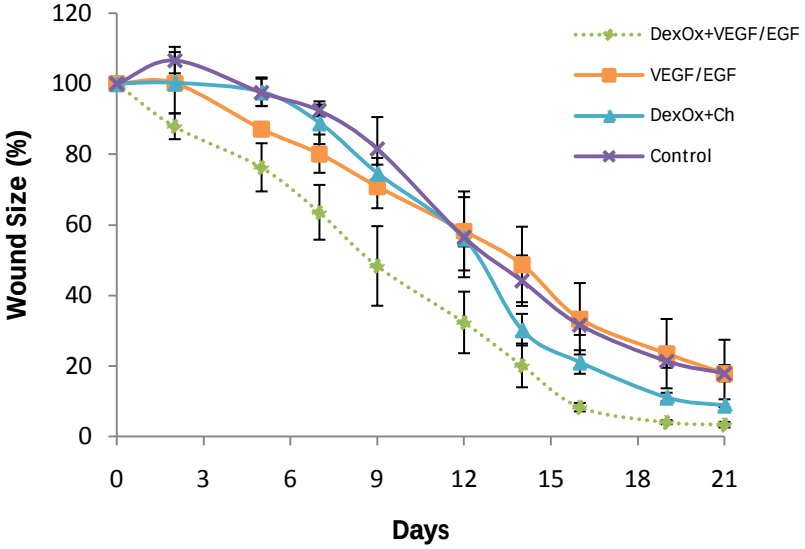

Figure 35 - Effect of DexOx+VEGF/EGF on burn wound compared to VEGF/EGF, DexOx+Ch and control group. The surface area of the burn wounds was calculated as described in methods and reported at each time point as the percentage of the surface area at baseline. Each point represents the mean ± standard error of the mean of at least three independent experiments.

It is important to mention that the animals' group treated only with VEGF and EGF (group 5) received several doses (10µg/wound site) every two days, while the groups treated with DexOx+VEGF, DexOx+EGF, DexOx+VEGF/EGF and DexOx+Ch received a single dose per week based on the protein release profile described in the chapter 3. VEGF proved to be a crucial growth factor in the wound healing process since that even when used alone accelerates this process, as observed in Figures 33, 34 and 35. However, the combination of the capacities to promote endothelial cells proliferation of EGF with the promotion of angiogenesis of VEGF, proved to decrease even more the duration of the wound healing process. Other studies revealed that angiogenesis, the primary effect of VEGF, was clearly improved by encapsulation of the growth factor (Rieux et al., 2010). Moreover, chitosan microparticles have proved to be good candidates to be used as drug delivery systems, since they not only allow that the drug has a controlled release profile, avoiding several administrations, but also the electrostatic interactions between the negative charge of skin and the positive charge of chitosan are suitable for skin regeneration, as described elsewhere (Ribeiro et al., 2009). Dextran hydrogels have been described in the literature as being good candidates for wound healing, since it reduces the wound area faster than the control groups (Jukes et al., 2009; Weng et al., 2008). Thus, the hydrogel not only functioned as a support to chitosan microparticles, but also prolonged the time during which the growth factors were released.

4.5.4. Histological study

The histological sections of wound beds receiving the DexOx+VEGF/EGF, VEGF/EGF, DexOx+Ch and PBS are depicted in Figure 36. From the observation of the histological data it is possible to say that the epithelial layer thickness increased progressively from days 7 to 21. In groups treated with DexOx+VEGF/EGF and VEGF/EGF, the granulation tissue layer and epithelial layer thicknesses increased faster with the formation of new blood vessels, compared with DexOx+Ch and normal control groups. On day 21, all the skin lesions exhibited complete epithelization, although these was higher for DexOx+VEGF/EGF and VEGF/EGF treated groups, as described before. Neither specific inflammation nor reactive granulomas to the presence of DexOx, chitosan and growth factors were observed. No microorganisms were observed in skin lesions. No pathological abnormalities were observed in brain, lung, liver, spleen or kidney obtained during necropsy. These results support the local and systemic histocompatibility of the carriers. Furthermore, the increasing thickness of the epithelial layer during the experiment and the presence of complete epithelization in all the skin samples treated by the developed biomaterials and growth factors used, suggest that they may aid the re-establishment of tissue architecture.

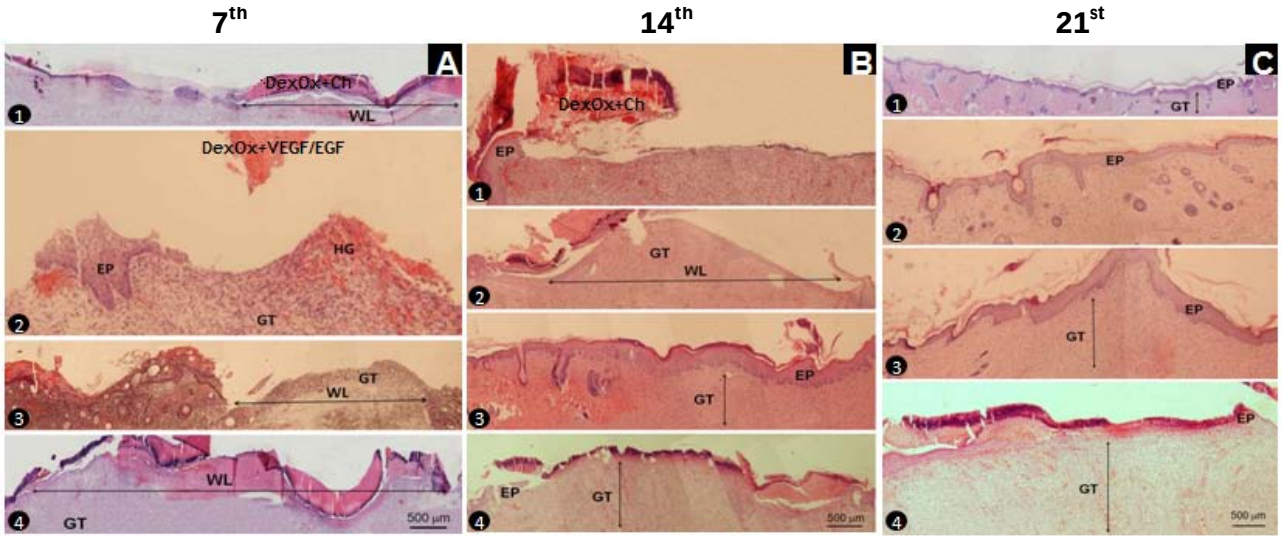

Figure 36 – Hematoxylin and eosin-stained sections of biopsies for the morphological evaluation of skin lesions after 7 days, scale bar 500µm (A), 14 days, scale bar 500µm (B) and 21 days, scale bar 500µm (C) treated with oxidized dextran loaded with chitosan microparticles (DexOx+Ch) (1), oxidized dextran loaded with chitosan microparticles containing vascular endothelial and endothelial growth factors (DexOx+VEGF/EGF) (2), vascular endothelial and endothelial growth factors (VEGF/EGF) (3) and phosphate-buffered saline (PBS) (4). EP: epithelial membrane; GT: granulation tissue; HG: hemorrhage; WL: wound length.

4.6. Conclusion

A versatile, non-toxic, *in situ* crosslinkable, biodegradable hydrogel has been successfully prepared from DexOx in order to be used as a wound dressing. Since hydrogels present rapid protein release profiles when used as drug delivery systems, chitosan microparticles were prepared by electrospraying, and two types of growth factors that have important roles in all phases of skin regeneration were encapsulated into them. The *in vitro* assays revealed that hydrogel and microparticles with and without the growth factors are both non-cytotoxic. The *in vivo* assays suggested that dextran hydrogel and chitosan microparticles with the two growth factors encapsulated promote faster wound healing with no signs of local or systemic inflammatory response. The results obtained here support the simultaneous application of the two different types of growth factors with combined roles in wound healing. VEGF and EGF together promote multiple mechanisms including collagen deposition, angiogenesis and epithelialisation. Moreover, chitosan microparticles were considered a good vehicle to deliver the growth factors herein studied, since a unique application per week of DexOx+VEGF/EGF in the wound site helps to reduce the wound area more rapidly than VEGF/EGF applied every two days. Furthermore, dextran hydrogel could be adapted as an *in situ* gelable wound dressing. The combination of these two systems (hydrogel and microparticles) can also be used as carrier for other growth factors in future studies for different application in the area of regenerative medicine.

Chapter 5
Concluding Remarks

5. Concluding Remarks

Wound healing is a major worldwide health problem that particularly affects the elderly patient population. According to the US Wound Healing Society, about 15% of older adults suffer from chronic, hard-to-heal wounds (Woodley et al., 2007). In recent years different therapeutic approaches have been proposed, among them the topical application of growth factors has been used to improve wound healing. Growth factors that play a key role in normal wound healing and, in addition, are often deficient or inactive in chronic wounds have been highlighted as attractive therapeutic agents. Among these factors are PDGF, EGF, TGF, keratinocyte growth factor, VEGF and FGF. The topical application of EGF has been shown to accelerate wound closure of acute human wounds (Escámez et al., 2008). Nevertheless, topical application of EGF never became a commercially viable therapy because of cost and practical considerations. Furthermore, VEGF is an angiogenic growth factor that promotes the closure of chronic wounds exhibiting hypoxia and compromised vascularity. One problem with the topical application of growth factors is that the wound bed is often laden with proteolytic enzymes that degrade and nullify the applied agent. A more sustained presence of the therapeutic agent may be desirable. In this regard, new skin substitutes with incorporated bioactive molecules are being developed to assure a continuous delivery of therapeutic agents to the wound site and overcome the limitations associated with topical application of growth factors. So far none of the skin substitutes developed completely replicates the anatomy, physiology, biological stability or aesthetic nature of uninjured skin. Skin substitutes should have some essential characteristics which include: being easy to handle and apply to the wound site; provide vital barrier function with appropriate water flux; be readily adherent; have appropriate physical and mechanical properties; undergo controlled degradation; be sterile, non-toxic and non-antigenic; and evoke minimal inflammatory reactivity (Metcalfe and Ferguson, 2007).

In the present research work a combination of hydrogels were produced. This kind of materials has been extensively used in the production of drug delivery systems and has been used as wound dressings. Thus, chitosan and alginate microparticles were produced to be used as drug delivery systems and a dextran hydrogel was produced to cover, protect and hydrate the wound and to act as a support for the microparticles introduced inside it. As described in other studies (Brandl et al., 2010; Hoare and Kohane, 2008), the drug release profile of drugs from hydrogels is faster, so the use of a second system containing the drug encapsulated (as depicted in Figure 8) is a way to overcome the restriction of hydrogels as drug delivery systems. During this practical work it was observed that chitosan and alginate microparticles have different swelling comportments. However, it is not possible to conclude that this behavior will always check, since it can change with the production method used, the temperature or with the solution used to do the studies (Agnihotri and Aminabhavi, 2004; El-Gibaly, 2002; Pasparakis and Bouropoulos, 2006). It was also verified that the release

profile of the protein used here (BSA) was faster for alginate microparticles than for chitosan ones, despite their macroscopic structural surface appeared to be similar. Furthermore, this release profile was independent of pH. When microparticles were introduced into dextran hydrogel the quantity of BSA released from both microparticles, in the same period of time, was lower, as expected. In this case, the protein must overcome two barriers: first, it must overcome the microparticle barrier and second, it must overcome the hydrogel matrix until reach the outside solution. The mathematical model developed, based on the swelling and *in vitro* protein release studies was tested with success, and in future it will be useful to develop other drug delivery systems with different or equal materials and drugs, as explained in chapter 3.

Moreover, it was also possible to verify that the dextran hydrogel loaded with chitosan microparticles containing growth factors can be used to improve the wound healing mechanism. Dextran and chitosan are two natural polysaccharides that have been used as drug delivery systems and as wound dressings (Huang and Fu, 2010; Maia et al., 2009; Ribeiro et al., 2009). As described before, EGF and VEGF are two crucial growth factors involved in the wound healing process. The *in vitro* release studies, made first, were useful to know how many times the carriers composed by dextran hydrogel loaded with chitosan microparticles containing VEGF and EGF would be applied to the wounds of animals. Based on *in vivo* studies the presence of VEGF and EGF, incorporated in the carriers, makes the wound healing process faster, with total epithelization and formation of new vessels after 21 days.

In future studies, other drug delivery systems could be produced with the help of mathematical model here developed, and the combination of these two systems (hydrogel and microparticles) produced with other materials can also be used as carriers for other growth factors that can be involved in other pathways of the human metabolism.

Bibliography

Bibliography

Acharya, G., Shin, C., McDermott, M., Mishra, H., Park, H., Kwon, I., Park, K., 2010. The hydrogel template method for fabrication of homogeneous nano/microparticles. Journal of Controlled Release 141, 314-319.

Agnihotri, S.A., Aminabhavi, T.M., 2004. Controlled release of clozapine through chitosan microparticles prepared by a novel method* 1. Journal of Controlled Release 96, 245-259.

Albrecht, C., Scherbart, A.M., Berlo, D., Braunbarth, C.M., Schins, R.P.F., Scheel, J., 2009. Evaluation of cytotoxic effects and oxidative stress with hydroxyapatite dispersions of different physicochemical properties in rat NR8383 cells and primary macrophages. Toxicology in vitro 23, 520-530.

Alemdaroglu, C., De im, Z., Çelebi, N., Zor, F., Oztürk, S., Erdo an, D., 2006. An investigation on burn wound healing in rats with chitosan gel formulation containing epidermal growth factor. Burns: journal of the International Society for Burn Injuries 32, 319-327.

Anumolu, S.N.S., Menjoge, A.R., Deshmukh, M., Gerecke, D., Stein, S., Laskin, J., Sinko, P.J., 2010. Doxycycline hydrogels with reversible disulfide crosslinks for dermal wound healing of mustard injuries. Biomaterials 32, 1204-1217.

Arya, N., Chakraborty, S., Dube, N., Katti, D.S., 2009. Electrospraying: A facile technique for synthesis of chitosan based micro/nanospheres for drug delivery applications. Journal of Biomedical Materials Research Part B: Applied Biomaterials 88, 17-31.

Auger, F., Lacroix, D., Germain, L., 2009. Skin substitutes and wound healing. Skin Pharmacology and Physiology 22, 94-102.

Badylak, S., Taylor, D., Uygun, K., 2010. Whole-Organ Tissue Engineering: Decellularization and Recellularization of Three-Dimensional Matrix Scaffolds. Annual review of biomedical engineering 13, 27-53.

Balasubramani, M., Kumar, T.R., Babu, M., 2001. Skin substitutes: a review. Burns 27, 534-544.

Bao, P., Kodra, A., Tomic-Canic, M., Golinko, M.S., Ehrlich, H.P., Brem, H., 2009. The role of vascular endothelial growth factor in wound healing. Journal of Surgical Research 153, 347-358.

Barrientos, S., Stojadinovic, O., Golinko, M.S., Brem, H., Tomic Canic, M., 2008. Growth factors and cytokines in wound healing. Wound Repair and Regeneration 16, 585-601.

Beldon, P., 2010. Basic science of wound healing. Surgery (Oxford) 28, 409-412.

Bhavsar, M.D., Jain, S., Amiji, M.M., 2009. Nanotechnology to improve oral drug delivery. Drug Efficacy, Safety, and Biologics Discovery: Emerging Technologies and Tools, Chapter 10, 231.

Bell, E., Ehrlich, H.P., Buttle, D.J., Nakatsuji, T., 1981. Living tissue formed in vitro and accepted as skin-equivalent tissue of full thickness. Science 211, 1052.

Boateng, J., Matthews, K., Stevens, H., Eccleston, G., 2008. Wound healing dressings and drug delivery systems: A review. Journal of pharmaceutical sciences 97, 2892-2923.

Böttcher-Haberzeth, S., Biedermann, T., Reichmann, E., 2010. Tissue engineering of skin. Burns 36, 450-460.

Brandl, F., Kastner, F., Gschwind, R., Blunk, T., Teßmar, J., Göpferich, A., 2010. Hydrogel-based drug delivery systems: Comparison of drug diffusivity and release kinetics. Journal of Controlled Release 142, 221-228.

Branski, L., Pereira, C., Herndon, D., Jeschke, M., 2006. Gene therapy in wound healing: present status and future directions. Gene therapy 14, 1-10.

Breen, E.C., 2007. VEGF in biological control. Journal of cellular biochemistry 102, 1358-1367.

Caldorera-Moore, M., Peppas, N.A., 2009. Micro-and nanotechnologies for intelligent and responsive biomaterial-based medical systems. Advanced drug delivery reviews 61, 1391-1401.

Capasso, J.M., Cossio, B.R., Berl, T., Rivard, C.J., Jimenez, C., 2003. A colorimetric assay for determination of cell viability in algal cultures. Biomolecular Engineering 20, 133-138.

Chen, F., Zhao, Y., Wu, H., Deng, Z., Wang, Q., Zhou, W., Liu, Q., Dong, G., Li, K., Wu, Z., 2006. Enhancement of periodontal tissue regeneration by locally controlled delivery of insulin-like growth factor-I from dextran-co-gelatin microspheres. Journal of Controlled Release 114, 209-222.

Clark, R., Ghosh, K., Tonnesen, M., 2007. Tissue engineering for cutaneous wounds. Journal of Investigative Dermatology 127, 1018-1029.

Crapo, P.M., Gilbert, T.W., Badylak, S.F., 2011. An overview of tissue and whole organ decellularization processes. Biomaterials 32, 3233-3243.

Dai, N., Williamson, M., Khammo, N., Adams, E., Coombes, A., 2004. Composite cell support membranes based on collagen and polycaprolactone for tissue engineering of skin. Biomaterials 25, 4263-4271.

Davidovich-Pinhas, M., Harari, O., Bianco-Peled, H., 2009. Evaluating the mucoadhesive properties of drug delivery systems based on hydrated thiolated alginate. Journal of Controlled Release 136, 38-44.

Delair, T., 2010. Colloidal polyelectrolyte complexes of chitosan and dextran sulfate towards versatile nanocarriers of bioactive molecules. European journal of pharmaceutics and biopharmaceutics 78 (1), 10-18.

Desai, T., 2000. Micro-and nanoscale structures for tissue engineering constructs. Medical Engineering and Physics 22, 595-606.

Dos Santos, K., Coelho, J., Ferreira, P., Pinto, I., Lorenzetti, S., Ferreira, E., Higa, O., Gil, M., 2006. Synthesis and characterization of membranes obtained by graft copolymerization of 2-hydroxyethyl methacrylate and acrylic acid onto chitosan. International journal of pharmaceutics 310, 37-45.

Draget, K., Skjåk-Bræk, G., Smidsrød, O., 1997. Alginate based new materials. International journal of biological macromolecules 21, 47-55.

Eisenbarth, E., 2007. Biomaterials for tissue engineering. Advanced Engineering Materials 9, 1051-1060.

Eldin, M.S.M., Soliman, E., Hashem, A., Tamer, T., 2010. Chitosan Modified Membranes for Wound Dressing Applications: Preparations, Characterization and Bio-Evaluation. Trends in Biomaterials and Artificial Organs 22, 158-168.

El-Gibaly, I., 2002. Development and in vitro evaluation of novel floating chitosan microcapsules for oral use: comparison with non-floating chitosan microspheres. International journal of pharmaceutics 249, 7-21.

Eming, S.A., Krieg, T., Davidson, J.M., 2007. Inflammation in wound repair: molecular and cellular mechanisms. Journal of Investigative Dermatology 127, 514-525.

Enoch, S., Leaper, D.J., 2008. Basic science of wound healing. Surgery (Oxford) 26, 31-37.

Escámez, M.J., Carretero, M., García, M., Martínez-Santamaría, L., Mirones, I., Duarte, B., Holguín, A., García, E., García, V., Meana, A., 2008. Assessment of optimal virus-mediated growth factor gene delivery for human cutaneous wound healing enhancement. Journal of Investigative Dermatology 128, 1565-1575.

Gadad, A., Patil, M., Naduvinamani, S., Mastiholimath, V., Dandagi, P., Kulkarni, A., 2009. Sodium alginate polymeric floating beads for the delivery of cefpodoxime proxetil. Journal of Applied Polymer Science 114, 1921-1926.

Ganapathy-Kanniappan, S., Geschwind, J.F.H., Kunjithapatham, R., Buijs, M., Syed, L.H., Rao, P.P., Ota, S., Vali, M., 2010. The Pyruvic Acid Analog 3-Bromopyruvate Interferes With the Tetrazolium Reagent MTS in the Evaluation of Cytotoxicity. ASSAY and Drug Development Technologies 8, 258-262.

Gaspar, V., Sousa, F., Queiroz, J., Correia, I., 2011. Formulation of chitosan–TPP–pDNA nanocapsules for gene therapy applications. Nanotechnology 22, 015101.

Grech, J., Mano, J., Reis, R., 2010. Processing and characterization of chitosan microspheres to be used as templates for layer-by-layer assembly. Journal of Materials Science: Materials in Medicine 1(6), 1855-1865.

Green, H., Rheinwald, J., 1975. Serial cultivation of strains of human epidermal keratinocytes: the formation of keratinizing colonies from single cells. Cell 6, 331-344.

Gurtner, G., Werner, S., Barrandon, Y., Longaker, M., 2008. Wound repair and regeneration. Nature 453, 314-321.

Guse, C., Koennings, S., Kreye, F., Siepmann, F., Goepferich, A., Siepmann, J., 2006. Drug release from lipid-based implants: elucidation of the underlying mass transport mechanisms. International journal of pharmaceutics 314, 137-144.

Hamidi, M., Azadi, A., Rafiei, P., 2008. Hydrogel nanoparticles in drug delivery. Advanced drug delivery reviews 60, 1638-1649.

Harrison, B., Atala, A., 2007. Carbon nanotube applications for tissue engineering. Biomaterials 28, 344-353.

Hasiwa, M., Kylián, O., Hartung, T., Rossi, F., 2008. Removal of immune-stimulatory components from surfaces by plasma discharges. Innate Immunity 14(2), 88-97.

Heile, A., Wallrapp, C., Klinge, P., Samii, A., Kassem, M., Silverberg, G., Brinker, T., 2009. Cerebral transplantation of encapsulated mesenchymal stem cells improves cellular pathology after experimental traumatic brain injury. Neuroscience letters 463, 176-181.

Hiemstra, C., Zhong, Z., van Steenbergen, M., Hennink, W., Feijen, J., 2007. Release of model proteins and basic fibroblast growth factor from in situ forming degradable dextran hydrogels. Journal of Controlled Release 122, 71-78.

Higuchi, T., 1960. Physical chemical analysis of percutaneous absorption process from creams and ointments. J. Soc. Cosmet. Chem 11, 85-97.

Hoare, T., Kohane, D., 2008. Hydrogels in drug delivery: Progress and challenges. Polymer 49, 1993-2007.

Huang, G.Y., Zhou, L.H., Zhang, Q.C., Chen, Y.M., Sun, W., Xu, F., Lu, T.J., 2011. Microfluidic hydrogels for tissue engineering. Biofabrication 3, 012001.

Huang, M., Berkland, C., 2009. Controlled release of Repifermin® from polyelectrolyte complexes stimulates endothelial cell proliferation. Journal of pharmaceutical sciences 98, 268-280.

Huang, S., Fu, X., 2010. Naturally derived materials-based cell and drug delivery systems in skin regeneration. Journal of Controlled Release 142, 149-159.

Huebsch, N., Mooney, D., 2009. Inspiration and application in the evolution of biomaterials. Nature 462, 426-432.

ISO, I.S.O., 2003. Biological evaluation of medical devices - Part 10: Tests for irritation and delayed-type hypersensitivity. International Organisation of Standardisation, Geneve.

Ito, A., Ino, K., Hayashida, M., Kobayashi, T., Matsunuma, H., Kagami, H., Ueda, M., Honda, H., 2005. Novel methodology for fabrication of tissue-engineered tubular constructs using magnetite nanoparticles and magnetic force. Tissue engineering 11, 1553-1561.

Jayakumar, R., Prabaharan, M., Kumar, P., Nair, S., Tamura, H., 2011. Biomaterials based on chitin and chitosan in wound dressing applications. Biotechnology Advances 29(3), 322-337.

Jin, C.M., Kaewintajuk, K., Jiang, J.H., Jeong, W.J., Kamata, M., KIM, H.S., Wataya, Y., Park, H., 2009. Toxoplasma gondii: A simple high-throughput assay for drug screening in vitro. Experimental Parasitology 121, 132-136.

Jones, I., Currie, L., Martin, R., 2002. A guide to biological skin substitutes. British journal of plastic surgery 55, 185-193.

Jukes, J.M., van der Aa, L.J., Hiemstra, C., van Veen, T., Dijkstra, P.J., Zhong, Z., Feijen, J., van Blitterswijk, C.A., de Boer, J., 2009. A Newly Developed Chemically Crosslinked Dextran–Poly (Ethylene Glycol) Hydrogel for Cartilage Tissue Engineering. Tissue Engineering Part A 16, 565-573.

Karakeçili, A.G., Satriano, C., Gümüsderelioglu, M., Marletta, G., 2008. Enhancement of fibroblastic proliferation on chitosan surfaces by immobilized epidermal growth factor. Acta Biomaterialia 4, 989-996.

Kenawy, E., Abdel-Hay, F., El-Newehy, M., Wnek, G., 2009. Processing of polymer nanofibers through electrospinning as drug delivery systems. Materials Chemistry and Physics 113, 296-302.

Kim, I., Seo, S., Moon, H., Yoo, M., Park, I., Kim, B., Cho, C., 2008. Chitosan and its derivatives for tissue engineering applications. Biotechnology Advances 26, 1-21.

Kim, S., Kim, J., Jeon, O., Kwon, I., Park, K., 2009. Engineered polymers for advanced drug delivery. European journal of pharmaceutics and biopharmaceutics: official journal of Arbeitsgemeinschaft fur Pharmazeutische Verfahrenstechnik eV 71(3), 420-430.

Kirkpatrick, C.J., Peters, K., Hermanns, M., Bittinger, F., Krump-Konvalinkova, V., Fuchs, S., Unger, R.E., 2005. In vitro methodologies to evaluate biocompatibility: status quo and perspective. Itbm-Rbm 26, 192-199.

Kiyozumi, T., Kanatani, Y., Ishihara, M., Saitoh, D., Shimizu, J., Yura, H., Suzuki, S., Okada, Y., Kikuchi, M., 2007. The effect of chitosan hydrogel containing DMEM/F12 medium on full-thickness skin defects after deep dermal burn. Burns 33, 642-648.

Klenkler, B., Sheardown, H., 2004. Growth factors in the anterior segment: role in tissue maintenance, wound healing and ocular pathology. Exp Eye Res 79, 677-688.

Ko, J., Park, H., Hwang, S., Park, J., Lee, J., 2002. Preparation and characterization of chitosan microparticles intended for controlled drug delivery. International journal of pharmaceutics 249, 165-174.

Kokabi, M., Sirousazar, M., Hassan, Z.M., 2007. PVA-clay nanocomposite hydrogels for wound dressing. European polymer journal 43, 773-781.

Kumar, R., Majeti, N., 2000. A review of chitin and chitosan applications. Reactive and functional polymers 46, 1-27.

Kumari, T., Vasudev, U., Kumar, A., Menon, B., 2010. Cell surface interactions in the study of biocompatibility. Trends in Biomaterials and Artificial Organs 15(2), 37-41.

Kumbar, S.G., Nukavarapu, S.P., James, R., Nair, L.S., Laurencin, C.T., 2008. Electrospun poly(lactic acid-co-glycolic acid) scaffolds for skin tissue engineering. Biomaterials 29, 4100-4107.

Kwon, Y., Kim, H., Roh, D., Yoon, S., Baek, R., Kim, J., Kweon, H., Lee, K., Park, Y., Lee, J., 2006. Topical application of epidermal growth factor accelerates wound healing by myofibroblast proliferation and collagen synthesis in rat. Journal of veterinary science 7, 105-109.

Li, J., Chen, J., Kirsner, R., 2007. Pathophysiology of acute wound healing. Clinics in dermatology 25, 9-18.

Lin, C., Metters, A., 2006. Hydrogels in controlled release formulations: network design and mathematical modeling. Advanced drug delivery reviews 58, 1379-1408.

Lo, C.W., Jiang, H., 2010. Photopatterning and degradation study of dextran glycidyl methacrylate hydrogels. Polymer Engineering & Science 50, 232-239.

Luangtana-anan, M., Limmatvapirat, S., Nunthanid, J., Chalongsuk, R., Yamamoto, K., 2010. Polyethylene Glycol on Stability of Chitosan Microparticulate Carrier for Protein. AAPS The American Association of Pharmaceutical Scientists 11, 1-7.

Lutolf, M., Hubbell, J., 2005. Synthetic biomaterials as instructive extracellular microenvironments for morphogenesis in tissue engineering. Nature biotechnology 23, 47-55.

MacNeil, S., 2007. Progress and opportunities for tissue-engineered skin. Nature 445, 874-880.

MacNeil, S., 2008. Biomaterials for tissue engineering of skin. Materials Today 11, 26-35.

Maeng, Y.J., Choi, S.W., Kim, H.O., Kim, J.H., 2010. Culture of human mesenchymal stem cells using electrosprayed porous chitosan microbeads. Journal of Biomedical Materials Research Part A 92, 869-876.

Maia, J., Ferreira, L., Carvalho, R., Ramos, M., Gil, M., 2005. Synthesis and characterization of new injectable and degradable dextran-based hydrogels. Polymer 46, 9604-9614.

Maia, J., Ribeiro, M., Ventura, C., Carvalho, R., Correia, I., Gil, M., 2009. Ocular injectable formulation assessment for oxidized dextran-based hydrogels. Acta Biomaterialia 5, 1948-1955.

Marques, A., Reis, R., Hunt, J., 2002. The biocompatibility of novel starch-based polymers and composites: in vitro studies. Biomaterials 23, 1471-1478.

Mazumder, M., Burke, N., Shen, F., Potter, M., Sto ver, H., 2009. Core-Cross-Linked Alginate Microcapsules for Cell Encapsulation. Biomacromolecules 10, 1365-1373.

Metcalfe, A., Ferguson, M., 2007a. Bioengineering skin using mechanisms of regeneration and repair. Biomaterials 28, 5100-5113.

Metcalfe, A., Ferguson, M., 2007b. Tissue engineering of replacement skin: the crossroads of biomaterials, wound healing, embryonic development, stem cells and regeneration. Journal of The Royal Society Interface 4, 413-437.

Norman, J., Desai, T., 2006. Methods for fabrication of nanoscale topography for tissue engineering scaffolds. Annals of biomedical engineering 34, 89-101.

Omokanwaye, T., Owens, D., Wilson Jr, O., 2010. Identification of Bacteria and Sterilization of Crustacean Exoskeleton Used as a Biomaterial. 26th Southern Biomedical Engineering Conferencesbec 2010 April 30-May 2, 2010 College Park, Maryland, USA 32, 418-421.

Orive, G., Hernandez, R., Gascon, A., Igartua, M., Pedraz, J., 2003. Survival of different cell lines in alginate-agarose microcapsules. European Journal of Pharmaceutical Sciences 18, 23-30.

Ousey, K., McIntosh, C., 2009. Physiology of Wound Healing, chapter 2.

Palmeira-de-Oliveira, A., Ribeiro, M., Palmeira-de-Oliveira, R., Gaspar, C., Costa-de-Oliveira, S., Correia, I., Pina Vaz, C., Martinez-de-Oliveira, J., Queiroz, J., Rodrigues, A., 2010. Anti-Candida Activity of a Chitosan Hydrogel: Mechanism of Action and Cytotoxicity Profile. Gynecologic and Obstetric Investigation 70, 322-327.

Park, J.B., Lakes, R.S., 2007. Biomaterials: an introduction. Springer Verlag, 3ª edition.

Pasparakis, G., Bouropoulos, N., 2006. Swelling studies and in vitro release of verapamil from calcium alginate and calcium alginate-chitosan beads. International journal of pharmaceutics 323, 34-42.

Paul, W., Sharma, C., 2004. Chitosan and alginate wound dressings: A short review. Trends Biomater. Artif. Organs 18, 18-23.

Peppas, N.A., Hilt, J.Z., Khademhosseini, A., Langer, R., 2006. Hydrogels in biology and medicine: from molecular principles to bionanotechnology. Adv Mater 18, 1345-1360.

Petrie, T.A., García, A.J., 2009. Extracellular Matrix-derived Ligand for Selective Integrin Binding to Control Cell Function. Biological Interactions on Materials Surfaces, chapter 7, 133-156.

Pham, C., Greenwood, J., Cleland, H., Woodruff, P., Maddern, G., 2007. Bioengineered skin substitutes for the management of burns: a systematic review. Burns 33, 946-957.

Potter, T.M., Stern, S.T., 2011. Evaluation of cytotoxicity of nanoparticulate materials in porcine kidney cells and human hepatocarcinoma cells. Methods in molecular biology (Clifton, NJ) 697(5), 157-165.

Prabaharan, M., Mano, J., 2008. Chitosan-based particles as controlled drug delivery systems. Drug Delivery 12, 41–57.

Promega, T., 2008. CellTiter 96® AQueous One Solution Cell Proliferation Assay. Promega Corporation.

Prow, T.W., Grice, J.E., Lin, L.L., Faye, R., Butler, M., Becker, W., Wurm, E.M.T., Yoong, C., Robertson, T.A., Soyer, H.P., 2011. Nanoparticles and microparticles for skin drug delivery. Advanced drug delivery reviews, article in press.

Ratner, B.D., 2004. Biomaterials science: an introduction to materials in medicine. Academic press, 2nd edition.

Reddy, P., Swarnalatha, D., 2010. Recent Advances in Novel Drug Delivery Systems. Recent Advances in Novel Drug Delivery 2, 2025-2027.

Ribeiro, M., Espiga, A., Silva, D., Baptista, P., Henriques, J., Ferreira, C., Silva, J., Borges, J., Pires, E., Chaves, P., Correia, I., 2009. Development of a new chitosan hydrogel for wound dressing. Wound Repair and Regeneration 17, 817-824.

Rieux, A., Ucakar, B., Mupendwa, B.P.K., Colau, D., Feron, O., Carmeliet, P., Preat, V., 2010. 3D systems delivering VEGF to promote angiogenesis for tissue engineering. Journal of Controlled Release 150(3), 272-278.

Roach, P., Eglin, D., Rohde, K., Perry, C., 2007. Modern biomaterials: a review—bulk properties and implications of surface modifications. Journal of Materials Science: Materials in Medicine 18, 1263-1277.

Rodrigues, A., Saraiva Sanchez, E., da Costa, A., Moraes, Â., 2008. The influence of preparation conditions on the characteristics of chitosan alginate dressings for skin lesions. Journal of Applied Polymer Science 109, 2703-2710.

Roskoski, R., Jr., 2007. Sunitinib: a VEGF and PDGF receptor protein kinase and angiogenesis inhibitor. Biochem Biophys Res Commun 356, 323-328.

Sachan, N., Pushkar, S., Jha, A., Bhattcharya, A., 2009. Sodium alginate: the wonder polymer for controlled drug delivery. Journal of pharmacy research 2, 1191-1199.

Sachs, D., Voorhees, J., 2010. Age-Reversing Drugs and Devices in Dermatology. Clinical Pharmacology & Therapeutics 89(1), 34-43.

Seal, B., Otero, T., Panitch, A., 2001. Polymeric biomaterials for tissue and organ regeneration. Materials Science and Engineering: R: Reports 34, 147-230.

Seeley, R.R., Stephens, T.D., Philip, T., 2003. Anatomia & Fisiologia 6th Edition, 150-169.

Sezer, A., Hatipoglu, F., Cevher, E., O urtan, Z., Bas, A., Akbu a, J., 2007. Chitosan film containing fucoidan as a wound dressing for dermal burn healing: preparation and in vitro/in vivo evaluation. AAPS PharmSciTech 8, 94-101.

Shaw, T., Martin, P., 2009a. Wound repair at a glance. Journal of cell science 122, 3209-3213.

Sheridan, R., Moreno, C., 2001. Skin substitutes in burns. Burns: journal of the International Society for Burn Injuries 27(1), 92.

Shevchenko, R., James, S., James, S., 2010. A review of tissue-engineered skin bioconstructs available for skin reconstruction. Journal of The Royal Society Interface 7(43), 229-258.

Siepmann, J., Siepmann, F., 2008. Mathematical modeling of drug delivery. International journal of pharmaceutics 364, 328-343.

Stamatialis, D.F., Papenburg, B.J., Gironès, M., Saiful, S., Bettahalli, S.N.M., Schmitmeier, S., Wessling, M., 2008. Medical applications of membranes: Drug delivery, artificial organs and tissue engineering. Journal of Membrane Science 308, 1-34.

Stojadinovic, O., Kodra, A., Golinko, M., Tomic-Canic, M., Brem, H., 2007. A novel, non-angiogenic mechanism of VEGF: Stimulation of keratinocyte and fibroblast migration. Wound Repair and Regen 15, 30-36.

Strodtbeck, F., 2001. Physiology of wound healing. Newborn and Infant Nursing Reviews 1, 43-52.

Supp, D., Boyce, S., 2005. Engineered skin substitutes: practices and potentials. Clinics in dermatology 23, 403-412.

Takka, S., Gürel, A., 2010. Evaluation of Chitosan/Alginate Beads Using Experimental Design: Formulation and In Vitro Characterization. AAPS PharmSciTech 11, 460-466.

Tsirogianni, A.K., Moutsopoulos, N.M., Moutsopoulos, H.M., 2006. Wound healing: immunological aspects. Injury 37, S5-S12.

Uludag, H., De Vos, P., Tresco, P., 2000. Technology of mammalian cell encapsulation. Advanced drug delivery reviews 42, 29-64.

Wang, H., Liu, Q., Yang, Q., Li, Y., Wang, W., Sun, L., Zhang, C., 2010. Electrospun poly (methyl methacrylate) nanofibers and microparticles. Journal of materials science 45, 1032-1038.

Watanabe, W., Sudo, K., Asawa, S., Konno, K., Yokota, T., Shigeta, S., 1995. Use of lactate dehydrogenase to evaluate the anti-viral activity against influenza A virus. Journal of virological methods 51, 185-191.

Weng, L., Romanov, A., Rooney, J., Chen, W., 2008a. Non-cytotoxic, in situ gelable hydrogels composed of N-carboxyethyl chitosan and oxidized dextran. Biomaterials 29, 3905-3913.

Wichterle, O., Lim, D., 1960. Hydrophilic gels for biological use. 185, 117-118.

Wong, D., Chang, H., 2009. Skin tissue engineering. The Stem Cell Research Community, StemBook 126(3), 858-868.

Woodley, D.T., Remington, J., Huang, Y., Hou, Y., Li, W., Keene, D.R., Chen, M., 2007. Intravenously injected human fibroblasts home to skin wounds, deliver type VII collagen, and promote wound healing. Molecular Therapy 15, 628-635.

Yang, X., Yang, K., Wu, S., Chen, X., Yu, F., Li, J., Ma, M., Zhu, Z., 2010. Cytotoxicity and wound healing properties of PVA/ws-chitosan/glycerol hydrogels made by irradiation followed by freeze-thawing. Radiation Physics and Chemistry 79, 606-611.

Yoo, H.J., Kim, H.D., 2008. Synthesis and properties of waterborne polyurethane hydrogels for wound healing dressings. Journal of Biomedical Materials Research Part B: Applied Biomaterials 85, 326-333.

Yu, C., Zhang, X., Zhou, F., Zhang, X., Cheng, S., Zhuo, R., 2008. Sustained release of antineoplastic drugs from chitosan-reinforced alginate microparticle drug delivery systems. International journal of pharmaceutics 357, 15-21.

Zhang, L., Webster, T., 2009. Nanotechnology and nanomaterials: Promises for improved tissue regeneration. Nano Today 4, 66-80.

Zhao, L., Mei, S., Wang, W., Chu, P.K., Wu, Z., Zhang, Y., 2010. The role of sterilization in the cytocompatibility of titania nanotubes. Biomaterials 31, 2055-2063.

Zuleta, F., Velasquez, P., De Aza, P., 2010. Effect of various sterilization methods on the bioactivity of laser ablation pseudowollastonite coating. Journal of Biomedical Materials Research Part B: Applied Biomaterials 94, 399-405.